# Generation of tools for real-time observation of neurodegenerative disease related cellular pathologies

A thesis submitted for the partial fulfilment of the requirements for the degree of Master of Research, Faculty of Medicine, Human, and Health Sciences,

Macquarie University, July 2021

Nicholas Kakaroubas

46041222

Primary Supervisor: Dr. Emily Don

Co-supervisors: Dr. Alison Hogan, Dr. Marco Mosrch, Dr. Angela Laird

Macquarie University Centre for Motor Neuron Disease Research,

Faculty Medicine, Health, and Human Sciences, Macquarie University, NSW, Australia.

Keywords: Amyotrophic Lateral Sclerosis, Danio rerio, stress granules, animal models.

This thesis has not been submitted for a higher degree to any other university or institution.

# Declaration

All material presented in this thesis, except were acknowledged in discipline specific manner, is original and has not been previously submitted in part or whole as a part of a degree in any university. No financial compensation was pursued or accepted for the completion of this thesis. There were no conflicts of interest in completing this thesis.

The research presented in this thesis was performed with the ethics approval from Macquarie University Animal Ethics Committee under Animal Research Authority (2015/033-26 and 2015/034-32) and Biosafety Approval (NLRD approval 5794). All experiments were conducted conforming to current regulatory standards.

Nicholas Gerasimos Kakaroubas

# Table of Contents

# List of Figures

# Abstract

Currently, the pathological biochemistry of Amyotrophic Lateral Sclerosis (ALS) is poorly understood resulting in limited treatment options. Emerging research has implicated aberrant stress granules in ALS pathology. Stress granules are accumulations of non-membrane bound RNA-protein assemblies which aggregate in the cytosol of cells as a natural response to external stimuli. These stress granule assemblies are a dynamic biological response to cellular stress, limiting mRNA translation initiation to help the cell survive short-term stresses such as thermal, metabolic, and oxidative stress. Chronic stress granules form when the cell does not disperse the RNA-protein assemblies leading to cell death. The objective of this thesis is to create models to study stress granule formation and disassembly in ALS in real time, in vivo.

Zebrafish are the most suitable model organism for this study. Their high reproduction rate, a well characterised gene altering 'toolkit', and transparency in their embryonic and larval stages allow for a high number of samples to be genetically altered and screened over short time frames. Zebrafish share up to 70% of exons and major organs of interest with humans which should enable sound comparison at the cellular level of stress granule dynamics. To study stress granule formation, this project aims to link known stress granule associated proteins with fluorescent markers to visualise stress granule dynamics, in real time, in vivo, through confocal microscopy.

In this thesis we have generated mRNA stress granule reporters. These mRNA stress granule reporters were injected into zebrafish embryos, allowing the visualisation of the formation of protein aggregates determined to be stress granules. These puncta were quantified and analysed with morphological assays to determine the effect on the zebrafish model. We have characterised and established the mVenus-G3bp1 mRNA transcript as a stress granule reporter and established direction for the future of this research.

# Materials Arising from this Candidature

Poster presentation:

**Mr. Nicholas Kakaroubas**, Dr. Alison Hogan, Dr. Marco Morsch, Dr. Angela Laird, Dr. Emily Don. 'Validation of Stress Granule Reporters in Zebrafish' presented at: 31st International Symposium on ALS/MND; 11 December 2020; Online.

Oral presentation:

**Mr. Nicholas Kakaroubas**, Dr. Alison Hogan, Dr. Marco Morsch, Dr. Angela Laird, Dr. Emily Don. 'The Generation and Validation of *in vivo* Stress Granule Reporters' presented at: Model Organisms Showcase; 12 March 2021; Centenary Institute, University of Sydney, NSW, Australia.

## Acknowledgements

I first and foremost want to thank my primary supervisor Dr. Emily Don. You helped me through more than this thesis – you mentored me in professionalism and lent a sympathetic ear when times were tough. With a keen eye to social causes, you are an inspiration to not just the scientist I want to be but to the person I want to grow into. I also want to thank my co-supervisors: Dr. Alison Hogan, Dr. Marco Morsch, and Dr. Angela Laird. You all fostered a productive and friendly work environment and helped shape this thesis.

I want to thank Macquarie University, the MND Team, the Lab Operations Team, and the Fish Room Team – I want to apologize for being a loud distraction in the office and lab but also thank you for your support, teaching, and teaching. I also want to acknowledge Dr. Jenifer Rowland for your help in editing.

I want to offer a huge thank you to all my friends and family, in particular to my parents. Mum, you were my paragon of strength growing up and in recent years have shown the world resilience I can only aspire to emulate. Dad, thank you for instilling in me the curiosity and confidence that made this possible. Thank you all, for your support and love through a challenging year. I promise to not talk as much about fish as I have been recently.

I finally want to dedicate this thesis to my nephew Jacob. As the next generation, you will benefit from the research done today. Science is more than playing around with tubes of DNA, but it is an applied curiosity. To be a scientist is to have the confidence to look at the world, stand up, and make your ideas known. Life like science is a team effort where you rely on your friends, family, and coworkers to support you through adversity and push you to be the best possible version of yourself. I hope that your curiosity and confidence never waiver.

# List of Abbreviations

ALS – Amyotrophic Lateral Sclerosis

U.S.A. – United States of America

fALS – familial Amyotrophic Lateral Sclerosis

sALS – sporadic Amyotrophic Lateral Sclerosis

gALS – Guamanian Amyotrophic Lateral Sclerosis

PIC – Preinitiation complexes

SOP – Standard operating procedure

E3 – Embryo medium

hpf – hours post fertilisation

WT – wild-type

CAT I – category 1

CAT II – category 2

CAT III – category 3

GGGS – Glycine-Glycine-Glycine-Serine

CRISPR – clustered regularly interspaced short palindromic repeats

ZFN – zinc finger

TALEN – transcription activator-like effector nucleases

BMAA – β-N-methylamino-L-alanine

# 1 Introduction

## 1.1 Amyotrophic Lateral Sclerosis

Amyotrophic Lateral Sclerosis (ALS) is a chronic and fatal neurodegenerative condition characterised by the degradation of motor neurons in the primary motor cortex, corticospinal tracts, brainstem and spinal cord resulting in total paralysis of the patient (1). Paralysis is progressive and most patients experience death within 2-3 years post diagnosis due to respiratory failure (2, 3). Roughly 10-20% of people living with ALS survive longer than 10 years post diagnosis (4). Currently there is no cure for ALS with only two drugs approved by the U.S.A. Food and Drug Administration for the treatment of ALS symptoms: riluzole, and edaravone (5, 6). There are multiple forms of ALS, each with similar clinical presentations yet categorised due to apparent cause - familial ALS (fALS) (relating to genetically inherited ALS) represents 5-10% of all cases (7), sporadic ALS (sALS) (relating to an unfamiliar cause) which represents roughly 90% of cases and Guamanian ALS (gALS) as caused by environmental factors in Guam which are included in the 90% of sALS cases (8, 9). Considered a rare disorder, ALS has an estimated global incidence of between 0.4 and 1.8 per 100 000 individuals (10). The incidence rate of gALS is higher than what is seen in other countries with a highly variable rate of up 50 times that of the global rate with much debate surrounding the severity and cause (of all ALS types) within the scientific community (11, 12). While incidence rates seem low and sporadic, clinical diagnosis of ALS is correct approximately in 95% of cases however there exists no formal assessment or diagnostic tool with most cases being confirmed post mortem meaning many people may suffer prior or without diagnosis (13). A major challenge faced with creating assessment tools is the mystery surrounding the genetic and environmental influences, and early pathogenesis of the condition. A component of ALS pathology which may provide insight to the early stages of the condition is the inclusion of protein aggregates in affected cells.

## 1.2 Protein Aggregates

Intracellular protein aggregates have been historically linked to ALS pathogenesis as far back as 1998 with ALS-linked mutations in the enzyme, superoxide dismutase 1 (SOD1) resulting in accumulations of SOD1 protein (14). More recently in 2009, "cytoplasmic FUS immunoreactive inclusions" were observed by Vance et. al showing common fALS and sALS associated gene mutations which resulted in cytoplasmic localized granules in lower motor neurones (15). Aberrant accumulations of the TAR DNA-binding of 43 kDa (TDP-43) protein in the cytoplasmic regions of motor neurons have also been noticed in most cases of ALS (16-19). It is unknown whether these protein aggregations are related to stress granules or whether they are similar but distinct pathological inclusions in ALS pathogenesis. What is apparent and needed is a characterisation of stress granules to better understand both protein aggregates and ALS.

## 1.3 Stress Granules

Stress granules are non-membrane bound, mRNA-protein assemblies accumulated within the cytoplasm of cells as a response to external cellular stress (20, 21). Stress granules were originally observed in cells as a response to heat shock (22, 23). It is now known that stress granules can form in response to a multitude of cellular stressors (24-26). Cellular stress can be defined as anything which presents an immediate threat to the life of the cell in question. This includes oxidative, nutritional, and thermal shocks (26-29). An example of cellular stress is an abundance of reactive oxygen species in a biological system inducing oxidative stress on cells, resulting in the stress granule response (26). Stress granules are a significant area of research as they have not only been implicated in the pathogenesis of ALS but have been also linked to a myriad of other conditions such as breast cancers, Huntington's disease, and Creutzfeldt-Jakob disease (30-33). Cell death as a response to chronic stress granules may provide insight to the premature motor neuronal death seen in cases of ALS.

The exact function of stress granules has not yet been characterized however it is speculated that they serve a protective purpose, by temporarily sequestering proteins and mRNA that are not essential to surviving the temporary stress, inhibiting their action. Stress granule formation and disassembly is a dynamic process as once the external stressor is removed; the stress granules typically disperse (34, 35). The components which make up stress granules have been found to be essential to cell proliferation such as G3BP1 and TIA1 proteins and as such, if the stress granule is not dispersed, the cell will die due to irregular metabolic process and translation inhibition (36-39). Chronic stress granules localising in motor neurons such as these may provide insight to the premature motor neuron death as seen in cases of ALS.

There are multiple biochemical signalling pathways which regulate stress granule formation with one of the most extensively studied being the mammalian target of rapamycin (mTOR)-eukaryotic translation initiation factor 4F (eIf4F) and eIf2α signalling pathways. Under optimal conditions within a cell, mTOR acts as a regulator of cellular metabolism and is required as a checkpoint for mRNA translation initiation. mTOR will constitutively phosphorylate the eIF4E-binding protein, preventing it from binding to the eIF4E allowing for the formation of the eIF4F complex at the 5’ cap of mRNA promoting translation initiation (30). Stress granules can form when cellular stressors inactivate mTOR, which leads to accumulation of hypophosphorylated 4E-binding protein. Accumulated 4E-binding protein will bind to the eIF4E (creating eIF4E-4E-binding protein complexes), displacing the scaffolding proteins (eIF4G) and RNA helicase (eIF4A) from the mRNA 5’ cap inhibiting translation. The eIF4E-4E-binding protein complexes and inhibited translation initiation form preinitiation complexes (PICs). These PICs recruit RNA-binding proteins to form ‘seeds’ which eventuate in the formation of stress granules (40, 41).

Once the speculated protective function of stress granules is served and the stressor is removed, healthy cells will work to remove the stress granules such as to allow for the cell to resume regular function. Although the literature is still divided on how stress granules form and disperse (42, 43), a well characterized dispersal pathway studied is the autolysomal cascade. This mechanism of clearing stress granules from the cytoplasm in cells involves valosin-containing proteins and the autolysosomal cascade working to disperse the stress granules from cells (44). More recent understanding of stress granule dynamics acknowledges that the RNA-binding proteins which make up stress granules exist in a dynamic state of liquid-liquid phases, changing their liquid density depending on the stage in which they exist (45-47). Despite the research regarding an autolysosomal cascade for the removal of stress granules, there is little more characterization surrounding the dynamic mechanisms and processes of stress granule assembly and disassembly.

Chronic stress granules form when the cell does not disperse of the stress granule formations once the stressor to the cell is removed. This leads to cell death (due to the sequestering of cell proliferation mRNA and protein in the stress granule complex) which has been implicated in the pathology of neurodegeneration and motor neuron disease (48). Chronic stress granules are characterized by a prolonged exposure to stress conditions, especially nutrient starvation, and persistent viral exposure, for upwards of 4-6 hours however this definition has been contested in literature (48-50). While external stressors can impact ALS pathogenicity, many cases of neurodegenerative disease are associated with mutations in heterogeneous nuclear ribonucleoprotein A (hnRNP A/B) family members. These mutant hnRNP A proteins promote the maturation of stress granules into irreversible fibrils which enhance the pathology of the neurodegenerative condition (45, 51). These chronic stress granules have been implicated in cases of ALS however research as to how chronic stress granule dynamics impact ALS pathogenesis is an area where more research is

required (48, 52). For this reason, the *in vivo* modelling of both chronic and acute stress granules is of utmost importance as to expand the understanding of their role in ALS.

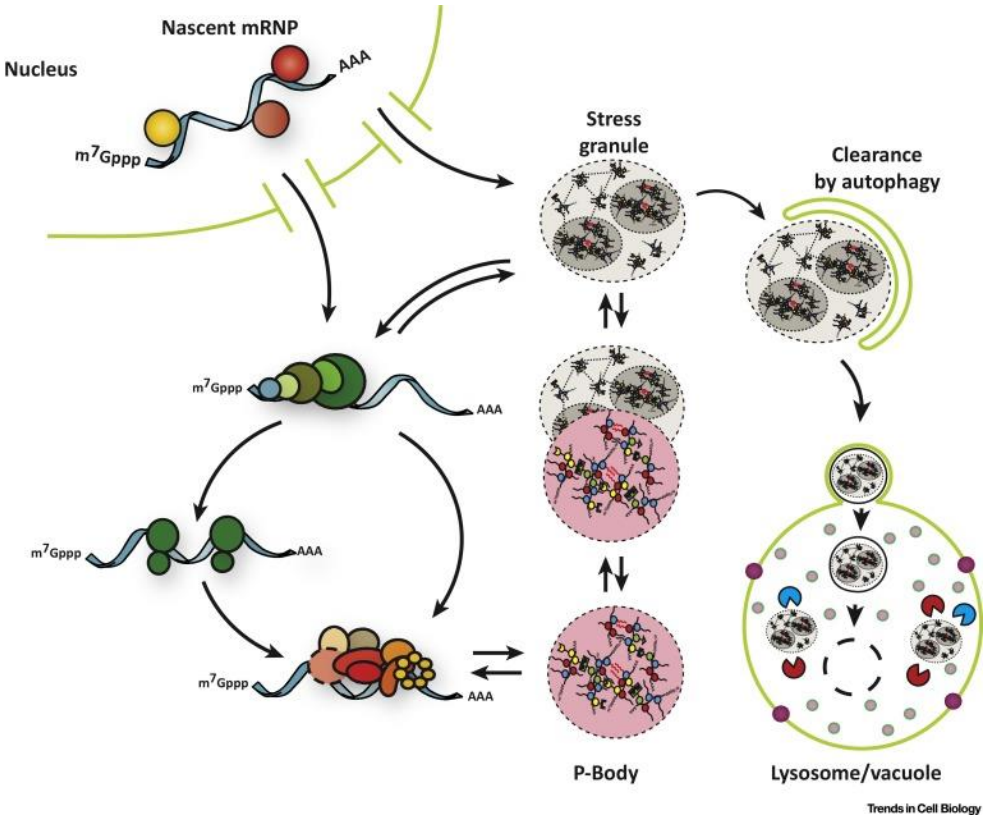


**Figure 1.** Stress granule assembly, disassembly, and autophagic clearance pathway. Adapted from Protter, Parker, 2016 (20).

## 1.4 Stress Granule Modelling

Historically, there have been many organisms utilised to model stress granules, ALS pathology, and interactions between the two. Models such as yeast cells (*Saccharomyces cerevisiae*), fruit flies (*Drosophila melanogaster*), round worms (*Caenorhabditis elegans*), zebrafish (*Danio rerio*), mice (*Mus musculus*), and Induced human Pluripotent Stem Cell-derived neurons have been used depending on their suitability for the experiment at hand (53-58). The *in vivo* modelling of ALS and stress granules is often favourable over *in vitro* and *in silico* experiments as *in vivo* modelling allows for the observation of the experimental effects on a living subject across different cell types and as such is a closer representation to what is seen in human ALS (59).

## 1.5 Advantages of Zebrafish as Disease Models

For the *in vivo* study of stress granules in ALS pathology, it is important to acknowledge the wider effect of the condition, namely how it will impact the motor neurons and different but neighbouring cells in the model. For this reason, it would be best to choose a model which reflects human physiology rather than single celled/cell type models such as yeast cells. Ease of imaging is also a consideration to be had. While the model may be appropriate to use for its biology, the stress granules and other cellular structures will still need to be imaged for analysis.

As the goal for this thesis is the *in vivo* modelling of stress granules, a high coverage of model in literature and high degree of similarity between human and model physiology is optimal. The zebrafish model's representation in ALS literature makes it the optimal model for this thesis (60). Zebrafish share up to 70% of their exons with humans (61), showing a higher (or comparable) degree of genetic similarity when compared with fruit flies, and roundworms (62, 63). Zebrafish also share anatomical features comparable to humans in muscle fibres and neurons (64) second only to mouse/murine models (65, 66). Furthermore, zebrafish are transparent in the embryonic and larval life stages enabling the *in vivo* imaging of cells and cell structures under light, fluorescent and confocal microscopy (67). Finally, zebrafish are continuous spawn breeders, mating all year round and producing large clutches every 1-1.9 days (68, 69) with optimal protocol suggesting breeding once every 1-2 weeks (70). Without a defined mating season, zebrafish models allow for continuous and yearlong research despite seasonal changes. For these reasons, the zebrafish is an appropriate model organism for some instances of *in vivo* modelling of stress granules and ALS biology as per this thesis investigation.

# 2 Aims of Thesis

This thesis is focused on the generation and validation of *in vivo* stress granule reporters in a zebrafish model. This project was conceived in the spirit of the larger research theme of the laboratory which is to understand the causes of and find cures for neurodegenerative diseases through observing protein aggregation and assembly in response to stimuli. Prior genetic and bioinformatic analysis has informed research efforts into potentially causative genes and processes. The purpose of this research is to investigate the dynamic processes of stress granule dynamics and what role they may be playing in the pathology of ALS and other neurodegenerative conditions. Therefore, there is a pertinent need to observe stress granule protein interaction in real time, hence *in vivo* reporters. Once a stress granule reporter is validated it will allow for the *in vivo* observation of dynamic stress granule formation and disassembly. Observing the cellular stress response will allow characterisation it with live imaging and lead to a deeper understanding of this response. Establishing an *in vivo* model will enable the observation of the stress granule response within a variety of cell types and the potential interactions between non-stressed cells and those which are stressed. In generating and validating an *in vivo* stress granule reporter, future research can be completed to further characterize stress granules in living systems and understand their role in ALS pathogenesis. There are three main aims of this research:

Aim 1: To express a transient stress granule reporter in zebrafish larvae.

Aim 2: To determine the optimal dose and timeframe for imaging the stress granule reporter.

Aim 3: To validate the stress granule reporter in response to cellular stress.

The investigation is outlined in the following chapters.

# 3 Methods and Materials

## 3.1 Zebrafish

The use of zebrafish for this project was approved by Macquarie University Animal Research Authority (AEC Reference Number: 2015/034 and 2015/033), Amendment 42 on the 23/04/2020 and Biosafety NLRD approval 5794.

### 3.1.1 Zebrafish Maintenance

Zebrafish were kept at a constant water temperature of 28°C, pH of 7.40, and conductivity of 1200 µS/m. The fish experienced a 14-hour day/10-hour night cycle with a simulated sunrise (from 7:30 am – 8:30 am) and sunset (from 9:00 pm – 9:30 pm). Fish were routinely fed twice a day on weekdays and once a day on weekends unless otherwise specified, adults receiving pellets of generic fish food and artemia crustaceans and juvenile zebrafish being fed a mix of washed artemia crustaceans, paramecium ciliates, and fry food depending on their age.

### 3.1.2 Zebrafish Husbandry and Embryo Collection

A single adult male and two adult female zebrafish were placed in specialty pair-mating tanks in the early evening the day before the eggs were to be collected. The pair-mating tanks featured a removable plastic divider to keep the males and the female separated overnight, and a false bottom mesh to allow for the eggs to fall through. In the morning, the plastic dividers were removed, and the tank placed on an angle to mimic a shoreline during the simulated sunrise to allow the fish to come into contact and initiate spawning of eggs. Mating fish were placed in a new pair-mating tank to continue spawning eggs as desired. Fertilised eggs were ready to be collected 5-15 minutes after allowing the males and female to interact.

The fertilised eggs were retrieved by draining the pair mating tank through a plastic tea strainer and washed with system water to remove faeces. Collected eggs were transferred

from the tea strainer to a Petri dish containing 30 ml of embryo medium (E3) (5 mM NaCl, 0.17 mM KCl, 0.33 mM CaCl2, and 0.33 mM MgSO4 buffered to 7.3 pH using carbonate hardness generator (Aquasonic), no methylene blue) at 28 °C)

## 3.2 Generation of Expression Transcripts

Plasmid construct previously created were utilised in generating the mRNA expression transcripts. All plasmids were generated in pCS2+ vectors (71). The mVenus associated plasmids were synthesised through zebrafish cDNA as generated from previous researcher (confirmed with gel electrophoresis). The mCherry associated plasmids were synthesised by ThermoFisher Scientific GeneArt Synthesis and subcloned into a pCS2+ vector.

### 3.2.1 Bioinformatic Alignments

Published gene and protein sequences were sourced from the National Center for Biotechnology Information database. Gene and protein alignment was completed through the European Molecular Biology Laboratory – European Bioinformatics Institute EMBOSS Water program, using the Smith-Waterman algorithm for pairwise alignment. The genetic alignments used the EDNAFULL matrix with a 10.0 gap penalty, and 0.5 extend penalty. The protein alignments used the EBLOSUM62 matrix, with a 10.0 gap penalty, and 0.5 extension penalty.

Translation of plasmid DNA derived protein sequences was completed through the Swiss Institute of Bioinformatic Expasy translate tool with output set to Compact.

### 3.2.2 Transformation

Plasmids were transformed into chemically competent *Escherichia coli* bacteria through heat-shock protocol, as follows; chemically competent *E. coli* were thawed on ice and incubated (on ice) for a minimum of 5 minutes in a vessel containing 2 µl of the plasmid DNA. These cells were heat-shocked at 42ºC for 30 seconds and immediately returned to ice. 250 µl of room-temperature Super Optimal Broth medium was added to the cells, which could recover

for 1 hour at 37ºC at 200 rpm. After recovery, 30- 250 µl of cells were spread over the surface of a Luria Broth agar plate containing the appropriate antibiotic using sterile glass beads. Plates were inverted and incubated at 37ºC overnight.

### 3.2.3 Miniprepreperation of plasmid DNA

Minipreperation of plasmid DNA was completed with the QIAprep Spin Miniprep Kit (cat. nos. 27104 and 27106) according to the manufacturer's instructions, utilizing the appropriate buffers and reactions.

### 3.2.4 Gel Extraction

Products separated through gel electrophoresis were purified by column with a QIAquick Gel Extraction Kit (Qiagen) following manufacturer's instructions with slight modifications. Five times the reaction volume of buffer QC was added to the PCR reaction tube and then the protocol was strictly followed. PCR products were eluted twice into 30 µl H2O.

### 3.2.5 Klenow Blunting, Phosphorylation, and Ligation

Klenow blunting of sticky-ended DNA fragments was performed with 1 µl of DNA polymerase I, large (Klenow) fragment (NEB). Approximately 5 µg of ligated vector was blunted in a 50 µl reaction suggested by the manufacturer. Reactions were incubated at 25ºC for 15 minutes for blunting and then subjected to 75ºC for 20 minutes for heat inactivation.

Phosphorylation of PCR fragments (150 ng) was performed utilising 0.5 µl of polynucleotide kinase (NEB) in a 9 µl reaction in ligation buffer (NEB). The reaction was incubated for 37ºC for 20 minutes for phosphorylation of insert and then incubated at 65ºC for 10 minutes for heat inactivation.

Ligations of DNA fragments and vectors were performed according to standard protocols. The amount of insert needed was determined according to the following formula, with an insert vector molar ration of 3:1.

$$ng\ of\ insert = \frac{ng\ of\ vector\ \times kb\ of\ insert}{kb\ of\ vector} \times insert{:}\ vector\ molar\ ratio$$

However, typically 150 ng of insert was used in a 20 µl reaction with 50-75 ng of vector. If multiple inserts required ligation, 100 ng of each insert was utilised. The ligation was performed with 1µl T4 DNA ligase (NEB) in ligation buffer (NEB) in a 20 µl reaction according to the manufacturer's instructions. Reactions were incubated overnight at 16ºC.

### 3.2.6 mRNA Transcription and Clean-Up

Plasmids were linearized through a restriction digest with Not1 restriction enzymes from NEB. mRNA was transcribed by combining 1 µg of the linearized pCS2+ plasmid vector (in 6 µl of water), 10 µl of 2x NTP/CAP, 2 µl 10x reaction buffer, and 2 µl of the transcriptase mix. This transcription reaction was set up in duplicate and left to incubate at 37ºC for 4 hours (or in the PCR machine overnight with program set to 37ºC for 240 minutes and then hold at 16ºC).

Transcribed mRNA was purified using the MEGAclear Kit Purification for Large Scale Transcription Reactions (catalogue number: AM1908). The contents of the 2x 20 µl mRNA transcription reactions were combined with 60 µl of elution solution added (mix by pipetting up and down). 350 µl of binding buffer was added (mix by pipetting up and down), then 250 µl of 100% ethanol was added (mix by pipetting up and down). This mixture was transferred to a filter tube and centrifuged at 12 000 rpm for 30 seconds at 4ºC. Flow through was discarded. 500 µl of wash buffer was added (after the 100% ethanol had been added to the wash buffer). The filter tube was again centrifuged at 12 000 rpm for 30 seconds at 4ºC. Again 500 µl of wash buffer was added. The filter tube was again centrifuged at 12 000 rpm for 30 seconds at 4ºC. Flow through was discarded. The filter tube was centrifuged at 12 000 rpm for 30 seconds at 4ºC to dry the filter membrane. This filter was transferred to a new tube with 30 µl of Milli-Q water to elute the mRNA in. The tube was incubated for 10 minutes on

a heat block set to 60ºC. The tube was centrifuged at 12 000 rpm for 1 minute. The supernatant was then quantified on the ThermoFisher NanoDrop spectrophotometer (ND-1000) and then stored at -80ºC.

## 3.3 Microinjection

Microinjection of wild-type (AB/TU) zebrafish embryos was completed at the single cell stage (15-30 minutes post fertilisation) to ensure even distribution of expression transcripts amongst cells.

### 3.3.1 Injection Plate

Injection plates were made as a 30 ml solution of molten 1.5% agarose made with Milli-Q water. An initial pour of half the molten solution into a 150 mm petri dish was left semi covered cool to a semi-solid state. The remaining molten solution was poured on top of the previous, now semi-solid agarose with a plastic mould lowered into it. Once all the agarose solution was solid, the plastic mould was removed. This injection plate was then covered and wrapped with Parafilm for storage at 4°C for 3 months at which point, the injection plate would be replaced with a new one to avoid contamination.

### 3.3.2 Microinjection Needles

Prior to injection a Model P-2000 Sutter Instrument Co. Laser-Based micropipette puller was allowed to heat up for 15 minutes with the following settings (values referring to undefined units specific to the Model P-2000): heat (HEAT) = 700, filament laser scanning (FIL) = 4, velocity of glass carriage system (VEL) = 60, pull force (PULL) = 175, and delay of pull function after heating (DEL) = 145.

After sufficient time, a single, sterile Harvard Apparatus borosilicate glass capillary (GC100FS-10) was placed in the micropipette puller. Two microinjection needles would be

created from a single glass capillary, excess needles were stored in a 150 mm petri dish secured with a strip of Blu Tack adhesive putty.

### 3.3.3 Injection of Expression Transcripts

Microinjection needles were carefully loaded with 2-3 µl of mRNA expression transcripts between concentration ranges of 50 – 175 ng/µl using an Eppendorf GELoader pipette tip and P20 pipette in such a way to avoid air bubbles. This needle was then placed into the micropipette holder where the tip of the micropipette was broken with a standard microscope slide. Once the tip is broken, a drop of mineral oil would be placed on a micrometer and the micropipette injected into the oil. This process would give the diameter (*d*) of the bolus (injected material volume as a sphere). Volume of bolus (*V*) was calculated as follows:

$$V = \frac{4}{3}\pi\left(\frac{d}{2}\right)^3$$

Gas pressure from the microinjector was altered to influence bolus size (higher pressure resulted in a larger bolus, lower pressure resulted in a smaller bolus). A bolus size of 10 µm was used to deliver an injection load of 0.5 pl for the injection of mRNA constructs.

Once the bolus was measured, embryos were collected at the single cell stage and aligned along the grooves of the injection plate. Once arranged with the single cell facing upward, the microinjection could take place with the expression constructs injected toward the animal pole of the developing embryo, within the chorion. After injection, the embryos were placed in a 150 mm petri dish containing 30 ml of E3 solution, stored in a 28.5°C incubator.

## 3.4 Inducing Cellular Stress and Dechorination

Cellular stress in the zebrafish models was achieved through the activation of heat shock proteins as per SOP 010 - Inducing cellular stress in zebrafish embryos/larvae. Cellular stress was achieved by removing 24-30 hpf zebrafish embryos from the 28.5°C incubator and

dechorinating them immediately with two Dumont #5 forceps. Dechorionated embryos to be heat shocked were placed in a 1.5 ml Eppendorf tube with 1.5 ml of E3 Embryo Medium, and then placed in a heat block set to 37°C for 1 hour. After 1 hour at 37°C, the embryos were returned to the 28.5°C incubator.

Dechorination of embryos was occasionally completed manually at 24-30 hpf within a 150 mm petri dish containing the embryos in 30 ml of E3 as per the AEC SOP – Dechorination of zebrafish embryos. This involved the use of two Dumont #5 watch maker forceps to pull the chorion from either side of the developing embryo in opposite directions. This resulted in the embryo falling out of the chorion.

## 3.5 Microscopy

For this thesis, microscopy including bright-field and fluorescent microscopy with a Leica M165 Fluorescence Microscope with attached Leica DFC550 camera and Leica Application Suite X (3.7.4.23463) software, and confocal microscopy with Leica SP5 with attached Leica DFC365FX camera and Leica Application Suite X (3.7.4.23463) software.

### 3.5.1 Screening and Brightfield Microscopy

Initial screening of fluorescence took place on fluorescent microscopes with relevant fluorescent filters with a Leica M165 Fluorescence Microscope with attached Leica DFC550 camera and Leica Application Suite X (3.7.4.23463) software. Fluorescence was determined through binary judgement.

### 3.5.2 Confocal Microscopy

Tissue-specific imaging at higher resolutions was performed on the Leica SP5 confocal microscope with attached Leica DFC350 camera and Leica Application Suit AF (3.0) software.

Zebrafish embryos were sedated for 5 minutes with Tricaine mesylate. Then the embryos were suspended in a low melting agarose cooled to 45°C within a 35 mm clear glass-bottom petri dish with a 10 mm microwell which was allowed to cool then covered in E3 for the duration of the imaging.

## 3.6 Image Processing, Quantification, and Statistical Analysis

A variety of methods and programs were utilized in processing microscopy images in this project for both presentation and quantification.

### 3.6.1 ImageJ (Fiji)

ImageJ version 1.53 with Fiji image processing packages was used to edit, process, and quantify images. Stacks were combined with ZProjection (Sum Slices) before being quantified.

Manual counts of puncta were aided by the Multi-point tool. Automated puncta counts were completed by splitting channels of confocal microscopy images, stacked through ZProjection (Sum Slices), and then changed image type to 8-bit. The images threshold was then adjusted to the triangle setting and calibrated to determine the brightest puncta. Once this was complete, noise was despeckled and resulting image was quantified through the Analyse Particle feature using size of 10-10000 pixel units and circularity of 0-1.

### 3.6.2 Zerine Stacker

Brightfield microscopy images taken at different focal lengths were aligned and stacked in Zerine Stacker Version 1.04 Build T2020-05-22-1330 using the PMax to preserve detail. These images were imported to Fiji (Image J) for analysis and editing.

### 3.6.3 GraphPad Prism 8

Statistical analysis was completed in GraphPad Prism 8 version 8.0.2 (263). Values in figures show mean (bar graphs) and individual data points, and error bars in all figures represent standard deviation (SD), ****$p < 0.0001$, ***$p < 0.001$, **$p < 0.01$, *$p < 0.05$.

### 3.6.4 Stress granule definition

In this thesis, stress granules were defined by a set of inclusion criteria. For puncta to be counted as a part of the stress granule count, they must be fluorescent aggregations between 0.1 µm and 4 µm in diameter, localised in the cytoplasm of cells.

### 3.6.5 Morphology assay

Morphology assay was conducted by injecting mRNA expression transcripts into fish and then quantified based off criteria adapted from Panzica-Kelly, et al., 2010 (72).

# 4 Results

To ensure the generation of mRNA transcripts that would induce transient expression of stress granules linked to fluorophores, plasmids used included appropriate digestion and transcription sites. After mRNA injection, the zebrafish embryos were initially screened at 24 hours post fertilization to ensure fluorescence. An embryo morphological and length experiment was used to determine whether the mRNA transcripts were impacting the development of the zebrafish embryos physiology. Injected fish displaying fluorescence were separated into treatment groups, a control kept at 27°C and a heatshock group at 37°C to induce cellular stress. These embryos were imaged at muscle five somite caudal to the yolk sac/yolk tube boundary and the spinal cord dorsal to the yolk sac/yolk tube boundary. These images were quantified through both automatic software-based approaches and manual counting to determine the protein accumulations that occurred under cellular stress.

## 4.1 Generation of Genetic Material

The G3bp1 and Tia1 proteins were identified as components which forms as a part of the stress granule complex. As such, both proteins were targets for observation in a zebrafish model. Zebrafish have their own *g3bp1* and *tia1* orthologs – for this reason it was important to conduct a sequence alignment of the genes if the model of stress granule formation outlined in this thesis can be comparable to human stress granules.

Complementary DNA (cDNA) gene sequences for human *G3BP1* (BC108278.1), human *TIA1* (BC015944.1), zebrafish *g3bp1* (BC045874.1), and zebrafish *tia1* (BC066734.1) were sourced from the National Center for Biotechnology Information (NCBI) database. Protein sequences were translated through Swiss Institute of Bioinformatics (SIB), Expasy tool.

From gene sequence alignment, there was a 55.7% similarity and identity between the human *G3BP1* and zebrafish *g3bp1* genes with a gap percentage of 27.3% (Figure 2.1). Due

to low genetic similarity, a subsequent protein alignment was conducted (Figure 2.2). These protein alignments showed a much higher degree of similarity with 78.7% similarity, 69.0% identity, and 2.7% gap between human G3BP1 and zebrafish G3bp1. This alignment can be found in Appendix 7.1 and 7.2.

The gene alignment between *TIA1/tia1* genes showed a lower similarity between human and zebrafish than what was seen in the *G3BP1/g3bp1* alignments. There was a 52.1% identity and similarity between human *TIA1* and zebrafish *tia1* with 34.8% gaps (Figure 2.2). Protein alignments between both human TIA1 and zebrafish Tia1 showed 79.4% identity, 90.7% similarity, and 5.7% gap (Figure 2.2). These alignments can be found in Appendix 7.3 and 7.4.

Plasmid maps were created for the pCS2+ plasmids being used in the generation of mRNA transcripts. Featured are the necessary promoter sites, cleavage sites, and flexible GGGS linker fusion protein which when transcribed fuses the stress granule associated proteins to the fluorophore.

Once the mRNA transcripts were derived from the plasmid assemblies, the mRNA was confirmed through gel electrophoresis. These mRNA injection transcripts were compared to DNA ladders to confirm the size and therefore construction. The spread of the mRNA transcript on an electrophoresis gel was used as a simplified mechanism to determine degradation with a higher degree of spread indicating a higher degree of mRNA degradation. Figure 3.7 shows mRNA bands on an electrophoresis gel suitable for injection into zebrafish embryos.

| Gene (cDNA) | Identity (%) | Similarity (%) | Gaps (%) |
|---|---|---|---|
| Human *G3BP1* compared to Zebrafish *g3bp1* | 55.7 | 55.7 | 27.3 |
| Human *TIA1* compared to Zebrafish *tia1* | 52.1 | 52.1 | 34.8 |

**Figure 2.1.** Gene alignment showing percentage identity, similarity, and gaps between published human *G3BP1* (BC108278.1), human *TIA1* (BC015944.1), zebrafish *g3bp1* (BC045874.1), and zebrafish *tia1* (BC066734.1) as used in the PCS2+ plasmid. Alignments were done through water program set to Pairwise alignment, EDNAFULL matrix, with a 10.0 gap penalty, and 0.5 extend penalty.

| Translated Protein | Identity (%) | Similarity (%) | Gaps (%) |
|---|---|---|---|
| Human G3BP1 compared to Zebrafish G3bp1 | 69.0 | 78.7 | 2.7 |
| Human TIA1 compared to Zebrafish Tia1 | 79.4 | 90.7 | 5.7 |

**Figure 2.2.** Protein alignment between translated human *G3BP1* (BC108278.1), human *TIA1* (BC015944.1), zebrafish *g3bp1* (BC045874.1), and zebrafish *tia1* (BC066734.1) genes. Translation was completed through the Swiss Institute of Bioinformatics, Expasy tool. Alignments were done through water program set to Pairwise alignment, EBLOSUM62 matrix, with a 10.0 gap penalty, and 0.5 extend penalty.

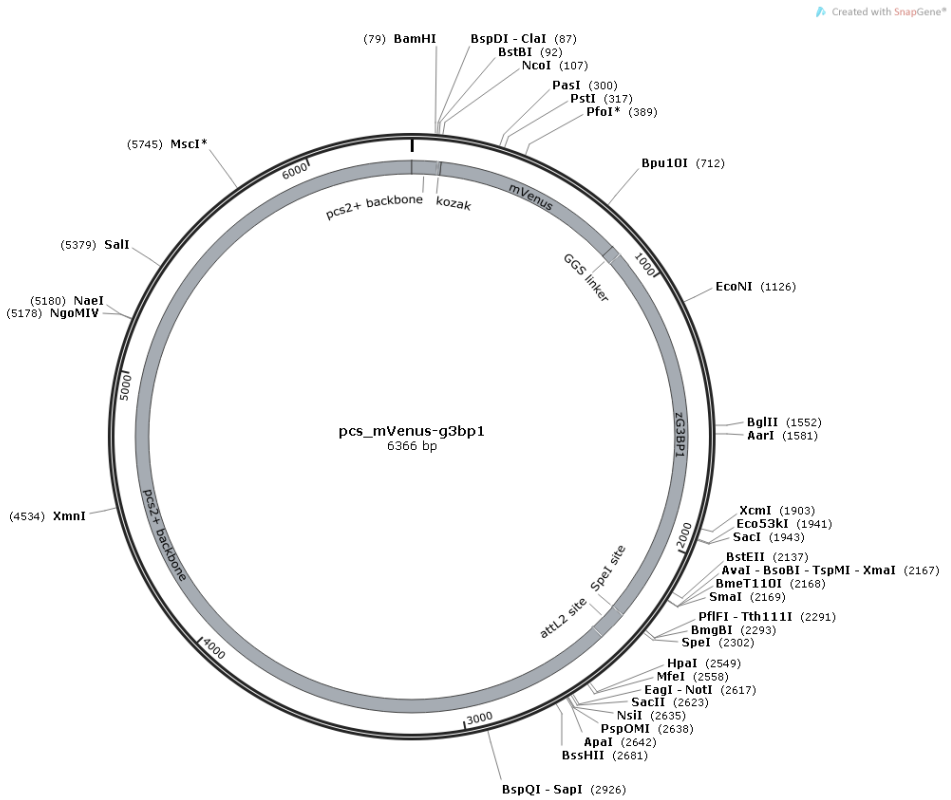


**Figure 3.1.** Plasmid map used for the generation of mVenus-G3bp1 mRNA.

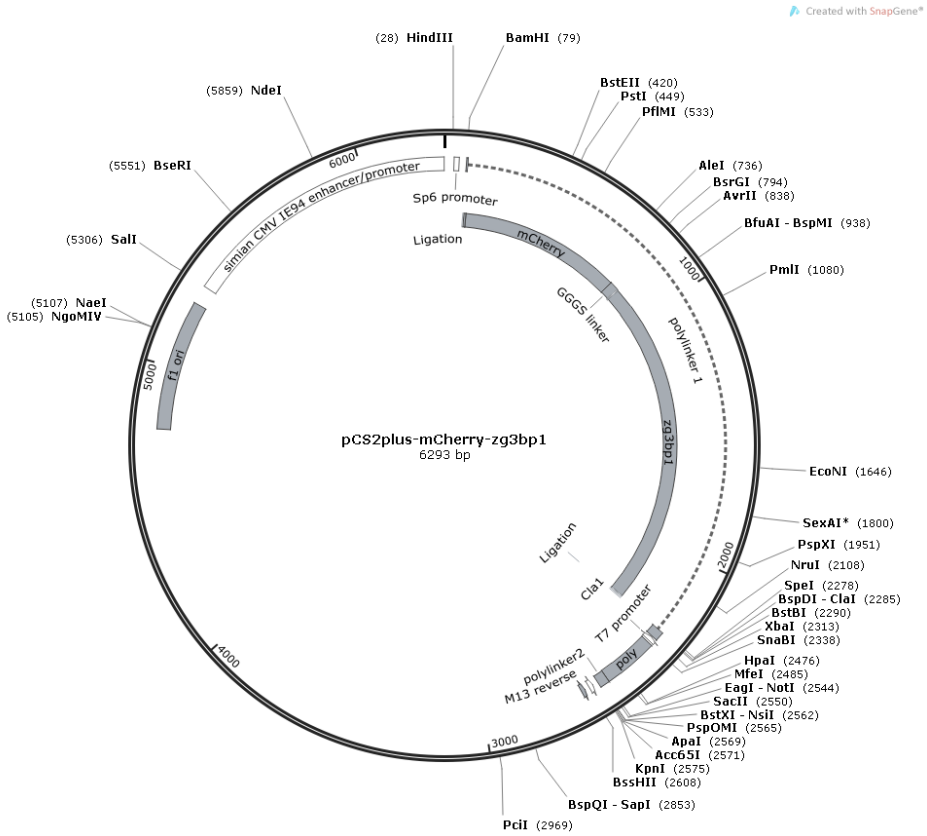


**Figure 3.2.** Plasmid map used for the generation of mCherry-G3bp1 mRNA.

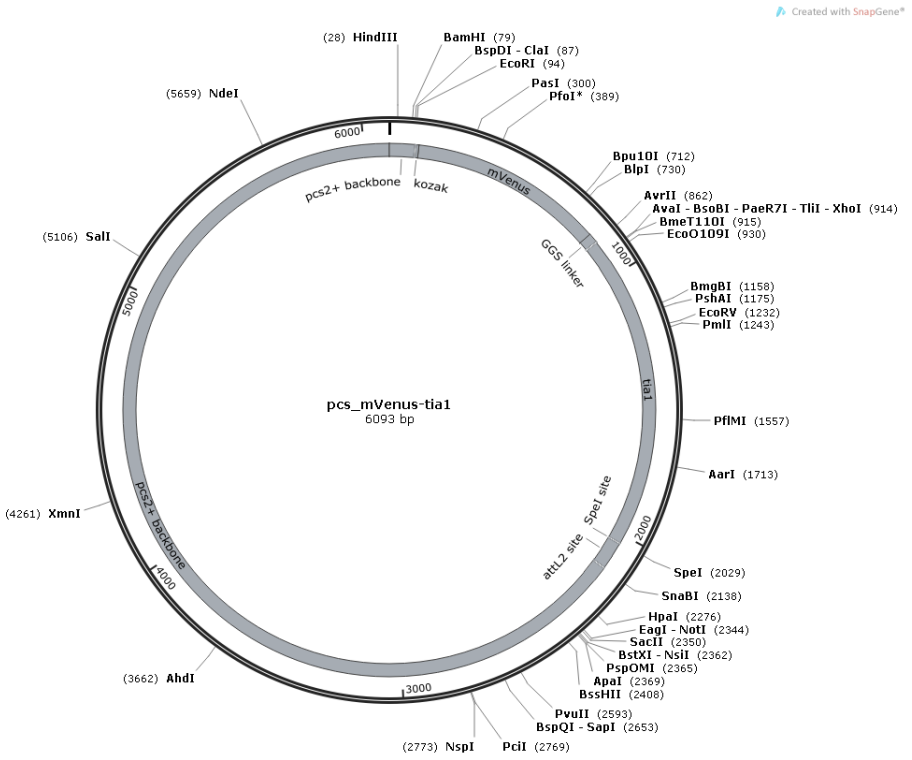


**Figure 3.3.** Plasmid map used for the generation of mVenus-G3bp1 mRNA.

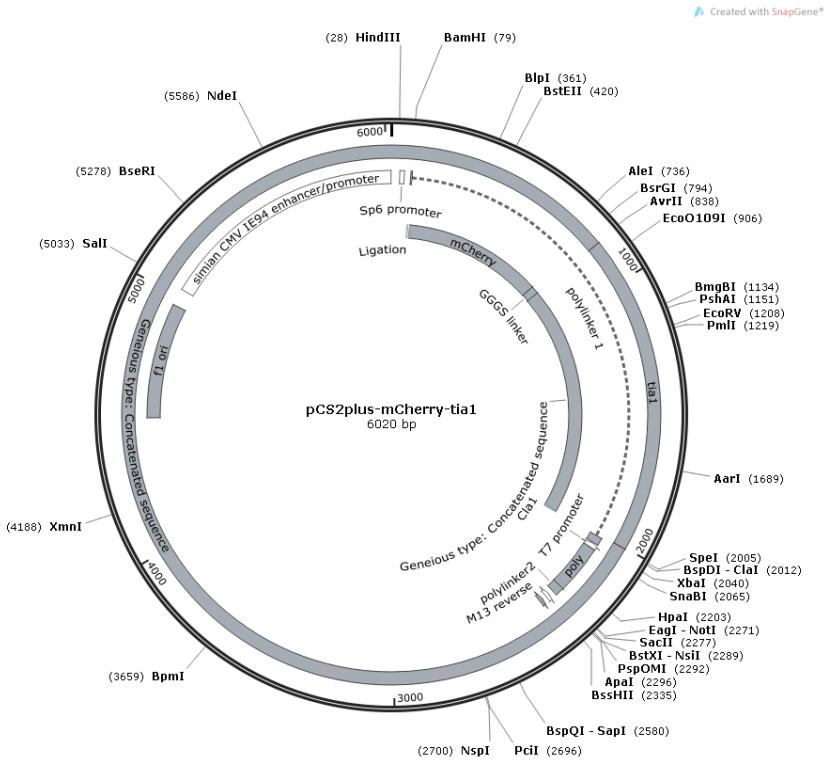


**Figure 3.4.** Plasmid map used for the generation of mCherry-Tia1 mRNA.

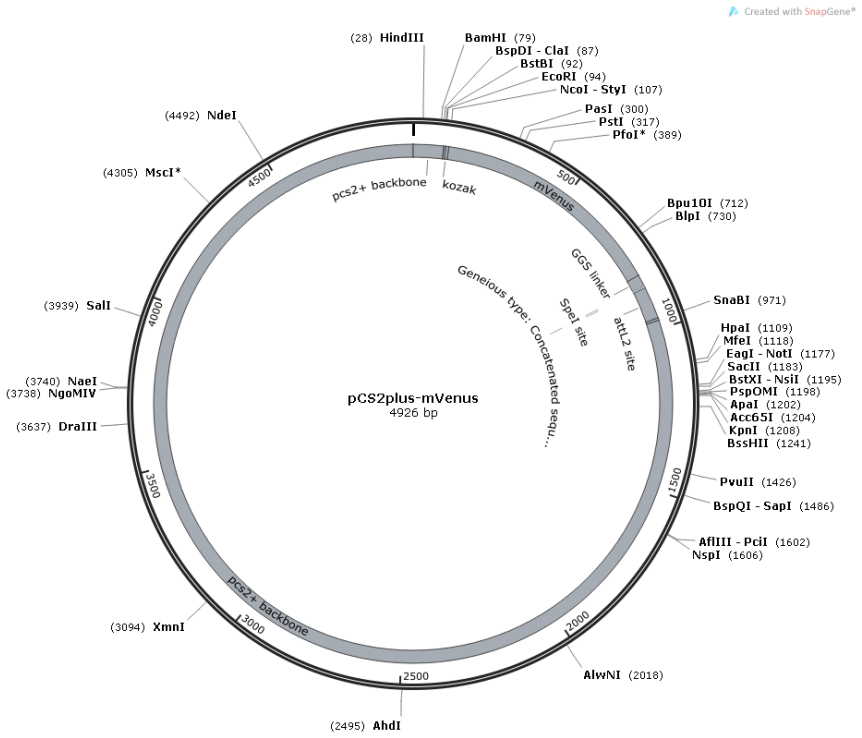


**Figure 3.5.** Plasmid map used for the generation of mVenus mRNA.

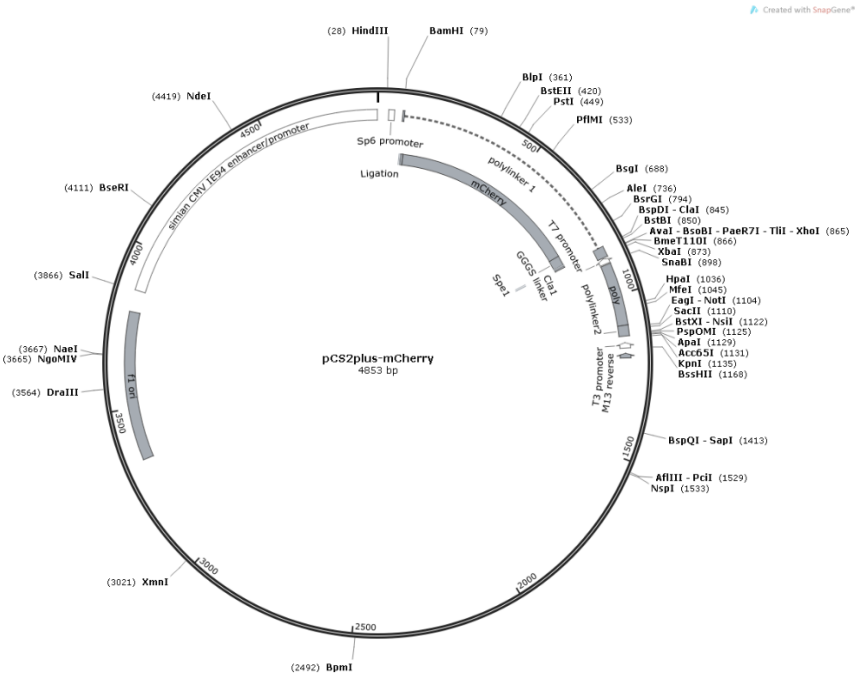


**Figure 3.6.** Plasmid map used for the generation of mCherry mRNA.

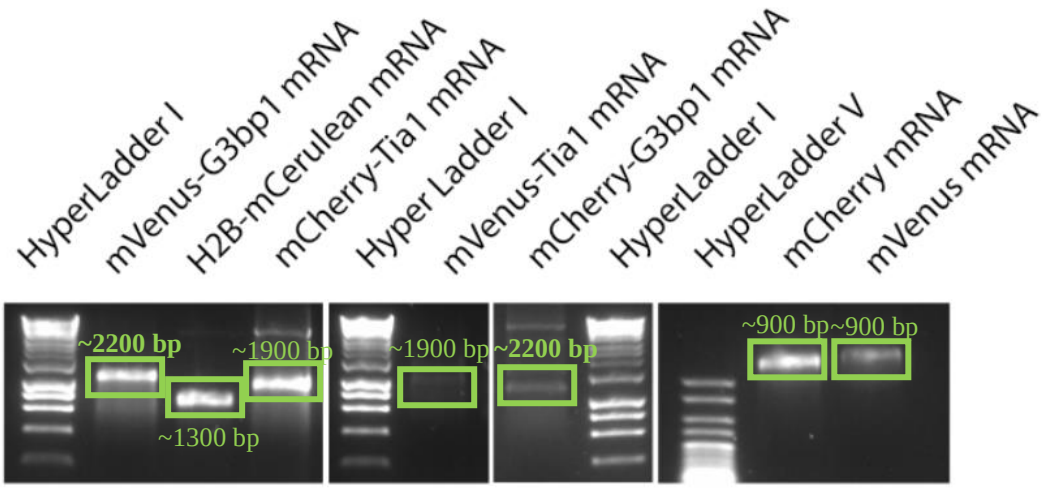


**Figure 3.7.** Gel electrophoresis of all mRNA constructs created for this thesis, derived from plasmid transcription confirming the generation of mRNA constructs. Expected band sized highlighted in green.

## 4.2 Transient Overexpression of mRNA Constructs

The mRNA transcripts used for this thesis are represented by the simplified models (Figure 4.1). The protien of interest (G3bp1/Tia1) is fused to the flurophore of choice (mVenus/mCherry) by a flexible GGGS linker. The "GGGS linker" referest to the structurally flexible, amino acid chain of glycine-glycine-glycine-serine. In the mRNA transcripts used in this thesis, the GGGS linkers were repeated three times (e.g. mVenus-GGGS-GGGS-GGGS-G3bp1).

The mRNA transcripts were initially injected into zebrafish embryos to ensure they translated into fluorescent proteins (Figure 4.2). Prior to confocal microscopy, the embryos were initially screened on the fluorescence microscope. While the fluorescent microscope could determine fluorescence, the maximum magnification (160x) of the Leica M165 Fluorescence Microscope was not high enough resulution for imaging subcellular stress granules.

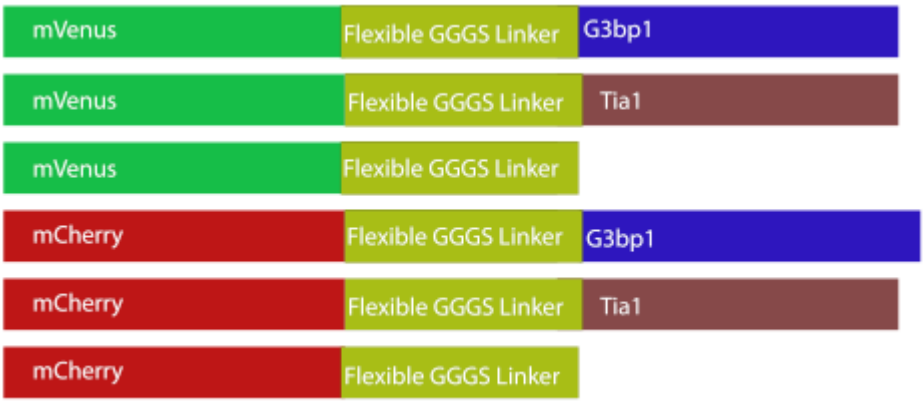


**Figure 4.1.** Diagram of the mRNA transcripts used for transient overexpression models.

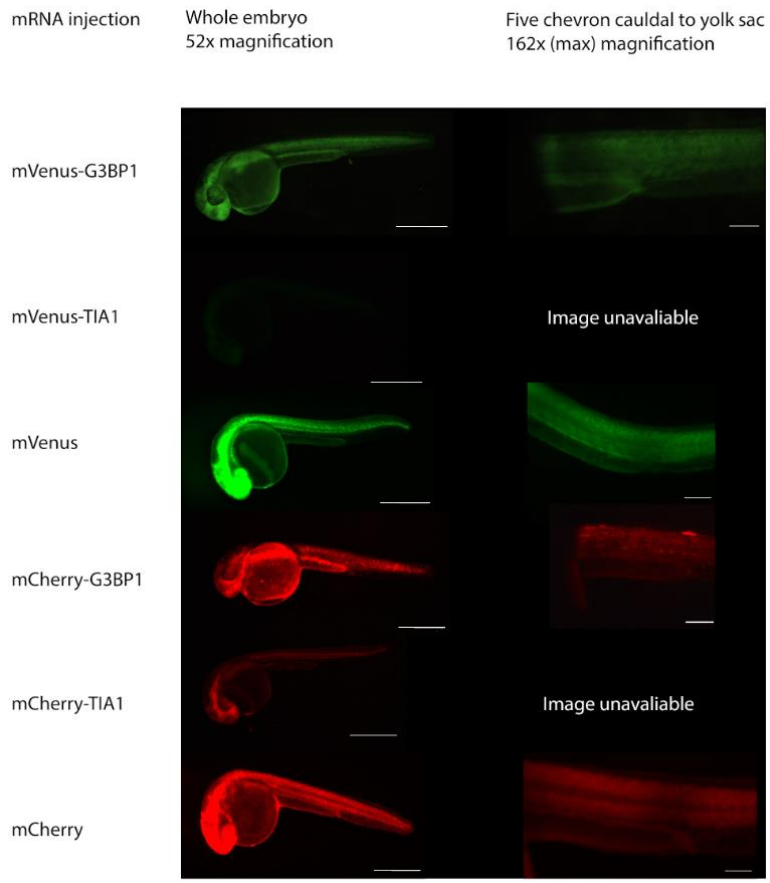


**Figure 4.2.** 24 hour post fertilisation embryos displaying expression of mRNA constructs injected at ~30 minutes post fertilisation. Scale bar is for images at 52x magnification is 500 μm, scale bar for images at 160x magnification is at 100 μm.

## 4.3 mRNA Dosage and Lifespan

Both the survival post-mRNA injection and the percentage of injected embryos displaying fluorescence was measured. Survival rates for control embryos is between 70-85% and the survival figure drops as low as <20% (embryos post mVenus-G3bp1 mRNA injection) at the 50 ng/ul concentration (Figure 5.1). Across all mRNA injections, the highest survival rates appear to be between 100 – 125 ng/ul (Figure 5.1). For an *in vivo* investigation, it is essential the embryos imaged are alive and fluorescent. As with survival, the highest consistent measures of embryo fluorescence appear to be between 100 – 125 ng/ul (Figure 5.1).

The mRNA transcripts were initially injected into embryos and screened at 24 hours post fertilization to confirm they fluoresce as seen in Figure 5.2. As different mRNA transcripts showed varying degrees of fluorescence, a timepoint experiment was conducted to determine the optimal time to screen fluorescent expression as well as determine how long zebrafish larvae fluoresce before the mRNA transcripts degrade in cells. From these experiments it was determined that 24 hours post fertilisation was the optimal time to screen a zebrafish embryo with a fluorescent mRNA transcript.

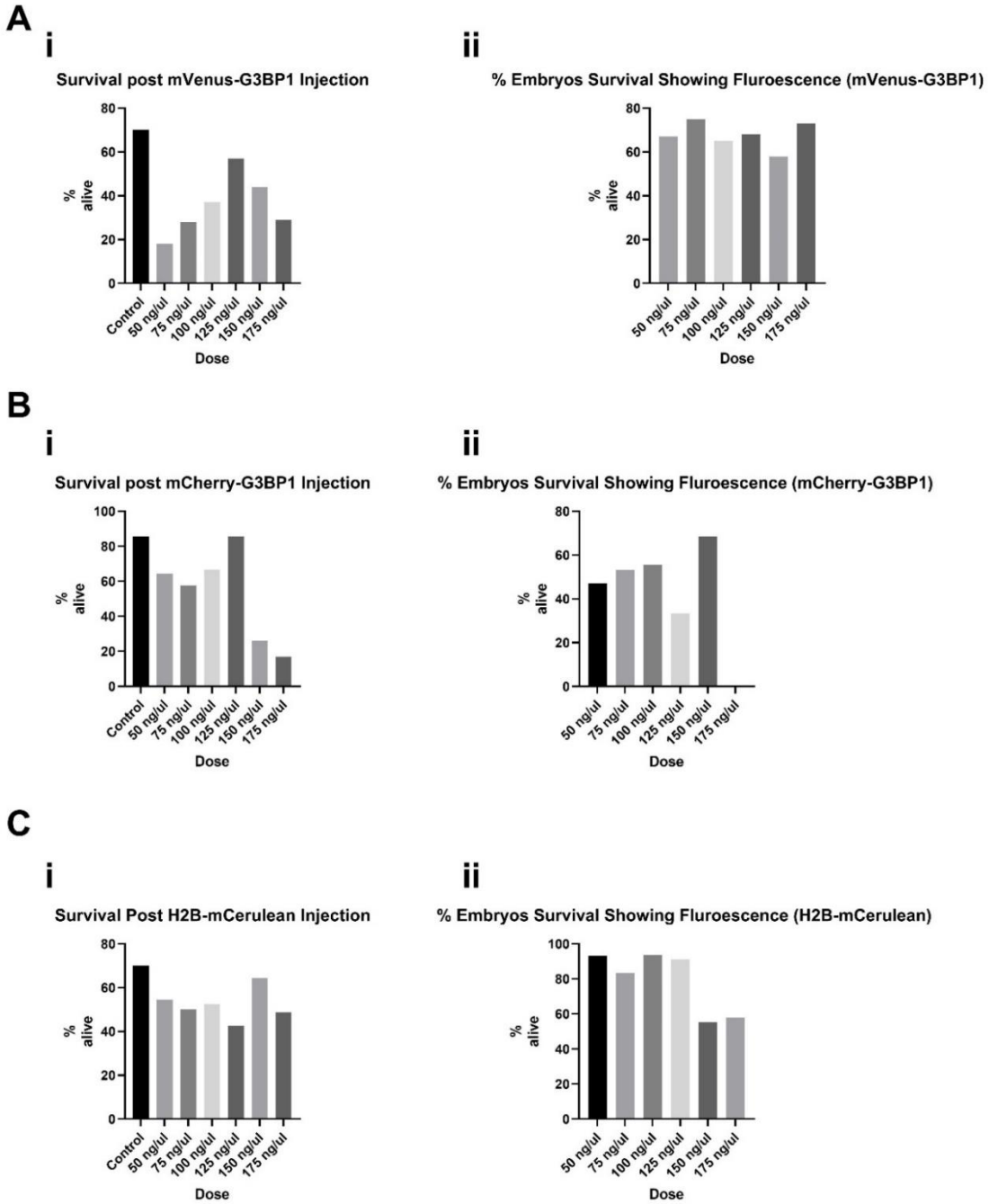


**Figure 5.1.** Timepoint fluorescence assay as measured through fluorescence microscopy. **A) i**. Graph showing survivability at 24 hours post injection of the mVenus-G3bp1 mRNA construct (n=1 experimental replicate, n= 283 biological replicates). **ii.** Graph showing the percentage of embryos which survived injection and displayed fluorescence compared to embryos which were alive and not displaying fluorescence (n=1 experimental replicate, n=406 biological replicates). **B) i.** Graph showing survivability at 24 hours post injection of the mCherry-G3bp1 mRNA construct (n=1 experimental replicate, n= 418 biological replicates). **ii.** Graph showing the percentage of embryos which survived injection and displayed fluorescence compared to

embryos which were alive and not displaying fluorescence (n=1 experimental replicate, n=178 biological replicates).**C) i.** Graph showing survivability at 24 hours post injection of the H2B-mCerulean mRNA transcript (n=1 experimental replicate, n=354 biological replicates). **ii.** Graph showing the percentage of embryos which survived injection and displayed fluorescence compared to embryos which were alive and not displaying fluorescence (n=1 experimental replicate, n=176 biological replicates).

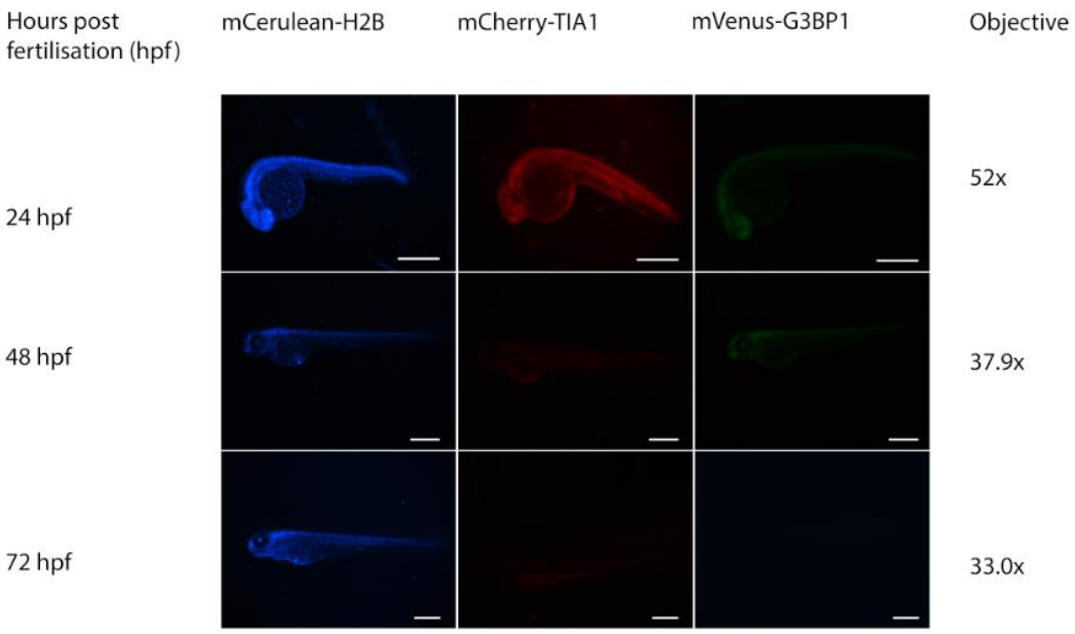


**Figure 5.2.** Fluorescence timepoint experiments (n=1 experimental replicate, n=9 biological replicates). Scale bar at 500 µm.

## 4.4 Morphology Experiments

A wild-type (WT) phenotype is preferred for morphology imaging as embryos which display these characteristics have readily identifiable structures, ideal for comparison between biological replicates. In the morphology experiments, we see that Cherry associated constructs have higher percentages of morphologies which deviate from the WT phenotype. mVenus associated constructs show higher percentages of WT embryos. As the goal of this thesis was to determine stress granules within an *in vivo* model, it was determined that embryos would require morphology comparable to wild type, control samples to aid in identifying structures in imaging. To do this, four categories of morphology were created: wild-type (WT), Category I (CAT I), Category II (CAT II), and Category III (CAT III). While WT embryos were preferred, CAT I embryos were acceptable. Embryo length was also measured. From this experiment we can see that the mCherry transcripts resulted in the most varied embryo length with the least amount of WT resulting embryos however a low number of biological replicates hinders this experiment with the embryos injected with mCherry mRNA as there was only three viable embryos for measurement. WT embryos were optimal for imaging experiments as the organs of the embryo are clear easily comparable to other biological replicates. Once extreme phenotypic deviations present themselves in the embryos (e.g., CAT I-III), comparisons are more difficult to make between embryos.

Embryo length was measured from the tip of the tail to the base of the hind brain. There is little variation between the mRNA injections except for the mCherry mRNA injection which shows the highest variability.

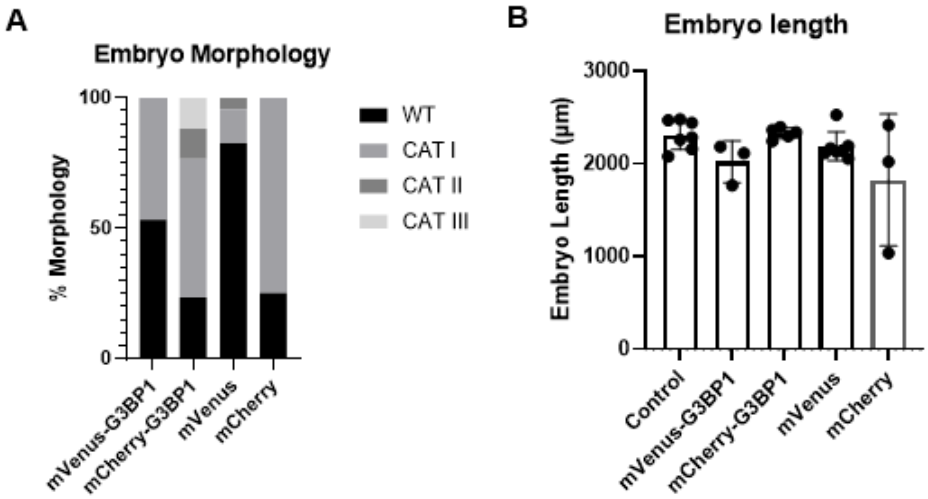


**C**

| Category | Phenotype | Example image |
|---|---|---|
| Wild-type | No discernible defects when compared to control fish. |   |
| CAT I | Slight variation in morphology resulting in 1 abnormality or developmental delay e.g., 1 spinal defect resulting in a bend when compared to control fish. | 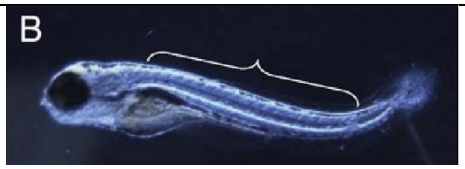  |
| CAT II | Moderate malformations with 2 or more abnormalities e.g., a spinal defect resulting in a bend and a shortened tail when compared to control fish. | 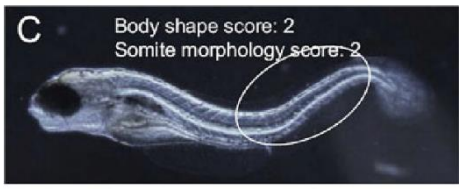  |

| | | |
|---|---|---|
| CAT III | Structure has severe morphological abnormalities e.g., delayed development resulting in multiple abnormalities. | 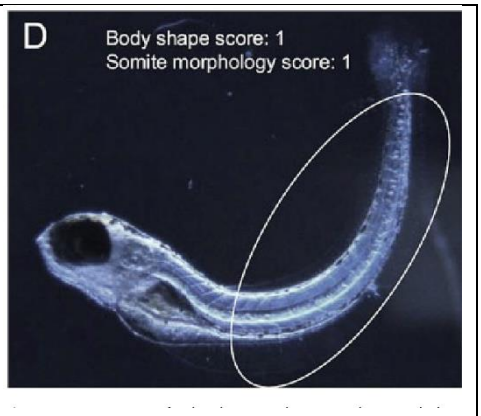  |

**Figure 6.** Morphology assay conducted to determine effect of expression transcripts on the developing physiology of zebrafish embryos. **A)** Categorizing the zebrafish embryos 24 hours post injection of mRNA constructs to determine effect on morphology (n= 1 experimental replicate, n=343 biological replicates). **B)** Embryo length 24 hours post injection of mRNA construct to determine effect on length. Individual data points represent each embryo measured. (n= 2 experimental replicates, n=25 biological replicates). **C)** Morphological quantification table and example images adapted based off criteria adapted from Panzica-Kelly, et al., 2010 (72).

## 4.5 Stress Response and Puncta Count

The mRNA used for imaging the stress response were coinjections of; 100ng/µl of mCherry-G3bp1 and 100ng/µl of H2B-mCerulean, 100ng/µl of mCherry and 100ng/µl of H2B-mCerulean, 100ng/µl of mVenus-G3bp1 and 100ng/µl of H2B-mCerulean, and 100ng/µl of mVenus and 100ng/µl of H2B-mCerulean mRNA as these concentrations provided a measurable effect on the embryos whilst keeping intervention to a minimum. The areas of the fish imaged were observed in the muscle fiber five somite caudal to the yolk sac/yolk tube boundary and the spinal cord dorsal to the yolk sac/yolk tube boundary (Figure 7.1). When counting stress granules, a set of inclusion criteria was developed. This inclusion criteria was used to determine whether the puncta seen in the confocal microscopy images was likely to be a stress granule due to its localization in the cytoplasm, fluorescence (showing G3bp1 protein inclusion), and diameter being between 0.1 µm and 4 µm. Automated counting was attempted in order to establish a standard and high throughput methodology in puncta counting and these were complimented with higher accuracy manual counts. Lower quality images where zebrafish physiology was not comprehensible were disqualified from the puncta counts.

A manual count of puncta forming in the mVenus-G3bp1 mRNA injected embryo's muscle images showed a mean number of 60.43 puncta forming in the cells of heatshock images, and a mean number of 4.714 puncta forming in the cells of control images. The highest puncta count was seen in a heatshocked image of 102 puncta (Figure 7.3 A). The heatshock and control images had a P value of 0.0003 (Figure 7.3 A).

An automated count of puncta forming in the mVenus-G3bp1 mRNA injected embryo's muscle images showed a mean number of 179.9 puncta forming in the cells of heatshock images, and a mean number of 46.29 puncta forming in the cells of control images

(Figure 7.3 B). The highest puncta count was seen in a heatshocked image of 383 puncta (Figure 7.3 B). The heatshock and control images had a P value of 0.0092 (Figure 7.3 B).

A manual count of puncta forming in the mVenus mRNA injected embryo's muscle images showed a mean number of 0.3333 puncta forming in the cells of heatshock images, and a mean number of 0.1429 puncta forming in the cells of control images (Figure 7.3 C). The highest puncta count was seen in a heatshocked image of 2 puncta (Figure 7.3 C). The heatshock and control images had a P value of 0.5902 (Figure 7.3 C).

A manual count of puncta forming in the mCherry-G3bp1 mRNA injected embryo's muscle images showed a mean number of 35.60 puncta forming in the cells of heatshock images, and a mean number of 15.80 puncta forming in the cells of control images (Figure 7.5 A). The highest puncta count was seen in a heatshocked image of 71 puncta (Figure 7.5 A). The heatshock and control images had a P value of 0.0974 (Figure 7.5 A).

An automated count of puncta forming in the mCherry-G3bp1 mRNA injected embryo's muscle images showed a mean number of 270.2 puncta forming in the cells of heatshock images, and a mean number of 45.80 puncta forming in the cells of control images (Figure 7.5 B). The highest puncta count was seen in a heatshocked image of 349 puncta (Figure 7.5 B). The heatshock and control images had a P value of 0.0974 (Figure 7.5 B).

A manual count of puncta forming in the mCherry mRNA injected embryo's muscle images showed a mean number of 77.67 puncta forming in the cells of heatshock images, and a mean number of 112.3 puncta forming in the cells of control images (Figure 7.5 C). The highest puncta count was seen in a heatshocked image of 189 puncta (Figure 7.5 C). The heatshock and control images had a P value of 0.4550 (Figure 7.5 C).

A manual count of puncta forming in the mVenus-G3bp1 mRNA injected embryo's spinal cord images showed a mean number of 3.500 puncta forming in the cells of heatshock images, and a mean number of 0.000 puncta forming in the cells of control images (Figure

7.7 A). The highest puncta count was seen in a heatshocked image of 6 puncta. The heatshock and control images had a P value of 0.2965 (Figure 7.7 A).

An automated count of puncta forming in the mVenus-G3bp1 mRNA injected embryo's spinal cord images showed a mean number of 10.50 puncta forming in the cells of heatshock images, and a mean number of 7.000 puncta forming in the cells of control images (Figure 7.7 B). The highest puncta count was seen in a heatshocked image of 11 puncta (Figure 7.7 B). The heatshock and control images had a P value of 0.2317 (Figure 7.7 B).

A manual count of puncta forming in the mVenus mRNA injected embryo's spinal cord images showed a no puncta forming and as such no calculatable P value (Figure 7.7 C).

A manual count of puncta forming in the mCherry-G3bp1 mRNA injected embryo's spinal cord images showed a mean number of 14.50 puncta forming in the cells of heatshock images, and a mean number of 12.33 puncta forming in the cells of control images (Figure 7.9 A). The highest puncta count was seen in a heatshocked image of 25 puncta. The heatshock and control images had a P value of 0.8274 (Figure 7.9 A).

An automated count of puncta forming in the mCherry-G3bp1 mRNA injected embryo's spinal cord images showed a mean number of 23.50 puncta forming in the cells of heatshock images, and a mean number of 20.00 puncta forming in the cells of control images (Figure 7.9 B). The highest puncta count was seen in a heatshocked image of 39 puncta (Figure 7.9 B). The heatshock and control images had a P value of 0.8371 (Figure 7.9 B).

A manual count of puncta forming in the mCherry mRNA injected embryo's spinal cord images showed a mean number of 58.67 puncta forming in the cells of heatshock images, and a mean number of 29.80 puncta forming in the cells of control images (Figure 7.9 C). The highest puncta count was seen in a heatshocked image of 103 puncta (Figure 7.9 C). The heatshock and control images had a P value of 0.1567 (Figure 7.9 C).

These results are presented in a summary table in Figure 7.10.

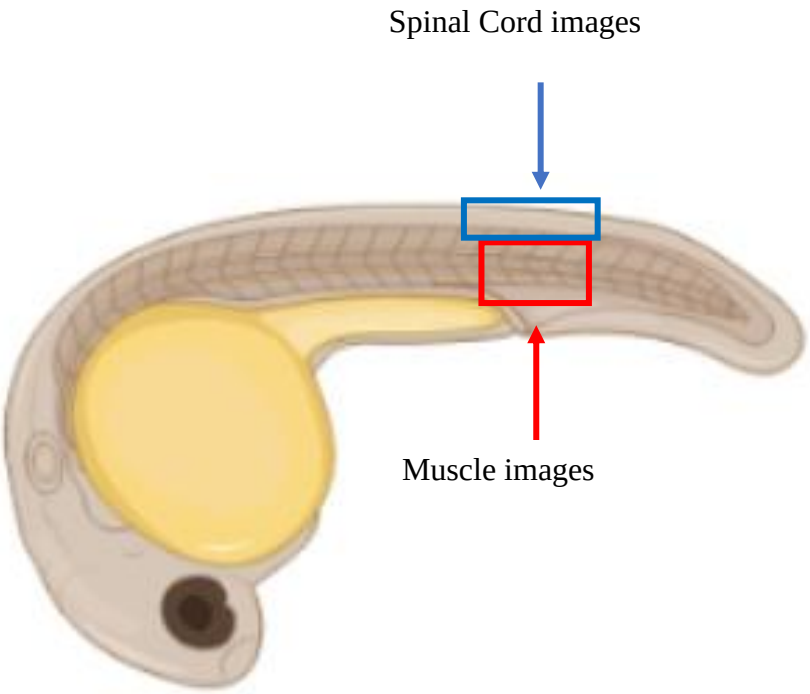


**Figure 7.1.** Imaging map of areas of interest for this thesis. Confocal muscle images were taken 5 somites caudal to the yolk sac and spinal cord images were taken in the area dorsal to 5 somite caudal to the yolk sac.

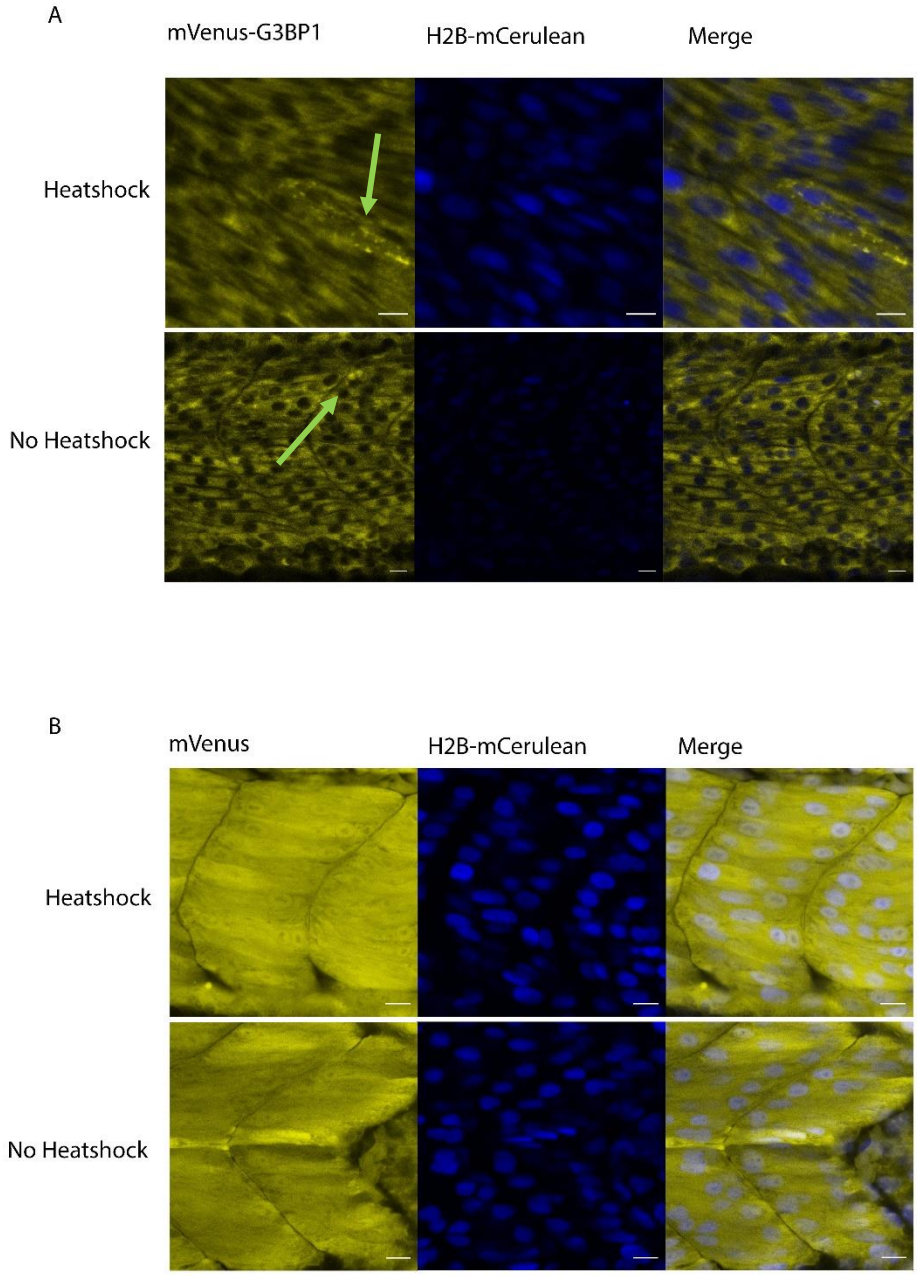


**Figure 7.2.** Representative images of heatshock and control mVenus-G3bp1/mVenus and H2B-mCerulean mRNA injected embryos muscle images (puncta of interest highlighted in green). Scale bars at 10 μm. **A)** Heatshock and control mVenus-G3bp1 and H2B-mCerulean mRNA coinjected embryos muscle images (n=2 experimental replicates, n=14 biological replicates). **B)** Heatshock and control mVenus and H2B-mCerulean mRNA injected embryos muscle images (n=2 experimental replicates, n=13 biological replicates).

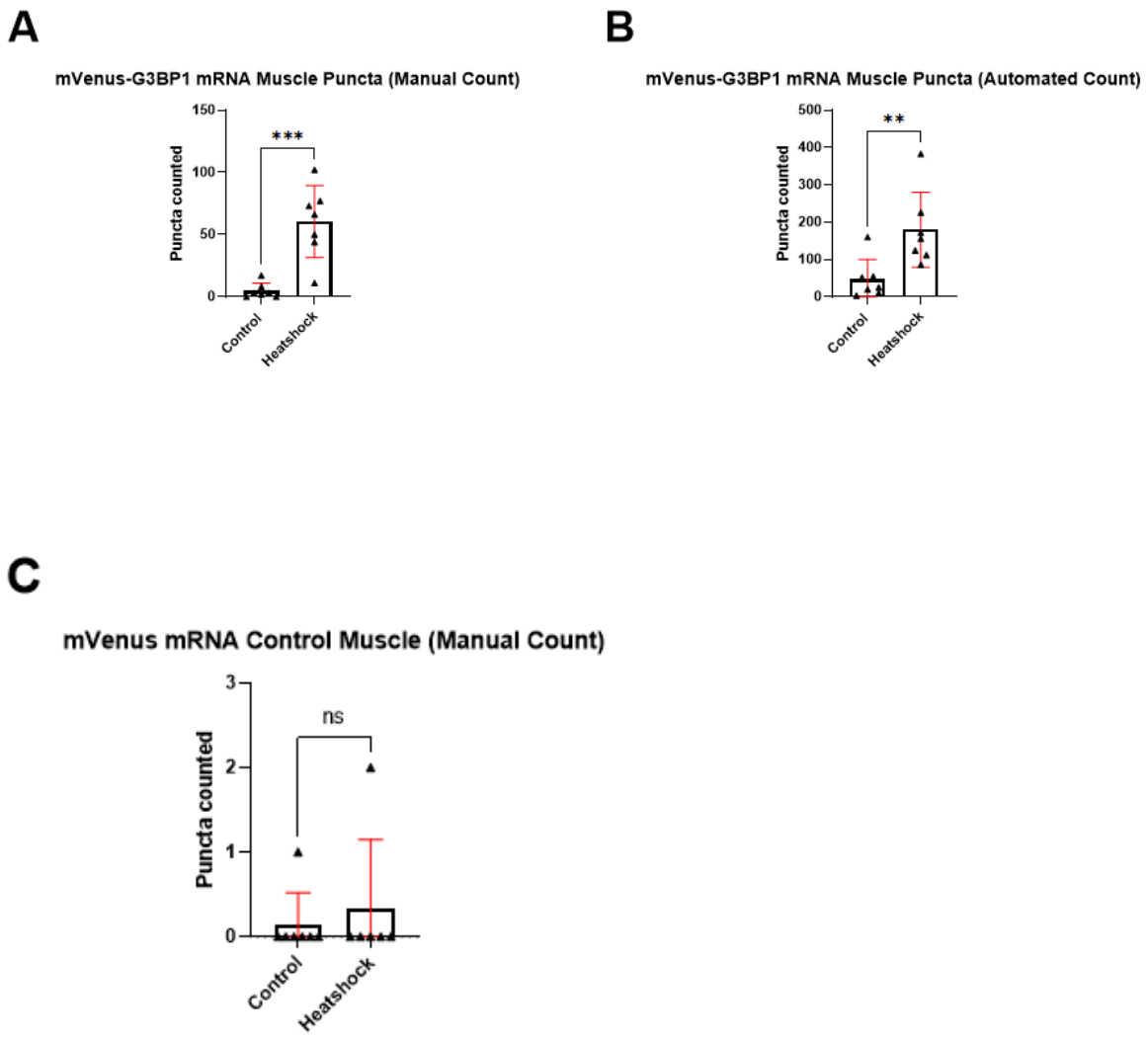


**Figure 7.3.** Counts of puncta within areas of interest in confocal microscopy muscle images of embryos injected with the mVenus-G3bp1 mRNA construct which fit the inclusion criteria for stress granules in heatshock and control images. Individual fish represented with triangle (▲) symbol. **A)** Manual count of mVenus-G3bp1 and H2B-mCerulean mRNA coinjected embryos muscle images puncta with unpaired t test showing P-value = 0.0003 (n=2 experimental replicates, n=14 biological replicates). **B)** Automated count of mVenus-G3bp1 and H2B-mCerulean mRNA coinjected embryos muscle images puncta with unpaired t test showing P-value 0.0092 (n=2 experimental replicates, n=14 biological replicates). **C)** Manual count of mVenus and H2B-mCerulean mRNA coinjected embryos muscle images with unpaired t test showing P-value 0.5902 (n=2 experimental replicates, n=13 biological replicates).

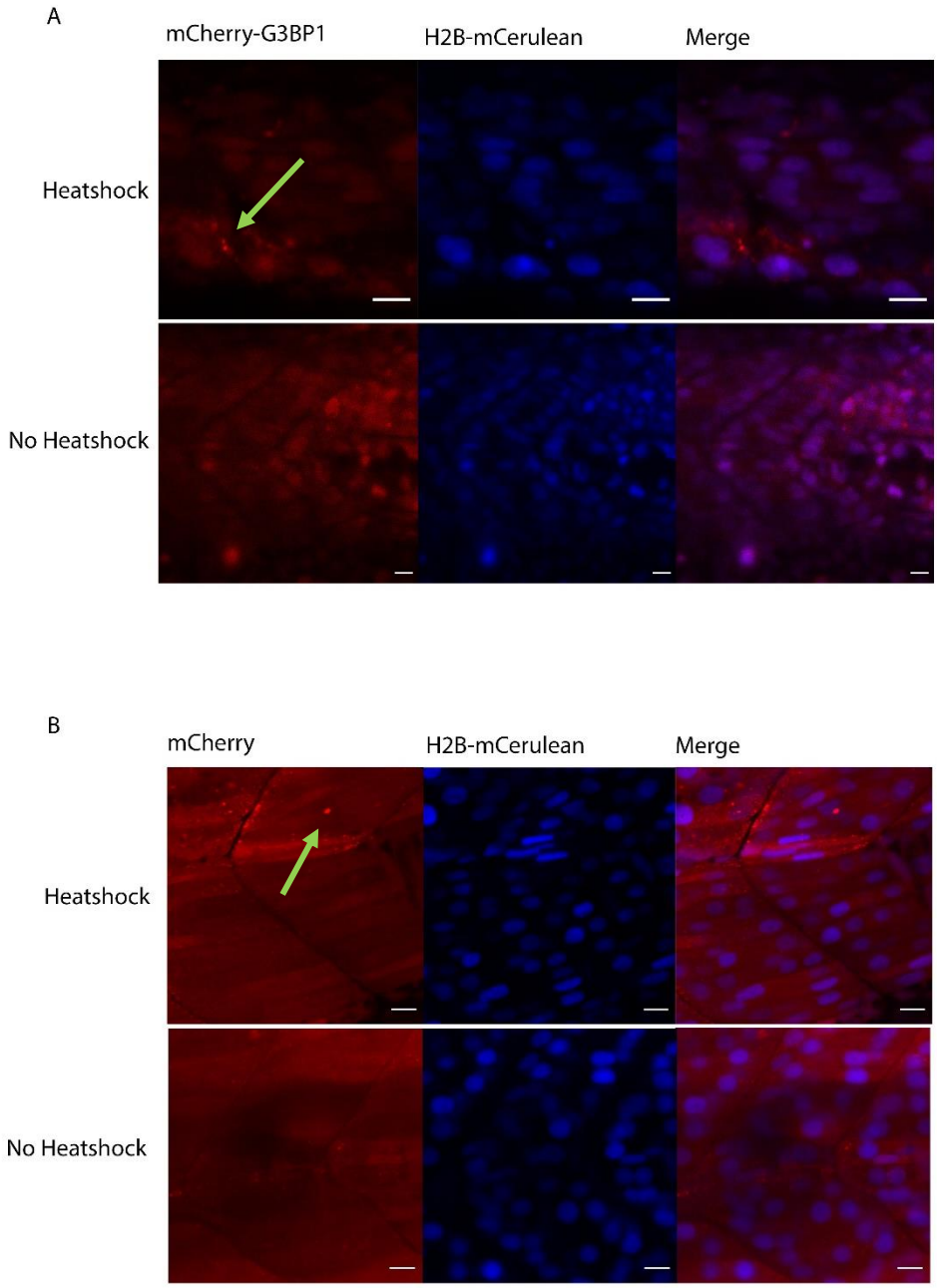


**Figure 7.4.** Representative images of heatshock and control mCherry-G3bp1/mCherry and H2B-mCerulean mRNA injected embryos muscle images. Scale bars at 10 μm (puncta of interest highlighted in green). **A)** Heatshock and treatment mCherry-G3bp1 and H2B-mCerulean mRNA coinjected embryos muscle images (n=2 experimental replicates, n=10 biological replicates). B**)** Heatshock and control mCherry and H2B-mCerulean mRNA injected embryos muscle images (n=2 experimental replicates, n=6 biological replicates).

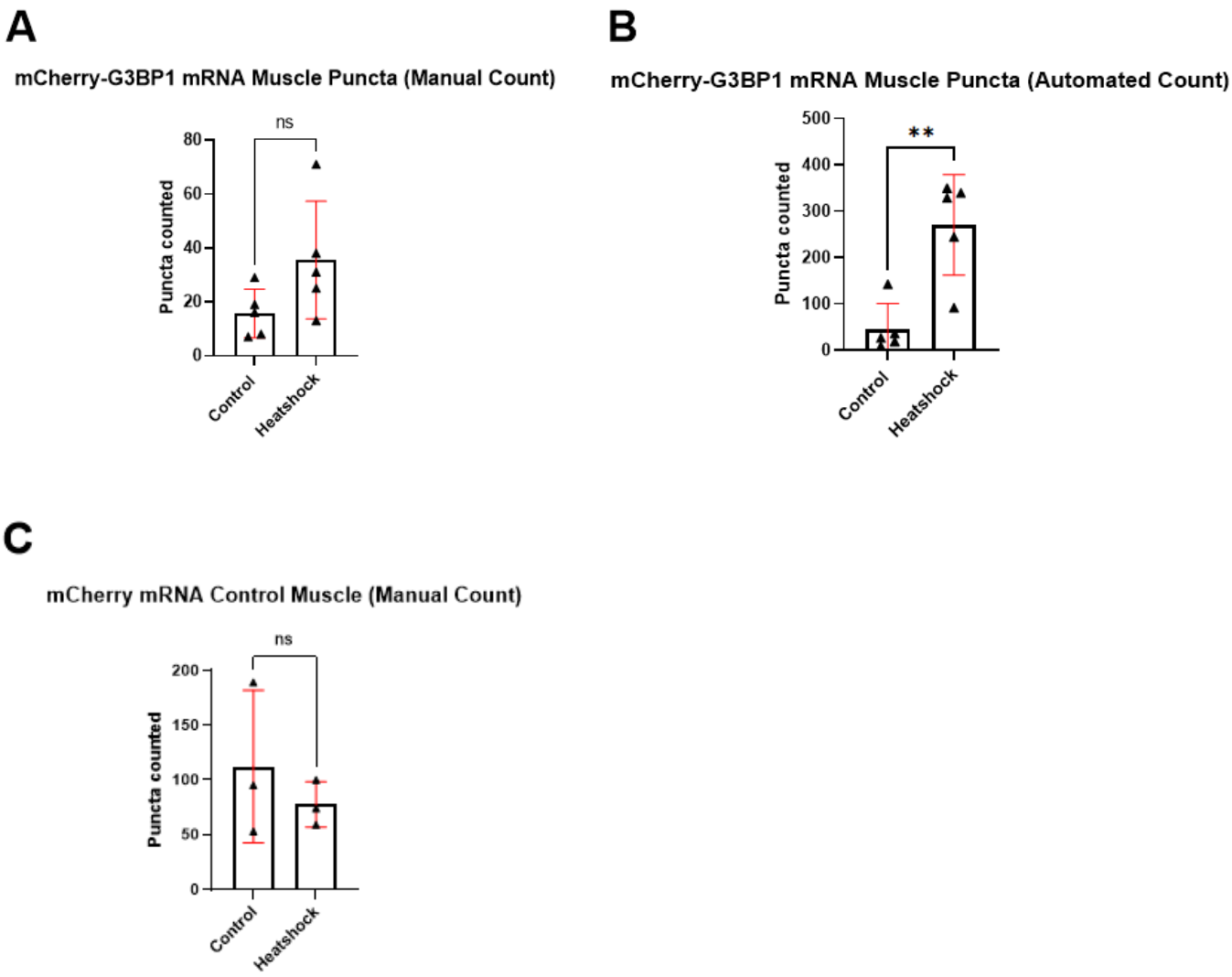


**Figure 7.5.** Counts of puncta within areas of interest in confocal microscopy muscle images of embryos injected with the mCherry-G3bp1/mCherry mRNA transcript which fit the inclusion criteria for stress granules in heatshock and control images. **A)** Manual count of mCherry-G3bp1 and H2B-mCerulean mRNA coinjected embryos muscle images puncta with unpaired t test showing P-value = 0.0974 (n=2 experimental replicates, n=10 biological replicates). **B)** Automated count of mVenus-G3bp1 and H2B-mCerulean mRNA coinjected embryos muscle images puncta with unpaired t test showing P-value 0.0033 (n=2 experimental replicates, n=10 biological replicates). **C)** Manual count of mVenus and H2B-mCerulean mRNA coinjected embryos muscle images with unpaired t test showing P-value 0.4550 (n=2 experimental replicates, n=6 biological replicates).

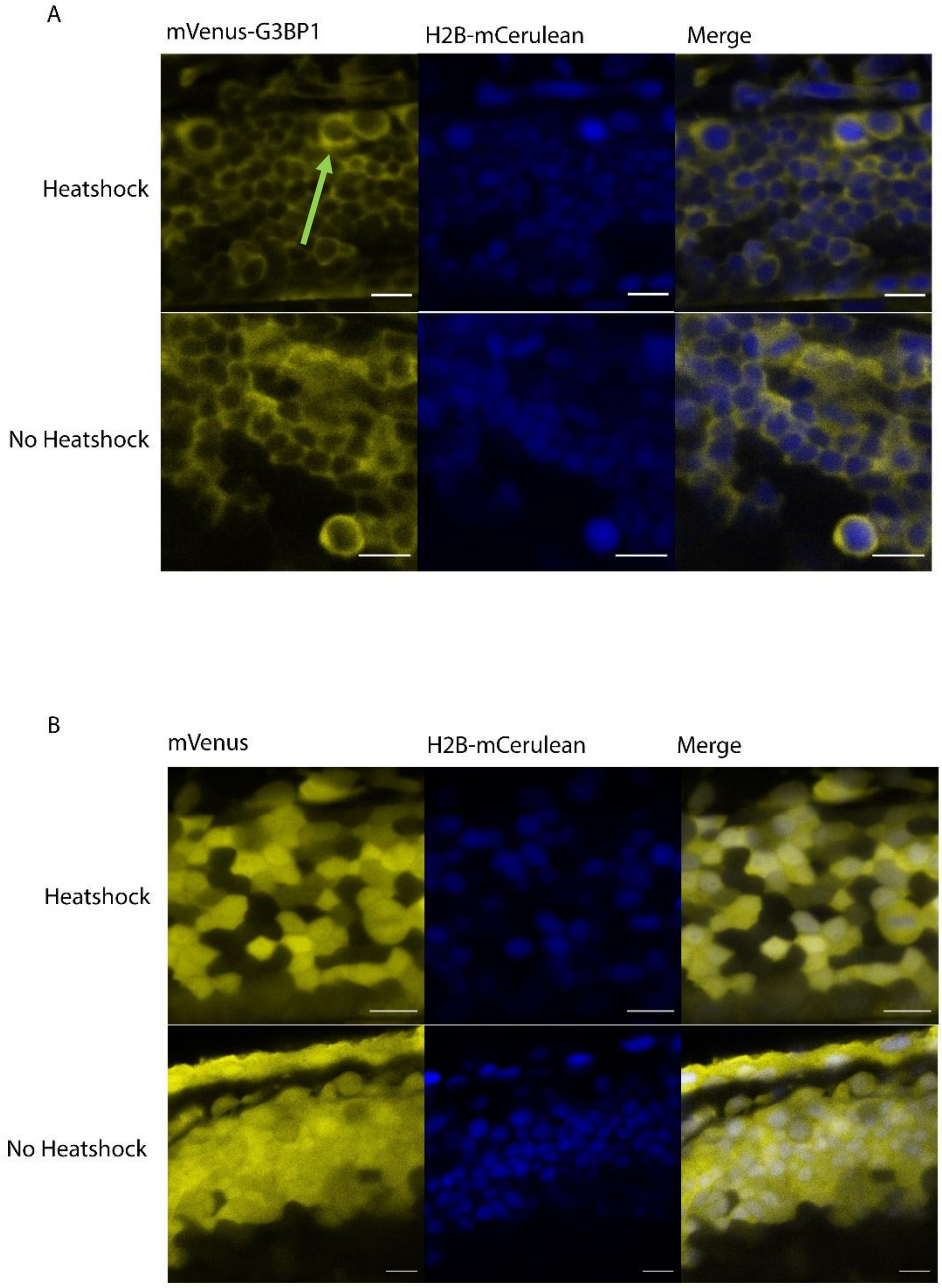


**Figure 7.6.** Representative images of heatshock and control mVenus-G3bp1/mVenus and H2B-mCerulean mRNA injected embryos spinal cord images. Scale bars at 10 µm (puncta of interest highlighted in green). **A)** Heatshock and control mVenus-G3bp1 and H2B-mCerulean mRNA coinjected embryos spinal cord images (n=2 experimental replicates, n=4 biological replicates). B**)** Heatshock and control mVenus and H2B-mCerulean mRNA injected embryos spinal cord images (n=2 experimental replicates, n=4 biological replicates).

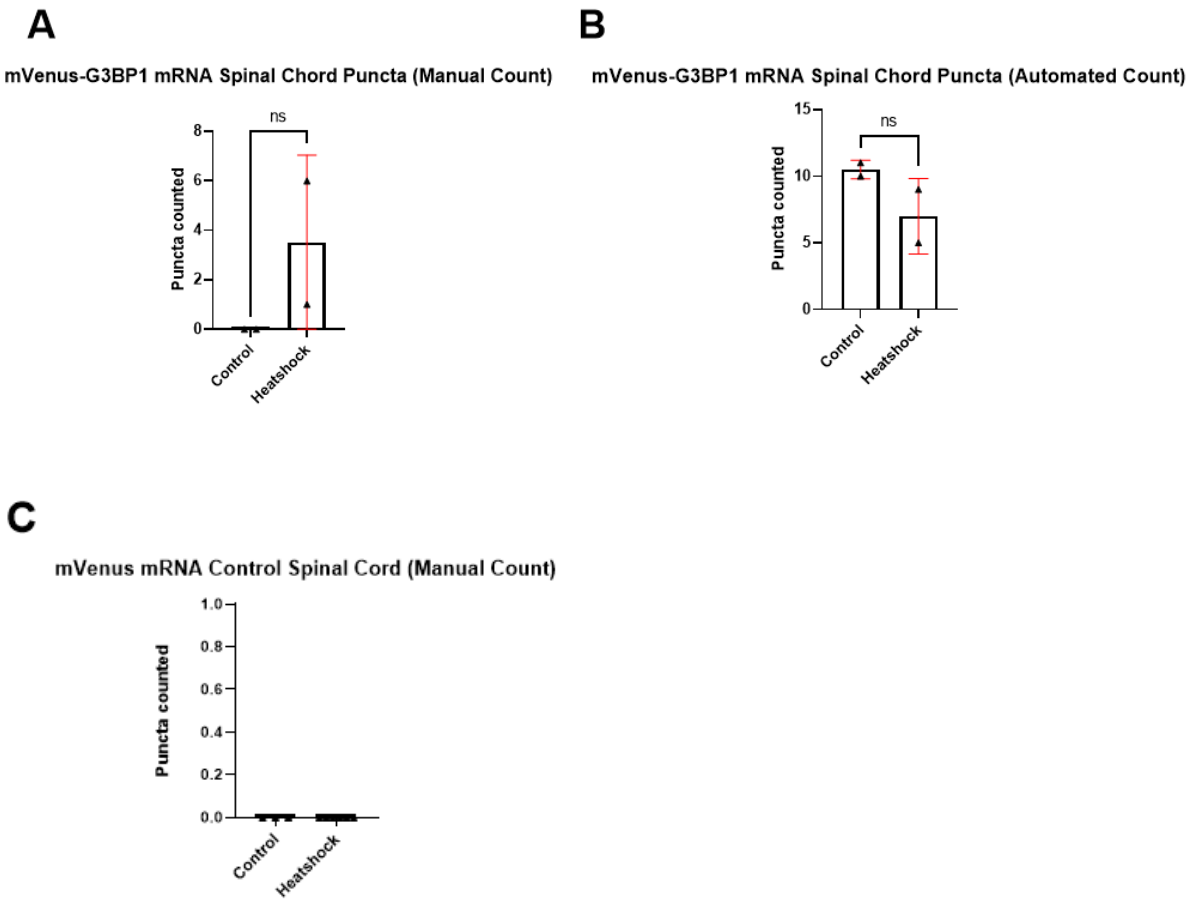


**Figure 7.7.** Counts of puncta within areas of interest in confocal microscopy spinal cord images of embryos injected with the mVenus-G3bp1 mRNA construct which fit the inclusion criteria for stress granules in heatshock and control images. **A)** Manual count of mVenus-G3bp1 and H2B-mCerulean mRNA coinjected embryos spinal cord images puncta with unpaired t test showing P-value = 0.2965 (n=2 experimental replicates, n=4 biological replicates). **B)** Automated count of mVenus-G3bp1 and H2B-mCerulean mRNA coinjected embryos spinal cord images puncta with unpaired t test showing P-value 0.2317 (n=2 experimental replicates, n=4 biological replicates). **C)** Manual count of mVenus and H2B-mCerulean mRNA coinjected embryos spinal cord images with unpaired t test showing no P-value (n=2 experimental replicates, n=9 biological replicates).

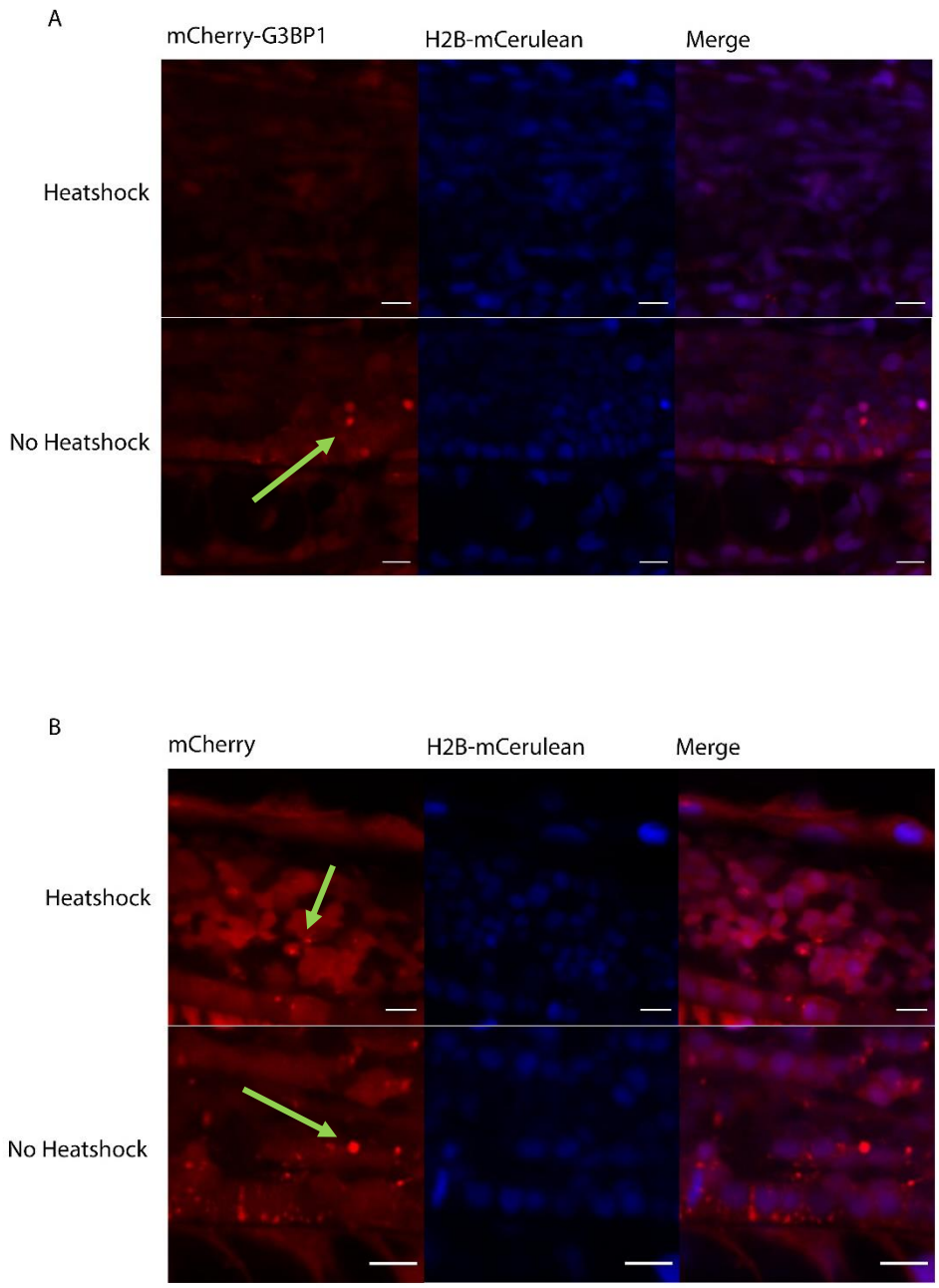


**Figure 7.8.** Representative images of heatshock and control mCherry-G3bp1/mCherry and H2B-mCerulean mRNA injected embryos spinal cord images. Scale bars at 10 μm (puncta of interest highlighted in green). **A)** Heatshock and control mCherry-G3bp1 and H2B-mCerulean mRNA coinjected embryos spinal cord images (n=2 experimental replicates, n=5 biological replicates). **B)** Heatshock and control mCherry and H2B-mCerulean mRNA injected embryos spinal cord images (n=2 experimental replicates, n=5 biological replicates).

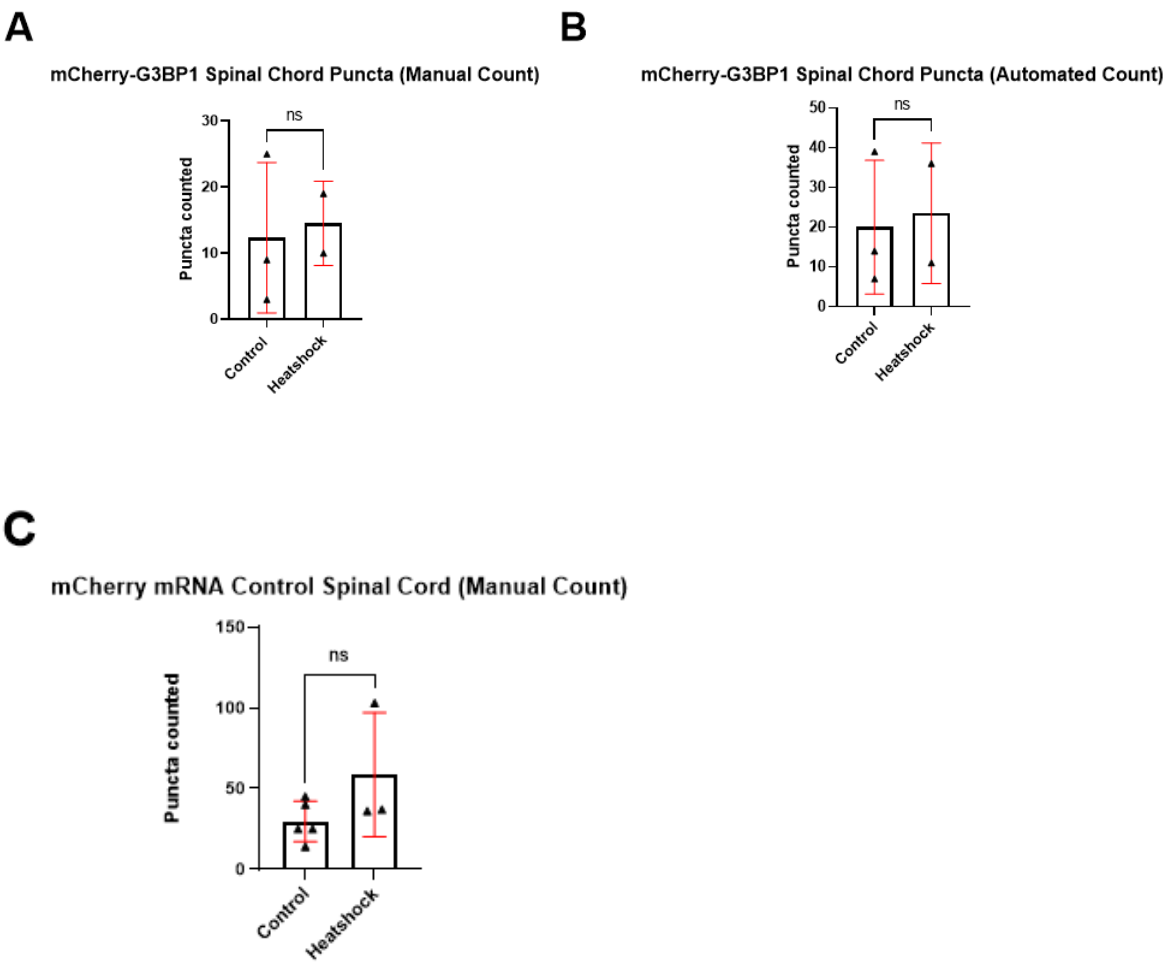


**Figure 7.9.** Counts of puncta within areas of interest in confocal microscopy spinal cord images of embryos injected with the mCherry-G3bp1 mRNA construct which fit the inclusion criteria for stress granules. **A)** Manual count of mCherry-G3bp1 and H2B-mCerulean mRNA coinjected embryos spinal cord images puncta with unpaired t test showing P-value = 0.8274 (n=2 experimental replicates, n=5 biological replicates). **B)** Automated count of mCherry-G3bp1 and H2B-mCerulean mRNA coinjected embryos spinal cord images puncta with unpaired t test showing P-value 0.8371 (n=2 experimental replicates, n=5 biological replicates). **C)** Manual count of mCherry and H2B-mCerulean mRNA coinjected embryos spinal cord images with unpaired t test showing P-value 0.1567 (n=2 experimental replicates, n=8 biological replicates).

| Structure | mRNA Injection | Heatshock Manual Puncta Count (average) | Control Manual Puncta Count (average) | Heatshock Automated Puncta Count (average) | Control Automated Puncta Count (average) |
|---|---|---|---|---|---|
| Muscle | mVenus-G3bp1 H2B-mCerulean | 60.43 | 4.7143 | 179.9 | 46.29 |
| | mVenus H2B-mCerulean | 0.3333 | 0.1429 | N/A | N/A |
| | mCherry-G3bp1 H2B-mCerulean | 35.60 | 15.80 | 270.2 | 45.80 |
| | mCherry H2B-mCerulean | 77.67 | 112.3 | N/A | N/A |
| Spinal Cord | mVenus-G3bp1 H2B-mCerulean | 3.500 | 0 | 10.50 | 7.000 |
| | mVenus H2B-mCerulean | 0 | 0 | N/A | N/A |
| | mCherry-G3bp1 H2B-mCerulean | 14.50 | 12.33 | 23.50 | 20.00 |
| | mCherry H2B-mCerulean | 58.67 | 29.80 | N/A | N/A |

**Figure 7.10.** Summary of average puncta counts across all imaged areas to 4 significant figures.

# 5 Discussion

There were three major aims of this thesis: to express a transient stress granule reporter in zebrafish larvae, to determine the optimal dose and timeframe for imaging the stress granule reporter, and to validate the stress granule reporter in response to cellular stress. These aims were completed through the transient over expression of stress granule reporters, timepoint and morphology screening, and through heatshock and control experiments imaged through confocal microscopy. Analysis of these results will be found in the following chapter.

## 5.1 Preliminary Bioinformatic Alignment

A preliminary bioinformatic alignment was preformed to determine genetic similarity between what was present in the plasmids and what would be of value to this research. The genetic similarity between these sequences were lower than expected however it was suspected that the low degree of similarity was likely due to evolutionary differences between the human *G3BP1* and zebrafish *g3bp1* sequences. As such we conducted a subsequent protein alignment which reflected the expected outcomes of the initial alignment. A high degree of similarity between both human G3BP1 and zebrafish G3bp1 proteins makes sense considering the biochemical action of G3BP1 as a Ras-GTPase-activating protein by associating with its SH3 domain (73). These proteins are responsible for the accelerating the GTPase function of Ras, associated with multiple pro-survival and cellular senescence functions (73, 74). The function of G3BP1 protein is an important mainstay in many multicellular organisms (35, 75, 76).

In addition to human and zebrafish G3BP1 proteins being orthologous, G3BP1 has historically been used as a marker for stress granule development (20, 77). Other stress granule proteins were considered for this thesis such as TIA1 as its involvement in stress granule assembly has been previously noted in literature (78). Ultimately TIA1 was not pursued as a stress granule marker due to difficulties in observing fluorescence post

mCherry-Tia1 and mVenus-Tia1 mRNA injection. The decision was made for this thesis to focus on the creation and characterisation of the G3BP1 protein as a stress granule marker.

## 5.2 Generation and Confirmation of Genetic Material

Gel electrophoresis acted as a simple method of confirming mRNA transcription and degradation. The mRNA transcripts generated for this thesis are outlined in the gels, including the Tia1 associated proteins. Tia1 was considered as an additional stress granule associated protein, however it failed to express within an *in vivo* zebrafish embryo model. The initial thought behind incorporating Tia1 and G3bp1 proteins with fluorophores was to image the two as stress granule formed. When difficulties with Tia1 expression in zebrafish embryos were made present, focus shifted to the G3bp1 protein as the stress granule marker for this thesis. The mRNA transcripts encode for the G3bp1 protein bound to either an mVenus or mCherry fluorophore by a flexible GGGS (glycine – glycine - glycine -serine) linker. Fusion proteins such as the GGGS linker are highly successful in that they allow for the independent folding of two proteins while during fusion (79). Flexible GGGS linkers also can be designed with higher glycine or serine contents to depending on the required linker length and flexibility (79). In generating the mRNA with genes tagged with fluorophores, previous literature has identified optimal gene functionality at the 3’ end and as such genes of interest were tagged at this site (80). This approach in previous literature was completed with a CRISPR/Cas9 method differing from a transient mRNA overexpression model. Due to time constraints, there was little requirement to investigate further functionality by tagging the fluorophore at the 5’ end as the initial attempt was successful. The optimisation of the technique outlined in this thesis may be a potential future direction of this project.

The gel electrophoresis of the mCherry-G3bp1 mRNA (Figure 3.7) showed multiple distinct bands as opposed to the expected, single band. The mRNA stock used for this electrophoresis gel was also used for injection into embryos and evidentially resulted in

fluorescence. It is unknown why there were multiple bands in the gel electrophoresis of mCherry-G3bp1 mRNA however it may potentially be the result of contamination in the plasmid preparation (multiple, unintended SP6 promotors), unintended products/contamination, or other unique circumstances. As the mRNA functioned as intended, there was little need to investigate the multiple bands in the electrophoresis gel.

The results clearly show that fluorescence of the mRNA transcripts is detectable through fluorescence microscopy. This initial screening was to confirm that the G3bp1 bound fluorophores expressed within an *in vivo* zebrafish embryo model. While they are detectable through Leica M165 Fluorescence Microscope, the resolution of the screening scope was not of a high enough resolution to image intracellular protein accumulations.

### 5.3 Optimal dose and Timeframe for Imaging

It was important to establish an optimal dose for mRNA injections to minimise the toxic effect of exogeneous material injected in an embryo, as it is statistically optimal to have high number of viable embryos for treatment and puncta quantification. Higher concentrations of mRNA in injections appears to be consistent with lesser survivability with the highest and most consistent mRNA concentration to be around 100-125 ng/µl. It was decided that 100ng/ul was an optimal dose to avoid potential additional stresses to the embryo whilst still achieving fluorescence.

It is widely known in literature that mRNA is a temporary means of expression within an *in vivo* model (81). Zebrafish embryos develop rapidly and within 24 hours post fertilisation (hpf) have developed anatomical features worthy of comparison to human physiology. We conducted an experiment to determine how long the various fluorophore bound stress granule proteins express fluorescence in the embryonic model at 24 hour increments. There was some variability seen in the mCerulean-H2B expressed embryos with stable expression up until the 72 hpf mark however the mCherry-Tia1 and mVenus-G3bp1

mRNA injected fish showed little fluorescence after the 24 hpf point. This may be a result of the H2B protein being a histone protein and having a different expression pattern when compared to Tia1 and G3bp1. Despite relatively strong fluorescence shown in the mCherry-Tia1 mRNA injected zebrafish shown when compared to the mVenus-G3bp1 mRNA injected fish at the 24 hpf timepoint, the inconsistency in expression pattern across Tia1 associated constructs solidified their removal from the study. If they were seen to be expressing fluorescence into the 48 or 72 hpf timepoints, they may have been reconsidered however G3BP1 associated constructs displayed limited but noticeable fluorescence into the 48 hpf timepoint.

Morphology of developing zebrafish is a wide area of research with much nuance in determining morphological variance. It was impotant for the mRNA transcripts to have as little effect on the morphology of the zebrafish as possible, to ensure survivability and allow for the comparison between animals. To keep the examination simplified, two experiments were conceived to determine morphological abnormalities – a morphology chart and quantifying zebrafish length. The morphology chart was adapted from literature and classified zebrafish embryos at the 24 hpf stage into one of four categories. The wild-type (WT) morphology was indistinguishable from wild-type, control embryos, the Category 1 (CAT I) displayed slight a variation in morphology resulting in 1 abnormality or developmental delay, Category 2 (CAT II) embryos displayed moderate malformations with 2 or more abnormalities, and Category 3 (CAT III) embryos showed structures which have severe morphological abnormalities. The higher the category of morphology, the more the embryo was affected by the mRNA injection. The highest category seen was CAT III in the mCherry-G3bp1 mRNA injected fish which also resulted in the lowest WT values. The next lowest number of WT zebrafish embryos was seen in the mCherry mRNA control fish which had a majority of animals in the CAT I category. Both mVenus and mVenus-G3bp1 mRNA

injected embryos showed a high number of WT phenotype embryos. These results imply that an over expression of mCherry is detrimental to the development of the zebrafish, potentially due to the self-aggregative properties of mCherry (82), sequestering G3bp1 protein and disrupting cellular function.

Embryo length was also measured from the tip of the tail to the base of the hind brain in the animals used in the morphology experiments. The measurement of zebrafish from tip of the tail to the base of the hind brain as chosen as an encompassing indicator of length. Length of the embryo's was not a component of the morphology assay and yet may be an indicator of delayed development. There was little variation across all mRNA injected animals except in the mCherry mRNA injected zebrafish embryos. This may be a result of a low biological replicate number which was n = 3. Little variation in embryo length across the mRNA injected and control samples indicates that length is largely unaffected by the presence of mRNA however to definitively conclude that would require more experimental and biological replicates and as such, the results of this study should be considered a pilot study, used for power calculations to determine statistically significant biological and experimental replicate numbers.

## 5.4 Validation of stress granule reporters in response to cellular stress

The two structures were imaged in the stress response experiments were the muscle fibres five somite caudal to the yolk sac/yolk tube boundary and spinal cord cells dorsal to the yolk sac/yolk tube boundary. These two areas were identified to be of importance in keeping within the scope of ALS as it is a condition characterized by the degradation of motor neurons. By focusing the imaging to these two areas of physiological importance, comparisons may be made between treatment groups. The Tia1 protein was excluded from the validation of stress granule reporters as the initial attempts at imaging fish injected with the mRNA transcripts resulted in embryos displaying little to no fluorescence. To determine

the validity of stress granule reporters generated, a set of stress granule inclusion criteria were developed as an accessible definition of protein accumulations, based off contemporary literature. What was counted in the imaged zebrafish embryos were protein accumulations (as evident by fluorescent G3bp1 protein aggregation) between 0.1 µm and 4 µm in diameter, localised in the cytoplasm of cells (29, 77, 83). Defining stress granules in this way allowed for their quantification to be made possible by microscopy however it fails in confirming that the puncta counted are definitively stress granules. Furthermore, stress granule counts were defined by an area imaged rather than per cell. As images used for stress granule/puncta counts were taken across comparable areas at the same magnification, the comparison is valid for this thesis. To be a definitive quantification of puncta, puncta counts need to be per cell and not across an area. Confirmation that the puncta as reported by this thesis are stress granules and quantifying puncta as a function of cell rather than area are both technical limitations of this study and thus immediate future directions.

When looking to the fluorophore only controls, mVenus associated mRNA injections resulted in the puncta counts as hypothesised, with close to no puncta counted in either the muscle or spinal cord images. There were two images which depicted higher than expected puncta counts in the muscle images of the mVenus mRNA experiments. There is an unexpectedly high number of puncta visible in both the mCherry mRNA muscle and spinal cord images with the highest value being seen in a control group muscle image with 189 puncta counted. This is surprising for two reasons, mainly that the embryo which displayed this high puncta count was not subjected to heatshock and even so, the mCherry expressed in the embryo's cells was not tagged to a G3bp1 protein. An explanation for the large puncta count discrepancy between the mCherry fluorophore mRNA muscle/spinal cord and mVenus fluorophore mRNA muscle/spinal cord puncta counts is seen in the literature where mCherry fluorophores have been described in specific conditions to self-aggregate (84). This initially

may be grounds for the dismissal of the mCherry and mCherry-G3bp1 mRNA transcript injected embryos puncta counts. However a difference in heatshock and control puncta counts seen in the mCherry-G3bp1 mRNA injected images could have meant that the results needed to be normalised against the mCherry mRNA injected images puncta counts to account for the inflated mCherry aggregation. Such large P values between the control and heatshock puncta quantifications in the: mVenus mRNA muscle, mVenus mRNA spinal cord, mCherry mRNA muscle, and mCherry mRNA spinal cord imply that the heatshock treatment did not influence the appearance of puncta in either the mVenus or mCherry mRNA injected muscle and spinal cord images.

The graph for the manually counted mCherry-G3bp1 mRNA injected muscle visualized non-significant P value = 0.0974 (as noted by the “ns” representing a value higher than 0.05). Whilst not conventionally an ideal P value, there is higher significance seen than what was in the mCherry mRNA injection muscle heatshock and control images (P value = 0.4550). Such a difference in the statistical significance between the mCherry-G3bp1 mRNA injected muscle control and treatment group when compared to the mCherry mRNA muscle images suggests a higher confidence interval for a difference between the mCherry-G3bp1 mRNA injected heatshock and control muscle than what was seen in the mCherry mRNA injection. This may be explained by the G3bp1 localizing and thus influencing the puncta counts, leading to additional puncta in the heatshock mCherry-G3bp1 mRNA injected embryos. The same cannot be said for the mCherry-G3bp1 mRNA injected spinal cord images as the puncta counted fluctuates seemingly sporadically with large error bars. While not a conventional method of interoperating P values, there is mounting support for the meta-analysis of P values, specific to the investigation at hand (85). These results may also be a result of low biological and experimental replicates as many of the confocal images were

unusable. These experiments can be considered pilot experiments for power calculations to be made before a conclusion can be reached.

The mVenus-G3bp1 mRNA injected muscle images resulted in puncta counts as hypothesised with the average puncta per muscle image within the treatment group at 35.6 and 15.8 for the control group. The treatment and control embryo muscle puncta counts were statistically significant with a P value = 0.0003. While such high statistical significance is not seen in the P value for the mVenus-G3bp1 mRNA injected spinal cord images (P value = 0.2965), this may be reflective of, as with the mCherry-G3bp1 mRNA injected spinal cord images, a low number of experimental and biological replicates (n=2 and n=4, respectively). An alternative explanation for such low puncta counts in the spinal cord may be that the spinal cord, being deeper within the tissue of the embryo, may have had a somewhat protective effect to the conditions of heatshock, dampening the sudden temperature change that lateral muscle would be exposed to however this is an unlikely explanation. Heatshock conditions were kept uniform across all tests as this was a primary investigation and variation would complicate comparisons between spinal cord and muscle puncta counts. To investigate this idea of deeper tissue experiencing less of a heatshock effect, the heatshock protocol used would need to be varied to observe the effects of differing heatshock time periods. In this investigation, heatshock conditions between the spinal cord imaged embryos and muscle somite imaged embryos were kept consistent. With higher biological replicates in the mVenus mRNA spinal cord puncta count, the data appears to be more uniform with zero puncta counts across both control and heatshock.

A nuclear marker (H2B-mCerulean mRNA) was co-injected with the mCherry and mVenus associated transcripts. H2B-mCerulean acted as a nuclear marker to aid with image quantification and confirm the proteins localize outside of the nucleus, within the cytoplasm of cells. Puncta within the H2B-mCerulean marked nuclei were not included in the puncta

counts to exclude nuclear localisation of protein granules. H2B tagged to mCerulean was an appropriate choice for nuclear marker as it is a histone protein, only appearing with DNA and as such is bound to the nucleus. The choice of fluorophore, mCerulean, was also appropriate as it's unique excitation (Ex $\lambda$ = 433) and emission (Em $\lambda$ = 475) spectra can be co-imaged with both mVenus (Ex $\lambda$ = 515, Em $\lambda$ = 527) and mCherry (Ex $\lambda$ = 587, Em $\lambda$ = 610) fluorophores (86-88).

Automated image quantification was attempted in this thesis as a means of establishing a novel and batch mechanism to count puncta formation through software. The attempts at this are explored in relation to the mVenus-G3bp1 and mCherry-G3bp1 mRNA injected muscle and spinal cord counts. All instances of automated counting resulted in wildly exaggerated puncta counts as evident by the inflated puncta counts across all automated counts. The puncta counts resulting from the automated counting were identified as being inflated as visual confirmation and comparison to manual counts showed that the software was counting non-stress granule puncta (as defined in Methods 3.6.4) and microscopy artifacts as puncta of relevance to the investigation. This is especially noticeable in the manually counted mVenus-G3bp1 mRNA injected muscle images where the mean value for heatshock puncta was 60.43 and the mean puncta count for control images was 4.714, vastly lower puncta counts than in the automated count of the same image set, showing a mean of 179.9 puncta forming in the heatshock images and a mean of 46.29 puncta appearing in the cells of control images. While the automated counting method of quantifying cellular stress derived puncta proved to be inaccurate, the knowledge gained from a failed experiment lends itself well to future endeavours.

## 5.5 Limitations

While robust, this thesis has several limitations which hold it back from being a definitive conclusion to the characterisation of stress granules and the stress response within an *in vivo* zebrafish model. The limitations outlined in this thesis are areas which have been identified as non-technical, conceptual shortcomings of the research. While the conclusions derived from the evidence presented in this thesis are valid, identifying the limitations of a research project is the first step to further developing the study.

### 5.5.1 Self-Aggregation of Red Fluorophore

Zebrafish embryos injected with mCherry associated fluorophore's mRNA (both mCherry and mCherry-G3bp1) showed significantly higher puncta counts in the untreated control samples than their mVenus associated samples. This is especially seen when comparing the mCherry and mVenus mRNA injected samples. While the inclusion criteria for counting puncta which were thought to be stress granules was a specific attempt at avoiding puncta counts that are not stress granules, it appears that some protein accumulations were included. The spontaneous aggregation of mCherry proteins identified in this thesis defies conventional thought as mCherry was designed as a true monomeric fluorophore (87). In contrast to the results presented in this thesis, there is literature suggesting that mCherry fused proteins do not spontaneously aggregate even in conditions of over-expression (82). Despite this, there is also literature describing multiple cases of the spontaneous aggregation of mCherry as identified in this thesis through speculated non-specific subcellular localization and/or secondary protein-protein interactions (84, 89). It is of interest to note that the literature both in support and denial of self-aggregating mCherry are not within zebrafish models, nor the conditions by which the mCherry associated injections within the model were put through (control groups at 28°C and treatment groups at 37°C). Regardless of what previously

published material claim, it is clear that in this instance mCherry was not an appropriate fluorophore for the experiments conducted in this thesis.

### 5.5.2 Zebrafish as a Model Organism

While a suitable model organism for this thesis, an *in vivo* zebrafish model is not without it's limitations. Zebrafish like many fish species are ectothermic in nature, and as such the zebrafish G3bp1 would have evolved over time with the zebrafish to function optimally at 28°C (90). Increasing the external temperature of the zebrafish to 37°C as was done in the heatshock for the treatment group represents a significant increase to the internal temperature of an ectotherm. While necessary to induce cellular stress, this form of cellular stress is far outside of what can be reasonable comparable to an endothermic human with ALS. The zebrafish G3bp1 protein would presumable not be behaving in a regular manner and may not be an accurate portrayal of larval zebrafish cells responding to cellular stress.

Stress granules are a ubiquitous response of cells exposed to cellular stressors. There were many viable structures within the zebrafish model that could have been used to image and visualize stress granules. To allow for a deeper analysis and ease of imaging, the scope of where stress granules were imaged for this thesis was limited to five somite caudal to the yolk sac/yolk tube boundary and the spinal cord cells dorsal to the yolk sac/yolk tube boundary. Limiting the scope of imaging in such a way allows for a faster turnover of image sets as the structure is readily recognized. Despite benefits, limiting the image range of zebrafish embryo physiology that was imaged presented some drawbacks in the application of this model. The context of this project was surrounding that of ALS pathogenesis and as such, it would have been of interest to image motor neurones. This limitation would be the primary focus of the continuation of this project as it would aid in refining the model to a higher degree of specificity towards the inclusion of stress granules in cases of ALS.

### 5.5.3 Overexpression of Stress Granule Proteins

A potential drawback of the use of utilizing an mRNA transient overexpression model for the visualization of stress granule proteins is in that the proteins expressed from the mRNA are in addition to the endogenous proteins produced from the zebrafish. This is an issue for measuring stress granule formation as an overexpression of stress granule associated genes such as G3BP1, TIA-1, TIAR, TTP, FMRP, CPEB, SMN, DYRK3 can induce the formation of stress granules within a cell (77, 91). The while the control (non-heatshocked) datasets showed a lesser protein accumulation counts in stress granule formation when compared to the treatment datasets (heatshocked), the overall measure of stress granules may have been inflated due to the overexpression of G3bp1. It is important for an *in vivo* model to accurately represent the intracellular environment and as such there are two solutions to this issue of protein overrepresentation.

The first solution to the over expression of stress granule associated proteins is by creating a model by knocking-in fluorescent proteins such that the naturally translated G3bp1 within the zebrafish embryo's cells is tagged with the fluorescent reporter. Due to the accuracy required to knock in these genes, it would be ideal to utilize a CRISPR/Cas9 insertion method due to its accuracy.

A second solution is in utilizing nuclear fractionation in combination with mass spectroscopy to quantify the number of proteins present in stress granules in the nucleus and compare to the proteins found in stress granules in the cytoplasm (92). This method represents significant cost and considerable labor however it will give an accurate idea of how intracellular stress granules behave without the influence of altering gene expression. Nuclear fractionation and mass spectroscopy changes the scope of this thesis and as such potentially would be better suited as a potential future direction of the research,

looking into the proteomics of stress granules, rather than a solution to a problem faced during the research.

## 5.6 Future Directions

This project has laid the initial groundwork for the *in vivo* characterisation of stress granule reporters within zebrafish. This thesis has also opened a door for a multitude of ground-breaking projects which can expand on outlined principles. The simplicity of stress granule reporting model established lends itself well to future projects which will result in a greater understanding of the stress granule response and its relation to ALS.

### 5.6.1 mScarlet to Replace mCherry Fluorophore

There is a need for a red fluorescent protein to be in use in zebrafish modelling, especially regarding studies concerning ALS pathology. A variety of fluorophores with different excitement and emission wavelengths allow for multiple proteins of interest to be identified through microscopy simultaneously, allowing for protein interactions and dynamics within ALS pathology to be studied. For this reason, when the action of mCherry was identified to be problematic for this study, it was decided that monomeric mScarlet was an appropriate substitution as it is reported in literature to be brighter than mCherry and have higher quantum yields (70%) above that of mCherry (<50%) without reported self-aggregation (93). Furthermore, mScarlet has similar excitation (Ex $\lambda$ = 569) and emission (Em $\lambda$ = 594) spectra as mCherry (Ex $\lambda$ = 587, Em $\lambda$ = 610), allowing it to be substituted into the coimaging efforts with mCerulean (Ex $\lambda$ = 433, Em $\lambda$ = 475) and mVenus (Ex $\lambda$ = 515, Em $\lambda$ = 527) (86-88, 93). As with the mCherry in this thesis, the action of mScarlet will need to test for it's appropriateness as a fluorescent tag for G3bp1 and cellular stress in an *in vivo* zebrafish model.

### 5.6.2 Transgenic Stress Granule Reporter Zebrafish Lines

While the transient overexpression model developed for this thesis was robust in its applications, it falls short in the longevity of the model as a whole and potentially impacts the accuracy of results. Transient overexpression of mRNA transcripts within zebrafish was found to be usable up until the 24 hpf timepoint – after this the detection of the transcript through its fluorescence begins to fail as the mRNA degrades within the zebrafish cells. While 24 hpf was seemingly ample time, it required multiple, labour intensive steps to ensure success. At 15-30 minutes post fertilisation, the transcript needed to be injected with embryos selected for survival and viability. Then at 20-24 hours post fertilisation, embryos were again screened for survival and mRNA transcript uptake. The positive embryos were then embedded and taken for confocal imaging. With multiple steps, the margin for error increases while embryo survivability and fluorescence of proteins decreases over time. Establishing a transgenic zebrafish line with these stress granule reporting constructs will streamline this process of stress granule detection as well as allowing for the stress granule reporting constructs to be reported over a longer timeframe. To overcome the concessions of transient over expression models, a knock-in transgenic model will need to be established.

The Tol2 transposon is a well-documented, historically used gene transfer vector used to create stably expressing transgenic zebrafish. Originally conceived in the medaka fish (*Oeyzuas latipes*), the Transposase enzyme allows a Tol2 flanked DNA construct to be inserted into the target genome (94). Tol2 transposon mediated mutagenesis operates with the transposase-donor DNA plasmid being designed with a promoter and the gene of interest. This is then co-injected with a synthetic transposase mRNA into early fertilized zebrafish egg (95). The injected genetic material is integrated at the multiple randomly located Tol2 locations throughout the genome and the construct becomes part of the zebrafish genome (94, 95). A major concession of the Tol2 transposon mediated genetic editing of zebrafish is the

lack of specific integration sites meaning the inserted DNA can be theoretically translocated anywhere along a chromosome – this high variability is a major consideration to be had when implementing this technique as it lacks a specific and accurate integration site. While Tol2 transposon mediated transgenesis is widely utilised in zebrafish studies, the lack of specific integration sites makes it unsuitable for this investigation as the knock-in gene will need to be integrated at a precise location such as to not overexpress the Tia1 and G3bp1 proteins, skewing results.

Endonucleases such as zinc finger nucleases (ZFNs), transcription activator-like effector nucleases (TALENs), and CRISPR (Clustered Regularly Interspaced Short Palindromic Repeats) are artificial, restriction enzyme systems often used in attempts at generating transgenic zebrafish lines (96-98). These endonuclease techniques work to edit the genome by inducing a double-stranded DNA break in a region of interest and allowing for the insertion of DNA to reintegrate into the specific site (99-101). All three systems have been employed for genome editing in zebrafish, however CRISPR is currently viewed as a higher accuracy alternative to ZFNs and TALENs for targeted genetic alterations (102, 103).

CRISPR was originally derived from the adaptive immune system of *Streptococcus pyogenes* (104). This technique employs a guide RNA (gRNA) bound to the Cas9 enzyme (CRISPR associated protein 9) and the target sequence of DNA (104). Once bound to the target sequence as defined by the gRNA, the Cas9 enzyme induces the double-stranded DNA break in the genome (101, 104). In the years following it's conception, CRISPR has been optimized as an effective and reliable mutagenesis technique in zebrafish for both gene knock-in and knock-out experiments (105). CRISPR/Cas9 shows potential to being the optimal method to take this project further through integrating the fluorophore of choice into the native gene locus of interest (e.g. G3bp1) as similar models have done in the past (35).

### 5.6.3 High-Throughput Stress Granule Quantification

A major bottleneck in data analysis within this thesis was the quantification of stress granules from microscopic images. This is due to the extensive time required to count the stress granules formed. There were multiple attempts to automate the stress granule quantification based off image analysis tools such as ImageJ (Fiji) however these attempts were unsuccessful due to the tendency of the analysis software to not count puncta that occur in clusters or over count images with high background fluorescence. The inclusion criteria for determining puncta to be stress granules was kept strict as it was the only mechanism of discrimination between stress granules and non-stress granule related aggregates. For this reason, automated counting was omitted for the mCherry and mVenus control images. Ultimately the most accurate method of quantifying stress granules was through a manual count however even manual counting was not without issues. Manual counting suffered from issues of uncertainty in counting puncta which occur in clusters or as with the automated counting, issues distinguishing puncta from images with high background fluorescence. Even with manual counting, statistical analysis through data normalization, determining stress granule puncta per cell, was impossible due to analysis of a two-dimensional image. Despite the difficulties in the approaches, thought was given as how to optimise this process through flow cytometric measurement of G3bp1 protein aggregation.

Flow cytometric analysis of inclusions and trafficking (FloIT), is a rapid and novel method for the quantification of protein inclusions larger than 0.5 µm within living cells (106). FloIT quantifies the number of inclusions present in the lysate of cells which is then normalized against the number of nuclei within the sample. Furthermore, FloIT has the ability to discriminate between inclusions formed by one protein and inclusions formed by multiple proteins – data such as this can aid in further characterising the stress granule response (106). FloIT has previously been utilised to determine intracellular TDP-43

aggregation as well as having been used with a zebrafish model (107, 108). Incorporating FloIT into this study will also aid in the identification of stress granules by the proteins found within. Identification of stress granules and discriminating them from other types of protein aggregation is an area of this thesis which is a natural progression of the study as it stands. The discrimination of protein aggregates in this study was defined by localisation and size as outlined in the methods. Establishing FloIT as a technique to be used in stress granule quantification will provide high-throughput and higher quality data than what can be accomplished through manual counting of microscopy images.

### 5.6.4 Further Characterization of Stress Response

As a speculated protective function of living cells, the stress granule response helps cells survive conditions that would otherwise lead to cell death through the stress response. Cellular stress goes beyond thermal stress tested as outlined in this thesis. It would be of benefit to test other types of cellular stresses and at varying concentrations on the model outlined in this thesis and future, potential models created. Characterizing other cellular stressors on this model will provide insight to how whether they differ in stress granule response intensity and duration. To understand the potentially differing stress granule responses, live imaging of the stress granules in the in vivo model of the various cellular stressors will show the assembly and disassembly of stress granule complexes over the duration of the response.

Cellular stress comes in multiple forms; oxidative stress, chemical exposures, thermal stress, and stress related to aging (26, 77, 109, 110). For the model outlined in this thesis, the focus was on thermal shock as a cellular stressor however literature regarding the difference between the stressors and their effect on a cell is sparse. There is value in examining the potential differences between cellular stressors as stress granules are implicated in a variety of diseases outside of ALS and if there is a difference between cellular stressors, it may

provide an insight to varying incidence rates and risk groups of different individuals (e.g. regular tobacco smokers are at higher risk of being exposed to oxidative stress) (111). Hydrogen peroxide has historically been used to test oxidative stress on cells due to the Fenton's reaction which between H2O2 and Fe2+ ions generating OH radicals which cause oxidative damage to the exposed cells (112). Utilizing this mechanism, it will be possible to determine the effect of oxidative stress on the zebrafish model.

While not necessarily reported as a cellular stressor, there may be potential benefit to testing the effect of β-N-methylamino-L-alanine (BMAA) on an *in vivo* model such as the one outlined in this thesis. BMAA is seen as the potential cause of Guamanian ALS (gALS) yet studies have not linked it to the formation of stress granules (113, 114). This link between BMAA and gALS is controversial in the neurodegeneration community (115). By testing the effect of BMAA and it's potential to impact stress granule formation, a novel link may be uncovered giving us deeper insight to not only the effect of BMAA on living cells but also the link between stress granules on the pathogenesis on ALS.

### 5.6.5 Characterisation of Stress Granule and ALS Associated Aggregates

Finally, the models testing in this thesis are wild-type zebrafish. While wild-type zebrafish are a robust model organism, there is a benefit to testing the stress granule response in transgenic zebrafish lines traditionally used in ALS modelling experiment to examine the potential interaction(s) of stress granules to other established aggregating structures associated with MND such as fluorophore fused FUS and TDP-43 models. Mutations within *FUS* genes and *TDP-43* genes have previously been linked to with both fALS, sALS and frontotemporal dementia (116, 117). Missense mutations in the *FUS* gene such as the R521G have been associated with fALS, resulting in dense protein aggregations and paraspeckles (RNA granules formed in the nuclear interchromatin space) of neuronal cells in fALS patients (116, 118). Furthermore, abnormal C-terminal fragments of TDP-43 have been

identified as cytoplasmic inclusions both lower motor neurons and glial cells in cases of fALS and sALS (117). Due to the observation of both FUS and TDP-43 proteins resulting in cytoplasmic protein granules, it is of interest to identify whether they are involved or influenced by the stress granule response.

This thesis provided the groundwork for mRNA transcripts to utilize in the modelling of stress granules within an *in vivo* zebrafish model. Wild-type zebrafish were used for the microinjection of mRNA transcripts however by injecting mVenus-G3bp1 mRNA transcripts as was done in this thesis into transgenic zebrafish lines producing fluorescently tagged FUS or TDP-43 mutants and subjecting them to conditions of cellular stress, the potential interactions between the FUS, TDP-43 and stress granules may be observable through confocal microscopy.

These interactions can be further characterized using the BioID screen for the potential interactions. BioID aids in the identification of relevant protein-protein interaction by utilizing a biotin ligase to biotinylate proteins based off their proximity (119). While utilizing this method would require further work, it may provide evidence to stress granules interacting with previously established ALS aggregations.

While both the injection of the mRNA transcripts outlined in this thesis into previously established transgenic ALS zebrafish lines and the characterisation of stress granule interactions through BioID are of significant research interest, a novel and exciting application of an *in vivo* modelling is the potential for live imaging to be combined with both future directions. Live imaging, when combined with the colocalization of mRNA transcripts, fluorescently tagged ALS transgenic zebrafish lines, and BioID showing interactions of interest will provide valuable insight characterising stress granules and the intracellular interactions of other proteins of interest.

## 5.7 Conclusion

This thesis was conceptualized under the context of widening the understanding of stress granules and their relation to intracellular protein accumulations as seen in cases of ALS. To accomplish this, stress granule reporting mRNA transcripts were created with G3bp1 expressed as a transient stress granule reporter in zebrafish larvae. The optimal dosage and timeframe for these stress granule reporters were determined through dose response experiments, morphology screening, and timeframe experiments. Dosages and imaging times were examined and chosen based off minimal mutagenesis, increased survival, and maximized fluorescence. Once the ideal dosages and imaging timeframe was understood, the zebrafish larvae were injected with the mRNA transcripts and separated into two groups – treatment to be exposed to a cellular stressor (heatshock) and control to remain at normal temperature. These groups were imaged on the confocal microscope to determine the subcellular localization of said stress granule reporters, and finally validate the stress granule reporter in its response to cellular stress. This thesis has successfully examined and characterised the use of mVenus-G3bp1 mRNA as a stress granule reporter in a zebrafish model. While there were several limitations with the study, the body of work within this thesis provides the initial investigation to rectify those limitations and move forward through to understanding the role stress granules play ALS pathogenesis.

# 6 References


1. Neary D, Snowden JS, Mann DM, Northen B, Goulding PJ, Macdermott N. Frontal lobe dementia and motor neuron disease. Journal of Neurology, Neurosurgery & Psychiatry. 1990;53(1):23-32.
2. Wijesekera LC, Nigel Leigh P. Amyotrophic lateral sclerosis. Orphanet Journal of Rare Diseases. 2009;4(1):3.
3. Mitsumoto H, Chad D, Pioro E. Amyotrophic Lateral Sclerosis (Philadelphia: Davis). 1998.
4. Chiò A, Logroscino G, Hardiman O, Swingler R, Mitchell D, Beghi E, et al. Prognostic factors in ALS: A critical review. Amyotroph Lateral Scler. 2009;10(5-6):310-23.
5. Jaiswal MK. Riluzole and edaravone: A tale of two amyotrophic lateral sclerosis drugs. Medicinal Research Reviews. 2019;39(2):733-48.
6. Bhandari R, Kuhad A, Kuhad A. Edaravone: a new hope for deadly amyotrophic lateral sclerosis. Drugs Today (Barc). 2018;54(6):349-60.
7. Valdmanis PN, Rouleau GA. Genetics of familial amyotrophic lateral sclerosis. Neurology. 2008;70(2):144.
8. Majoor-Krakauer D, Willems PJ, Hofman A. Genetic epidemiology of amyotrophic lateral sclerosis. Clinical Genetics. 2003;63(2):83-101.
9. Dunckley T, Huentelman MJ, Craig DW, Pearson JV, Szelinger S, Joshipura K, et al. Whole-Genome Analysis of Sporadic Amyotrophic Lateral Sclerosis. New England Journal of Medicine. 2007;357(8):775-88.
10. Gros-Louis F, Gaspar C, Rouleau GA. Genetics of familial and sporadic amyotrophic lateral sclerosis. Biochimica et Biophysica Acta (BBA) - Molecular Basis of Disease. 2006;1762(11):956-72.
11. Plato CC, Galasko D, Garruto RM, Plato M, Gamst A, Craig U-K, et al. ALS and PDC of Guam. Forty-year follow-up. 2002;58(5):765-73.
12. Plato CC, Garruto RM, Galasko D, Craig U-K, Plato M, Gamst A, et al. Amyotrophic Lateral Sclerosis and Parkinsonism-Dementia Complex of Guam: Changing Incidence Rates during the Past 60 Years. American Journal of Epidemiology. 2003;157(2):149-57.
13. Rowland LP. Diagnosis of amyotrophic lateral sclerosis. Journal of the Neurological Sciences. 1998;160:S6-S24.
14. Bruijn LI, Houseweart MK, Kato S, Anderson KL, Anderson SD, Ohama E, et al. Aggregation and motor neuron toxicity of an ALS-linked SOD1 mutant independent from wild-type SOD1. Science. 1998;281(5384):1851-4.
15. Vance C, Rogelj B, Hortobágyi T, De Vos KJ, Nishimura AL, Sreedharan J, et al. Mutations in FUS, an RNA processing protein, cause familial amyotrophic lateral sclerosis type 6. Science. 2009;323(5918):1208-11.
16. Giordana MT, Piccinini M, Grifoni S, De Marco G, Vercellino M, Magistrello M, et al. TDP-43 Redistribution is an Early Event in Sporadic Amyotrophic Lateral Sclerosis. Brain Pathology. 2010;20(2):351-60.
17. Mackenzie IR, Rademakers R, Neumann M. TDP-43 and FUS in amyotrophic lateral sclerosis and frontotemporal dementia. Lancet Neurol. 2010;9(10):995-1007.
18. Arai T, Hasegawa M, Akiyama H, Ikeda K, Nonaka T, Mori H, et al. TDP-43 is a component of ubiquitin-positive tau-negative inclusions in frontotemporal lobar degeneration and amyotrophic lateral sclerosis. Biochemical and Biophysical Research Communications. 2006;351(3):602-11.
19. Walker AK, Spiller KJ, Ge G, Zheng A, Xu Y, Zhou M, et al. Functional recovery in new mouse models of ALS/FTLD after clearance of pathological cytoplasmic TDP-43. Acta Neuropathologica. 2015;130(5):643-60.

20. Protter DSW, Parker R. Principles and Properties of Stress Granules. Trends Cell Biol. 2016;26(9):668-79.
21. Khalfallah Y, Kuta R, Grasmuck C, Prat A, Durham HD, Vande Velde C. TDP-43 regulation of stress granule dynamics in neurodegenerative disease-relevant cell types. Scientific Reports. 2018;8(1):7551.
22. Collier NC, Schlesinger MJ. The dynamic state of heat shock proteins in chicken embryo fibroblasts. Journal of Cell Biology. 1986;103(4):1495-507.
23. Nover L, Scharf KD, Neumann D. Cytoplasmic heat shock granules are formed from precursor particles and are associated with a specific set of mRNAs. Molecular and Cellular Biology. 1989;9(3):1298-308.
24. Palangi F, Samuel SM, Thompson IR, Triggle CR, Emara MM. Effects of oxidative and thermal stresses on stress granule formation in human induced pluripotent stem cells. PLOS ONE. 2017;12(7):e0182059.
25. Miller CL. Stress granules and virus replication. Future Virology. 2011;6(11):1329-38.
26. Chen L, Liu B. Relationships between Stress Granules, Oxidative Stress, and Neurodegenerative Diseases. Oxidative Medicine and Cellular Longevity. 2017;2017:1809592.
27. Malvezzi AM, Aricó M, Souza-Melo N, dos Santos GP, Bittencourt-Cunha P, Holetz FB, et al. GCN2-Like Kinase Modulates Stress Granule Formation During Nutritional Stress in Trypanosoma cruzi. Frontiers in Cellular and Infection Microbiology. 2020;10(149).
28. Alastalo T-P, Hellesuo M, Sandqvist A, Hietakangas V, Kallio M, Sistonen L. Formation of nuclear stress granules involves HSF2 and coincides with the nucleolar localization of Hsp70. Journal of Cell Science. 2003;116(17):3557-70.
29. Anderson P, Kedersha N. Stress granules. Current Biology. 2009;19(10):R397-R8.
30. Gupta N, Badeaux M, Liu Y, Naxerova K, Sgroi D, Munn LL, et al. Stress granule-associated protein G3BP2 regulates breast tumor initiation. Proceedings of the National Academy of Sciences. 2017:201525387.
31. Valentin-Vega YA, Wang Y-D, Parker M, Patmore DM, Kanagaraj A, Moore J, et al. Cancer-associated DDX3X mutations drive stress granule assembly and impair global translation. Scientific Reports. 2016;6(1):25996.
32. Waelter S, Boeddrich A, Lurz R, Scherzinger E, Lueder G, Lehrach H, et al. Accumulation of Mutant Huntingtin Fragments in Aggresome-like Inclusion Bodies as a Result of Insufficient Protein Degradation. Molecular Biology of the Cell. 2001;12(5):1393-407.
33. Goggin K, Beaudoin S, Grenier C, Brown A-A, Roucou X. Prion protein aggresomes are poly(A)+ ribonucleoprotein complexes that induce a PKR-mediated deficient cell stress response. Biochimica et Biophysica Acta (BBA) - Molecular Cell Research. 2008;1783(3):479-91.
34. Gonçalves AC, Towers ER, Haq N, Porco JA, Pelletier J, Dawson SJ, et al. Drug-induced Stress Granule Formation Protects Sensory Hair Cells in Mouse Cochlear Explants During Ototoxicity. Scientific Reports. 2019;9(1):12501.
35. Wang R, Zhang H, Du J, Xu J. Heat resilience in embryonic zebrafish revealed using an in vivo stress granule reporter. Journal of Cell Science. 2019;132(20):jcs234807.
36. Buchan JR, Parker R. Eukaryotic Stress Granules: The Ins and Outs of Translation. Molecular Cell. 2009;36(6):932-41.
37. Amorim IS, Lach G, Gkogkas CG. The Role of the Eukaryotic Translation Initiation Factor 4E (eIF4E) in Neuropsychiatric Disorders. Frontiers in Genetics. 2018;9(561).
38. Sahoo PK, Lee SJ, Jaiswal PB, Alber S, Kar AN, Miller-Randolph S, et al. Axonal G3BP1 stress granule protein limits axonal mRNA translation and nerve regeneration. Nature Communications. 2018;9(1):3358.
39. Gilks N, Kedersha N, Ayodele M, Shen L, Stoecklin G, Dember LM, et al. Stress granule assembly is mediated by prion-like aggregation of TIA-1. Mol Biol Cell. 2004;15(12):5383-98.
40. Cirillo L, Cieren A, Gotta M. Molecularly distinct cores coexist inside stress granules. bioRxiv. 2019:663955.

41. Panas MD, Ivanov P, Anderson P. Mechanistic insights into mammalian stress granule dynamics. The Journal of cell biology. 2016;215(3):313-23.
42. Wheeler JR, Matheny T, Jain S, Abrisch R, Parker R. Distinct stages in stress granule assembly and disassembly. Elife. 2016;5:e18413.
43. Buchan JR, Kolaitis R-M, Taylor JP, Parker R. Eukaryotic stress granules are cleared by autophagy and Cdc48/VCP function. Cell. 2013;153(7):1461-74.
44. Seguin SJ, Morelli FF, Vinet J, Amore D, De Biasi S, Poletti A, et al. Inhibition of autophagy, lysosome and VCP function impairs stress granule assembly. Cell Death Differ. 2014;21(12):1838-51.
45. Molliex A, Temirov J, Lee J, Coughlin M, Kanagaraj AP, Kim HJ, et al. Phase separation by low complexity domains promotes stress granule assembly and drives pathological fibrillization. Cell. 2015;163(1):123-33.
46. Dao TP, Kolaitis R-M, Kim HJ, O'Donovan K, Martyniak B, Colicino E, et al. Ubiquitin Modulates Liquid-Liquid Phase Separation of UBQLN2 via Disruption of Multivalent Interactions. Molecular Cell. 2018;69(6):965-78.e6.
47. Hyman AA, Weber CA, Jülicher F. Liquid-Liquid Phase Separation in Biology. Annual Review of Cell and Developmental Biology. 2014;30(1):39-58.
48. Reineke LC, Neilson JR. Differences between acute and chronic stress granules, and how these differences may impact function in human disease. Biochemical Pharmacology. 2019;162:123-31.
49. Reineke LC, Cheema SA, Dubrulle J, Neilson JR. Chronic starvation induces noncanonical pro-death stress granules. Journal of cell science. 2018;131(19):jcs220244.
50. Remenyi R, Gao Y, Hughes RE, Curd A, Zothner C, Peckham M, et al. Persistent Replication of a Chikungunya Virus Replicon in Human Cells Is Associated with Presence of Stable Cytoplasmic Granules Containing Nonstructural Protein 3. Journal of Virology. 2018;92(16):e00477-18.
51. Guo L, Kim HJ, Wang H, Monaghan J, Freyermuth F, Sung JC, et al. Nuclear-Import Receptors Reverse Aberrant Phase Transitions of RNA-Binding Proteins with Prion-like Domains. Cell. 2018;173(3):677-92.e20.
52. Smith HL, Mallucci GR. The unfolded protein response: mechanisms and therapy of neurodegeneration. Brain. 2016;139(8):2113-21.
53. Pioro EP, Mitsumoto H. Animal models of ALS. Clin Neurosci. 1995;3(6):375-85.
54. Van Damme P, Robberecht W, Van Den Bosch L. Modelling amyotrophic lateral sclerosis: progress and possibilities. Disease Models & Mechanisms. 2017;10(5):537-49.
55. Casci I, Pandey UB. A fruitful endeavor: modeling ALS in the fruit fly. Brain research. 2015;1607:47-74.
56. Botstein D, Chervitz SA, Cherry M. Yeast as a Model Organism. Science. 1997;277(5330):1259-60.
57. Li J, Le W. Modeling neurodegenerative diseases in Caenorhabditis elegans. Experimental Neurology. 2013;250:94-103.
58. Stephenson J, Amor S. Modelling amyotrophic lateral sclerosis in mice. Drug Discovery Today: Disease Models. 2017;25-26:35-44.
59. Gois AM, Mendonça DMF, Freire MAM, Santos JR. IN VITRO AND IN VIVO MODELS OF AMYOTROPHIC LATERAL SCLEROSIS: AN UPDATED OVERVIEW. Brain Research Bulletin. 2020;159:32-43.
60. Ramesh T, Lyon AN, Pineda RH, Wang C, Janssen PML, Canan BD, et al. A genetic model of amyotrophic lateral sclerosis in zebrafish displays phenotypic hallmarks of motoneuron disease. Disease Models & Mechanisms. 2010;3(9-10):652-62.
61. Howe K, Clark MD, Torroja CF, Torrance J, Berthelot C, Muffato M, et al. The zebrafish reference genome sequence and its relationship to the human genome. Nature. 2013;496(7446):498-503.

62. Mirzoyan Z, Sollazzo M, Allocca M, Valenza AM, Grifoni D, Bellosta P. Drosophila melanogaster: A Model Organism to Study Cancer. Frontiers in Genetics. 2019;10(51).
63. Simakov O, Kawashima T, Marlétaz F, Jenkins J, Koyanagi R, Mitros T, et al. Hemichordate genomes and deuterostome origins. Nature. 2015;527(7579):459-65.
64. Goldsmith JR, Jobin C. Think Small: Zebrafish as a Model System of Human Pathology. Journal of Biomedicine and Biotechnology. 2012;2012:817341.
65. Goodwin PC, Johnson B, Frevert CW. 4 - Microscopy, Immuno-Histochemistry, Digital Imaging, and Quantitative Microscopy. In: Treuting PM, Dintzis SM, Montine KS, editors. Comparative Anatomy and Histology (Second Edition). San Diego: Academic Press; 2018. p. 53-66.
66. Snyder JM, Hagan CE, Bolon B, Keene CD. 20 - Nervous System. In: Treuting PM, Dintzis SM, Montine KS, editors. Comparative Anatomy and Histology (Second Edition). San Diego: Academic Press; 2018. p. 403-44.
67. Lieschke GJ, Currie PD. Animal models of human disease: zebrafish swim into view. Nat Rev Genet. 2007;8(5):353-67.
68. Eaton RC, Farley RD, editors. Spawning Cycle and Egg Production of Zebrafish, Brachydanio rerio, in the Laboratory1974.
69. Spence R, Smith C. Male territoriality mediates density and sex ratio effects on oviposition in the zebrafish, Danio rerio. Animal Behaviour. 2005;69(6):1317-23.
70. Meyers JR. Zebrafish: Development of a Vertebrate Model Organism. Current Protocols Essential Laboratory Techniques. 2018;16(1):e19.
71. Wang H-Y, Li Y, Xue T, Cheng N, Du H-N. Construction of a series of pCS2+ backbone-based Gateway vectors for overexpressing various tagged proteins in vertebrates. Acta Biochimica et Biophysica Sinica. 2016;48(12):1128-34.
72. Panzica-Kelly JM, Zhang CX, Danberry TL, Flood A, DeLan JW, Brannen KC, et al. Morphological score assignment guidelines for the dechorionated zebrafish teratogenicity assay. Birth Defects Research Part B: Developmental and Reproductive Toxicology. 2010;89(5):382-95.
73. Omer A, Barrera MC, Moran JL, Lian XJ, Di Marco S, Beausejour C, et al. G3BP1 controls the senescence-associated secretome and its impact on cancer progression. Nature Communications. 2020;11(1):4979.
74. Omer A, Di Marco S, Gallouzi I-E. The senescence-associated secretory phenotype as a driver of tumor growth: does G3BP1 hold the key? Molecular & Cellular Oncology. 2021;8(1):1850161.
75. Abulfaraj AA, Mariappan K, Bigeard J, Manickam P, Blilou I, Guo X, et al. The Arabidopsis homolog of human G3BP1 is a key regulator of stomatal and apoplastic immunity. Life Science Alliance. 2018;1(2):e201800046.
76. Sidibé H, Dubinski A, Vande Velde C. The multi-functional RNA-binding protein G3BP1 and its potential implication in neurodegenerative disease. Journal of Neurochemistry. 2021;157(4):944-62.
77. Mahboubi H, Stochaj U. Cytoplasmic stress granules: Dynamic modulators of cell signaling and disease. Biochimica et Biophysica Acta (BBA) - Molecular Basis of Disease. 2017;1863(4):884-95.
78. Gilks N, Kedersha N, Ayodele M, Shen L, Stoecklin G, Dember LM, et al. Stress granule assembly is mediated by prion-like aggregation of TIA-1. Molecular biology of the cell. 2004;15(12):5383-98.
79. van Rosmalen M, Krom M, Merkx M. Tuning the Flexibility of Glycine-Serine Linkers To Allow Rational Design of Multidomain Proteins. Biochemistry. 2017;56(50):6565-74.
80. Chang N, Sun C, Gao L, Zhu D, Xu X, Zhu X, et al. Genome editing with RNA-guided Cas9 nuclease in Zebrafish embryos. Cell Research. 2013;23(4):465-72.
81. Howden SE, Voullaire L, Vadolas J. The transient expression of mRNA coding for Rep protein from AAV facilitates targeted plasmid integration. J Gene Med. 2008;10(1):42-50.

82. Revilla-García A, Fernández C, Moreno-Del Álamo M, de Los Ríos V, Vorberg IM, Giraldo R. Intercellular Transmission of a Synthetic Bacterial Cytotoxic Prion-Like Protein in Mammalian Cells. mBio. 2020;11(2).
83. Mahboubi H, Kodiha M, Stochaj U. Automated detection and quantification of granular cell compartments. Microsc Microanal. 2013;19(3):617-28.
84. Shemiakina II, Ermakova GV, Cranfill PJ, Baird MA, Evans RA, Souslova EA, et al. A monomeric red fluorescent protein with low cytotoxicity. Nature Communications. 2012;3(1):1204.
85. Amrhein V, Greenland S, McShane B. Scientists rise up against statistical significance. Nature. 2019;567(7748):305-7.
86. Rizzo MA, Piston DW. High-Contrast Imaging of Fluorescent Protein FRET by Fluorescence Polarization Microscopy. Biophysical Journal. 2005;88(2):L14-L6.
87. Shaner NC, Campbell RE, Steinbach PA, Giepmans BNG, Palmer AE, Tsien RY. Improved monomeric red, orange and yellow fluorescent proteins derived from Discosoma sp. red fluorescent protein. Nature Biotechnology. 2004;22(12):1567-72.
88. Kremers G-J, Goedhart J, van Munster EB, Gadella TWJ. Cyan and Yellow Super Fluorescent Proteins with Improved Brightness, Protein Folding, and FRET Förster Radius. Biochemistry. 2006;45(21):6570-80.
89. Shcherbo D, Merzlyak EM, Chepurnykh TV, Fradkov AF, Ermakova GV, Solovieva EA, et al. Bright far-red fluorescent protein for whole-body imaging. Nature Methods. 2007;4(9):741-6.
90. Stuart JA, Harper JA, Brindle KM, Brand MD. Uncoupling protein 2 from carp and zebrafish, ectothermic vertebrates. Biochimica et Biophysica Acta (BBA) - Bioenergetics. 1999;1413(1):50-4.
91. Anderson P, Kedersha N. Stress granules: the Tao of RNA triage. Trends Biochem Sci. 2008;33(3):141-50.
92. Gilchrist A, Au CE, Hiding J, Bell AW, Fernandez-Rodriguez J, Lesimple S, et al. Quantitative Proteomics Analysis of the Secretory Pathway. Cell. 2006;127(6):1265-81.
93. Bindels DS, Haarbosch L, van Weeren L, Postma M, Wiese KE, Mastop M, et al. mScarlet: a bright monomeric red fluorescent protein for cellular imaging. Nature Methods. 2017;14(1):53-6.
94. Kawakami K. Tol2: a versatile gene transfer vector in vertebrates. Genome Biol. 2007;8 Suppl 1(Suppl 1):S7-S.
95. Suster ML, Kikuta H, Urasaki A, Asakawa K, Kawakami K. Transgenesis in zebrafish with the tol2 transposon system. Methods Mol Biol. 2009;561:41-63.
96. Hwang WY, Peterson RT, Yeh J-RJ. Methods for targeted mutagenesis in zebrafish using TALENs. Methods. 2014;69(1):76-84.
97. Foley JE, Maeder ML, Pearlberg J, Joung JK, Peterson RT, Yeh JR. Targeted mutagenesis in zebrafish using customized zinc-finger nucleases. Nat Protoc. 2009;4(12):1855-67.
98. Hwang WY, Fu Y, Reyon D, Maeder ML, Kaini P, Sander JD, et al. Heritable and Precise Zebrafish Genome Editing Using a CRISPR-Cas System. PLOS ONE. 2013;8(7):e68708.
99. Do TU, Ho B, Shih SJ, Vaughan A. Zinc Finger Nuclease induced DNA double stranded breaks and rearrangements in MLL. Mutat Res. 2012;740(1-2):34-42.
100. Christian M, Cermak T, Doyle EL, Schmidt C, Zhang F, Hummel A, et al. Targeting DNA double-strand breaks with TAL effector nucleases. Genetics. 2010;186(2):757-61.
101. Brinkman EK, Chen T, de Haas M, Holland HA, Akhtar W, van Steensel B. Kinetics and Fidelity of the Repair of Cas9-Induced Double-Strand DNA Breaks. Mol Cell. 2018;70(5):801-13.e6.
102. Sertori R, Trengove M, Basheer F, Ward AC, Liongue C. Genome editing in zebrafish: a practical overview. Briefings in Functional Genomics. 2016;15(4):322-30.

103. Gaj T, Gersbach CA, Barbas CF, 3rd. ZFN, TALEN, and CRISPR/Cas-based methods for genome engineering. Trends Biotechnol. 2013;31(7):397-405.
104. Ran FA, Hsu PD, Wright J, Agarwala V, Scott DA, Zhang F. Genome engineering using the CRISPR-Cas9 system. Nature Protocols. 2013;8(11):2281-308.
105. Talbot JC, Amacher SL. A streamlined CRISPR pipeline to reliably generate zebrafish frameshifting alleles. Zebrafish. 2014;11(6):583-5.
106. Whiten DR, San Gil R, McAlary L, Yerbury JJ, Ecroyd H, Wilson MR. Rapid flow cytometric measurement of protein inclusions and nuclear trafficking. Scientific Reports. 2016;6(1):31138.
107. Zeineddine R, Whiten DR, Farrawell NE, McAlary L, Hanspal MA, Kumita JR, et al. Flow cytometric measurement of the cellular propagation of TDP-43 aggregation. Prion. 2017;11(3):195-204.
108. Robinson KJ, Tym MC, Hogan A, Watchon M, Yuan KC, Plenderleith SK, et al. Flow cytometry allows rapid detection of protein aggregates in cell culture and zebrafish models of spinocerebellar ataxia-3. bioRxiv. 2021:2021.03.09.434364.
109. Moujaber O, Mahboubi H, Kodiha M, Bouttier M, Bednarz K, Bakshi R, et al. Dissecting the molecular mechanisms that impair stress granule formation in aging cells. Biochimica et Biophysica Acta (BBA) - Molecular Cell Research. 2017;1864(3):475-86.
110. Hamada T, Yako M, Minegishi M, Sato M, Kamei Y, Yanagawa Y, et al. Stress granule formation is induced by a threshold temperature rather than a temperature difference in Arabidopsis. J Cell Sci. 2018;131(16).
111. Carnevale R, Sciarretta S, Violi F, Nocella C, Loffredo L, Perri L, et al. Acute Impact of Tobacco vs Electronic Cigarette Smoking on Oxidative Stress and Vascular Function. Chest. 2016;150(3):606-12.
112. Pereira TCB, Campos MM, Bogo MR. Copper toxicology, oxidative stress and inflammation using zebrafish as experimental model. Journal of Applied Toxicology. 2016;36(7):876-85.
113. Nunes-Costa D, Magalhães JD, G-Fernandes M, Cardoso SM, Empadinhas N. Microbial BMAA and the Pathway for Parkinson's Disease Neurodegeneration. Frontiers in Aging Neuroscience. 2020;12(26).
114. Chernoff N, Hill DJ, Diggs DL, Faison BD, Francis BM, Lang JR, et al. A critical review of the postulated role of the non-essential amino acid, β-N-methylamino-L-alanine, in neurodegenerative disease in humans. Journal of Toxicology and Environmental Health, Part B. 2017;20(4):183-229.
115. Ra D, Sa B, Sl B, Js M, Sj M, Da D, et al. Is Exposure to BMAA a Risk Factor for Neurodegenerative Diseases? A Response to a Critical Review of the BMAA Hypothesis. Neurotoxicity Research. 2021;39(1):81-106.
116. An H, Skelt L, Notaro A, Highley JR, Fox AH, La Bella V, et al. ALS-linked FUS mutations confer loss and gain of function in the nucleus by promoting excessive formation of dysfunctional paraspeckles. Acta Neuropathologica Communications. 2019;7(1):7.
117. Mackenzie IR, Rademakers R. The role of transactive response DNA-binding protein-43 in amyotrophic lateral sclerosis and frontotemporal dementia. Curr Opin Neurol. 2008;21(6):693-700.
118. Kwiatkowski TJ, Bosco DA, LeClerc AL, Tamrazian E, Vanderburg CR, Russ C, et al. Mutations in the FUS/TLS Gene on Chromosome 16 Cause Familial Amyotrophic Lateral Sclerosis. Science. 2009;323(5918):1205-8.
119. Roux KJ, Kim DI, Burke B, May DG. BioID: A Screen for Protein-Protein Interactions. Curr Protoc Protein Sci. 2018;91:19.23.1-19.23.15.

# 7 Appendix

## 7.1 Human *G3BP1* cDNA aligned with Zebrafish *g3bp1* cDNA

```
#######################################
# Program: water
# Rundate: Sun 19 Sep 2021 13:37:21
# Commandline: water
#    -auto
#    -stdout
#    -asequence emboss_water-I20210919-133829-0297-76475496-p2m.asequence
#    -bsequence emboss_water-I20210919-133829-0297-76475496-p2m.bsequence
#    -datafile EDNAFULL
#    -gapopen 10.0
#    -gapextend 0.5
#    -aformat3 pair
#    -snucleotide1
#    -snucleotide2
# Align_format: pair
# Report_file: stdout
#######################################

#=======================================
#
# Aligned_sequences: 2
# 1: BC045874.1
# 2: BC108278.1
# Matrix: EDNAFULL
# Gap_penalty: 10.0
# Extend_penalty: 0.5
#
# Length: 2457
# Identity:    1369/2457 (55.7%)
# Similarity:  1369/2457 (55.7%)
# Gaps:         671/2457 (27.3%)
# Score: 3806.0
#
#
#=======================================

BC045874.1        44 TAC------CGGCGCAGGAGGTGCTTCACCTAAATCACGTCAAACTCTTC     87
                     |||       |||.|| .|.||||| ..|.|||..||        ||||
BC108278.1         7 TACTATCCTCGGTGC-TGTGGTGC-AGAGCTAGTTC--------CTCT--     44

BC045874.1        88 CCAAAAACACATTACTGATTCCCTTTCGTTGAAACCAGTTGACCAAAGAA    137
                     |||          .||.|..|.|.|..||||||     ||||||||||.|
BC108278.1        45 CCA----------GCTCAGCCGCGTAGGTTGAA-----TTGACCAAAGCA     79

BC045874.1       138 ATGGTGATGGAGAAGCCAAGTGCCCAGCTTGTCGGGCGAGAGTTTGTCCG    187
                     |||||||||||||||||.|||.|||.|||.||||||||.||.||||||..|
BC108278.1        80 ATGGTGATGGAGAAGCCTAGTCCCCTGCTGGTCGGGCGGGAATTTGTGAG    129

BC045874.1       188 ACAGTATTACACCCTGCTGAACCAGGCTCCCGACTACCTGCACAGGTTTT    237
                     |||||||||||||.|||||||||||||||.||.|||...|||||.||.||||
BC108278.1       130 ACAGTATTACACACTGCTGAACCAGGCCCCAGACATGCTGCATAGATTTT    179

BC045874.1       238 ATGGCAAGAACTCCTCATATGTACATGGTGGACTGGA--CAACAATGGAA    285
                     ||||.||||||||.||.|||||.|||||.|||.||||  ||  |||||||
BC108278.1       180 ATGGAAAGAACTCTTCTTATGTCCATGGGGGATTGGATTCA--AATGGAA    227

BC045874.1       286 AACCAGCAGAAGCAGTATATGGACAGTCTGAAATCCATAAGAAGGTGATG    335
                     |.||||||||.||||||.||.||||||...||||||||.|.||||.||||||
BC108278.1       228 AGCCAGCAGATGCAGTCTACGGACAGAAAGAAATCCACAGGAAAGTGATG    277
```

```
BC045874.1       336 GCTCTAAGCTTCCGTGACTGTCACACTAAGATCAGACATGTCGATGCTCA    385
                     .|.|.||.||||....||||.|||||.||||||..|.||||||.||||||||
BC108278.1       278 TCACAAAACTTCACCAACTGCCACACCAAGATTCGCCATGTTGATGCTCA    327

BC045874.1       386 TGCCACCCTGAACGAGGGAGTGGTGGTTCAAGTTTTGGGGGGGTTGTCCA    435
                     ||||||.||.||.||.||.||||||.||.||.||..|||||....|.||.|
BC108278.1       328 TGCCACGCTAAATGATGGTGTGGTAGTCCAGGTGATGGGGCTTCTCTCTA    377

BC045874.1       436 ATAACATGCAACCCATGAGGAAGTTCATGCAGACATTTGTTTTGGCACCT    485
                     |.||||..||..|..||||||..||||||||.||.||||||..|.||.|||
BC108278.1       378 ACAACAACCAGGCTTTGAGGAGATTCATGCAAACGTTTGTCCTTGCTCCT    427

BC045874.1       486 GAGGGAACTGTTGCAAACAAGTTCTACGTACACAATGATATCTTCCGGTA    535
                     ||||||..||||||||||.||.||||||.||.||||||||||||||||.|.||
BC108278.1       428 GAGGGGTCTGTTGCAAATAAATTCTATGTTCACAATGATATCTTCAGATA    477

BC045874.1       536 CCAGGATGAAGTGTTTGGGGACTCTGACTCAGAACCTCCTGAGGAATCTG    585
                     |||.|||||.||.||||||.|..|.||.|.|.||.|||||..||||||.||||
BC108278.1       478 CCAAGATGAGGTCTTTGGTGGGTTTGTCACTGAGCCTCAGGAGGAGTCTG    527

BC045874.1       586 AGGAGGATGTGGAGG-AGCTG--GAGCGAGTGCACTCACCTGAGGTGGTC    632
                     |.||.||.||.|||| |.|||  ||..||..|||..||||||||||||||.
BC108278.1       528 AAGAAGAAGTAGAGGAACCTGAAGAAAGACAGCAAACACCTGAGGTGGTA    577

BC045874.1       633 CAAGAGGAGTCTTCTGG---GTATTACGAACAGACA-------------C    666
                     |..||.||   ||||||   .|..||.||.|||.||             .
BC108278.1       578 CCTGATGA---TTCTGGAACTTTCTATGATCAGGCAGTTGTCAGTAATGA    624

BC045874.1       667 CATGTGTAGAGCCT---GAGGTGCCCCAGGAAGAGGTGT--CTGTAACCC    711
                     |||| |.|||.|.|   ||||.|||           |||  |||.|   |
BC108278.1       625 CATG-GAAGAACATTTAGAGGAGCC-----------TGTTGCTGAA---C    659

BC045874.1       712 CAGAGCCCCAGCCTGAACCAGAAGTGGAGGTGGAGCCGGAGCCAGCAGCT    761
                     |||||||..|.||||||||||||            ||.||.|.||.|.||
BC108278.1       660 CAGAGCCTGATCCTGAACCAGAA------------CCAGAACAAGAACCT    697

BC045874.1       762 GTGGAGCTGAAA--------GCAGAGCCCATCAGCCAG------------    791
                     ||  |.||||||        |.|.||||  |.||||||
BC108278.1       698 GT--ATCTGAAATCCAAGAGGAAAAGCC--TGAGCCAGTATTAGAAGAAA    743

BC045874.1       792 -----CCTGAGGTTCATGTTGAGGAAAAGACTCAGAGATCTCCCCCATCG    836
                          |||||||   |||.|.||         .||||.|||      ||.
BC108278.1       744 CTGCCCCTGAGG---ATGCTCAG---------AAGAGTTCT------TCT    775

BC045874.1       837 CCCACACCTGCTGACACCGCACCCACCATGCCAGAGGACAACCGGCCATC    886
                     ||..|||||||.||||..||.|..||..|.|..||.|||....||.|||.
BC108278.1       776 CCAGCACCTGCAGACATAGCTCAGACAGTACAGGAAGACTTGAGGACATT    825

BC045874.1       887 TTCATGGGCTTCAGTCACTAGCAAGAATCTTCCACCTGGAGGAGTGGTCC    936
                     |||.|||||.||.||.||.||.||||||||||||||..|.||||..||.|
BC108278.1       826 TTCTTGGGCATCTGTGACCAGTAAGAATCTTCCACCCAGTGGAGCTGTTC    875

BC045874.1       937 CAGCCACAGGAGTCCCTCCACATGTTGTCAGAGTCCCATCAGCACAGCCA    986
                     |||..||.||..|.||.||.||||||||.|.|||.|||.|..||||||||.
BC108278.1       876 CAGTTACTGGGATACCACCTCATGTTGTTAAAGTACCAGCTTCACAGCCC    925

BC045874.1       987 CGTGTGGAGGTGAAAACAGAAACGCAGA--CCACAGCACAGAGACCCCAG   1034
                     |||...|||...||..|.|||.|.||||  ||||  ||||.|||||.|||
BC108278.1       926 CGTCCAGAGTCTAAGCCTGAATCTCAGATTCCAC--CACAAAGACCTCAG    973

BC045874.1      1035 AGAGATCAGAGACCACGTGACCAAAGA--------------CCA----GG   1066
                     .|.|||||.|||...||.||.|||.||               |||    ||
BC108278.1       974 CGGGATCAAAGAGTGCGAGAACAACGAATAAATATTCCTCCCCAAAGGGG   1023

BC045874.1      1067 ACCCTCTCCAGCTCACAGAACACCAAGGCCCGGAGTGGTACGAGAGGGTG   1116
                     ||||               |.|||||            |.||.|||||.|
BC108278.1      1024 ACCC---------------AGACCAA------------TCCGTGAGGCT-   1045
```

```
BC045874.1      1117 AGAGCGGGGAGTCAGAGGTG-----------CGACGAACAGTCCGATATC   1155
                          ||.||| || |||||           |||.|||..||..||.|.|
BC108278.1      1046 -----GGTGAG-CA-AGGTGACATTGAACCCCGAAGAATGGTGAGACACC   1088

BC045874.1      1156 CCGACAGTCACCAGCTCTTTGTTGGAAATGTACCTCATGATGTGGATAAG   1205
                     |.||||||||||||.||||||..||||.||..|.||||||||.||||||.|
BC108278.1      1089 CTGACAGTCACCAACTCTTCATTGGCAACCTGCCTCATGAAGTGGACA--   1136

BC045874.1      1206 AAT--GAGCTCAAGGAATTCTTTGAACAG-TACGGAACTGTCCTTGAGCT   1252
                     |||  |||||.||.||.||||||.|| || ||.||||..||..|.||||.|
BC108278.1      1137 AATCAGAGCTTAAAGATTTCTTTCAA-AGTTATGGAAACGTGGTGGAGTT   1185

BC045874.1      1253 GAGAATCAACAGTGGCGGGAAGCTGCCTAACTTTGGATTTGTGGTATTTG   1302
                     |.|.||.||||||||.||||||..|.||.||.||||||.||||||.||.||.|
BC108278.1      1186 GCGCATTAACAGTGGTGGGAAATTACCCAATTTTGGTTTTGTTGTGTTGG   1235

BC045874.1      1303 ATGATTCTGAGCCCGTGCAGAAGATCCTCAACAATCGGCCCATTAAACTG   1352
                     ||||||||||||||.||.||||||..|||||.|.||||..|||||||.|...|.
BC108278.1      1236 ATGATTCTGAGCCTGTTCAGAAAGTCCTTAGCAACAGGCCCATCATGTTC   1285

BC045874.1      1353 CGAGGAGATGTTCGGCTAAACGTAGAGGAAAAGAAGACCCGCTCAGCCCG   1402
                     .|||||.||.||.||.||.||.||.||.||.||||||||.||..|.||||.|
BC108278.1      1286 AGAGGTGAGGTCCGTCTGAATGTCGAAGAGAAGAAGACTCGAGCTGCCAG   1335

BC045874.1      1403 TGAAGGTGACCGACGAGACATCCGGCCCAGAGGCCCTGGGGGACCACGTG   1452
                     .||||||.||||||||||||.|..||.|...|.||.||||||.||.||.||.|
BC108278.1      1336 GGAAGGCGACCGACGAGATAATCGCCTTCGGGGACCTGGAGGCCCTCGAG   1385

BC045874.1      1453 ACCGGATAGGAGGGTCAA--GGGGGCCGCCTACCCGTGGAGGCATGGCTC   1500
                     ...||.|.||.||...||  .|.|||  |||.||||||||||||||||..|
BC108278.1      1386 GTGGGCTGGGTGGTGGAATGAGAGGC--CCTCCCCGTGGAGGCATGGTGC   1433

BC045874.1      1501 AGAAACCCAGTTTTGGAGCCGGTCGAGGCACAGGACCCAGCGAGGGC---   1547
                     |||||||..|.|||||||..||        .|||         ||||
BC108278.1      1434 AGAAACCAGGATTTGGAGTGGG--------AAGG---------GGGCTTG   1466

BC045874.1      1548 CGCTACACAGGACCACGTCAGTGATGCAGCTCCCACGTCA------TTCA   1591
                     ||          |||||.||||||   |.||      |||      ||||
BC108278.1      1467 CG----------CCACGGCAGTGA---ATCT------TCATGGATCTTCA   1497

BC045874.1      1592 CTGCTG--ATGCAAGTCACCCTGGTT--AACACAA------------GA-   1624
                      |||.|  ||.|||   |||||||||  ||||.||            ||
BC108278.1      1498 -TGCAGCCATACAA---ACCCTGGTTCCAACAGAATGGTGAATTTTCGAC   1543

BC045874.1      1625 ------TGG---CTT----------CCCTGTTCCCTGT------------   1643
                            |||   |||          |||.||   ||||
BC108278.1      1544 AGCCTTTGGTATCTTGGAGTATGACCCCAGT---CTGTTATAAACTGCTT   1590

BC045874.1      1644 ---------------------------------------------CTCC--A   1648
                                                                    ||||  .
BC108278.1      1591 AAGTTTGTATAATTTTACTTTTTTTGTGTGTTAATGGTGTGTGCTCCCTC   1640

BC045874.1      1649 TCCCTCACTCCAGGACCCAGGAGTGCGATTCTT---CTTTA-TCTGGACT   1694
                     ||||||.||              |.|..|||.|   ||||| ||| ..|.
BC108278.1      1641 TCCCTCTCT--------------TCCCTTTCCTGACCTTTAGTCT-TTCA   1675

BC045874.1      1695 CTTCC--TTTT---------TATTTCTGAGATTGAACTTGAATTTGTTGT   1733
                     |||||  ||||         |||||..|..||  |||  |.|.|| ||..
BC108278.1      1676 CTTCCAATTTTGTGGAATGATATTTTAGGAAT--AAC--GGACTT-TTAA   1720

BC045874.1      1734 AGAA--AAACAAAACTACTTGAATTGGGGAAAGGAGAAACCTAGC-----   1776
                     ||||  |||.|||||..|| ||||||             .|||.||
BC108278.1      1721 AGAAGCAAAAAAAAAGAC-TGAATT-------------TCCTTGCTTACT   1756

BC045874.1      1777 -----------------ATTTGGTTTT--------AGCGTTCTCTCCCTG   1801
                                      |||||..||||        |||..|.||.||
BC108278.1      1757 TTGCATATACAGACTGGATTTTTTTTTTTTTTTACAGCCATTTCCCC---   1803
```

```
BC045874.1      1802 TTTCTTAAAGGAACGTGT----TTTTACTG---CTTGG------GCAATC   1838
                          |||||||.||.|    |.||||||   .||||      .||.||
BC108278.1      1804 ------AAAGGAATGTCTTGCATATTACTGACATTTGGTATGTTTCATTC   1847

BC045874.1      1839 CTGTG---TATTGCT--------------------AGCACCCGCTTTCAG   1865
                     .| ||   ||||.||                    |||     ||.|.||
BC108278.1      1848 AT-TGGAATATTTCTTATTTTCTACGTGTTTGAAAAGC-----CTGTAAG   1891

BC045874.1      1866 GTCAAGTGCAAGTATGGTTTTATTTGGAATTGTTGCCAAGTC-----AAA   1910
                        ||.|.||.|         |||||..|.|.||..||||.|     |||
BC108278.1      1892 ---AAATACAGG---------ATTTGATAATATTTTCAAGGCAGGAAAAA   1929

BC045874.1      1911 TC---ATGG----TTGTGTGTGAG---TGACTA---TCTAGCATGTAAAG   1947
                     .|   ||.|    ||.|.||.|||   ||||||   |||.|  |||..||
BC108278.1      1930 CCCAAATTGTTTCTTCTTTGAGAGTCATGACTACCTTCTGG--TGTGGAG   1977

BC045874.1      1948 AA---TCC--TG-----TTTGCC--------TTCT---------------   1964
                     ||   .||  ||     ||||.|        ||||
BC108278.1      1978 AAATTGCCATTGGAAAATTTGACAATTTTGATTCTCACTGGTATGTTTAA   2027

BC045874.1      1965 --ACTG---------------------TTGCACTTCATCAAGAATGAC--   1989
                       ||||                     ||    ||.||.|||.||.||
BC108278.1      2028 AAACTGAATAAAAGGAATAGAATTTTTTT----TTGATAAAGGATCACAA   2073

BC045874.1      1990 AACATATTTTAACAACT-----------CCACTG---------TTGAGAG   2019
                     |||| |||.|||.|.||           |||.||         |||.||.
BC108278.1      2074 AACA-ATTCTAAAACCTAACTGTTTTTACCATTGAAATTTAAATTGTGAT   2122

BC045874.1      2020 AACA------AAAT----------AAAC-----------TCTATGTAC--   2040
                     ||.|      ||||          .|||           ||| ||.||
BC108278.1      2123 AATAGGTTTTAAATGTCTAGAATGCAACTGATAGGCTTTTCT-TGAACTG   2171

BC045874.1      2041 -----TATTTTGAA-----------------AA-----------AAAAAA   2057
                          |.|||||||                 ||           ||||||
BC108278.1      2172 TTAGTTTTTTTGAAGTAGTTTTTTCATGTTTAATTTGTATTTGTAAAAAA   2221

BC045874.1      2058 AAAAAAA   2064
                     |.|||||
BC108278.1      2222 ACAAAAA   2228


#---------------------------------------
#---------------------------------------
```

## 7.2 Translated human G3BP1 protein aligned with translated zebrafish G3bp1 protein

```
#######################################
# Program: water
# Rundate: Thu 27 May 2021 04:37:26
# Commandline: water
#    -auto
#    -stdout
#    -asequence emboss_water-I20210527-043724-0440-94769403-p2m.asequence
#    -bsequence emboss_water-I20210527-043724-0440-94769403-p2m.bsequence
#    -datafile EBLOSUM62
#    -gapopen 10.0
#    -gapextend 0.5
#    -aformat3 pair
#    -sprotein1
#    -sprotein2
# Align_format: pair
# Report_file: stdout
#######################################

#=======================================
#
# Aligned_sequences: 2
# 1: EMBOSS_001
# 2: EMBOSS_001
# Matrix: EBLOSUM62
# Gap_penalty: 10.0
# Extend_penalty: 0.5
#
# Length: 474
# Identity:     327/474 (69.0%)
# Similarity:   373/474 (78.7%)
# Gaps:          13/474 ( 2.7%)
# Score: 1636.5
#
#
#=======================================

EMBOSS_001         1 MVMEKPSAQLVGREFVRQYYTLLNQAPDYLHRFYGKNSSYVHGGLDNNGK
50
                     |||||||..||||||||||||||||||.||||||||||||||||||:|||
EMBOSS_001         1 MVMEKPSPLLVGREFVRQYYTLLNQAPDMLHRFYGKNSSYVHGGLDSNGK
50

EMBOSS_001        51 PAEAVYGQSEIHKKVMALSFRDCHTKIRHVDAHATLNEGVVVQVLGGLSN
100
                     ||:|||||.|||:|||:.:|.:|||||||||||||||||:||||||:|.|||
EMBOSS_001        51 PADAVYGQKEIHRKVMSQNFTNCHTKIRHVDAHATLNDGVVVQVMGLLSN
100

EMBOSS_001       101 NMQPMRKFMQTFVLAPEGTVANKFYVHNDIFRYQDEVFGDSDSEPPEESE
150
                     |.|.:|:||||||||||||:||||||||||||||||||||...:||.||||
EMBOSS_001       101 NNQALRRFMQTFVLAPEGSVANKFYVHNDIFRYQDEVFGGFVTEPQEESE
150

EMBOSS_001       151 EDVEE-LERVHSPEVVQEESSGYYEQTPCVEPEVPQ--EEVSVTPEPQPE
197
```

```
                    |:||| .||..:||||.::|..:|:|. .|..::.:  ||....|||.||
EMBOSS_001       151 EEVEEPEERQQTPEVVPDDSGTFYDQA-VVSNDMEEHLEEPVAEPEPDPE
199

EMBOSS_001       198 PEVEVEPEPAAVELKAEPISQPEVHVEEKTQRSPPSPTPADTAPTMPEDN
247
                    ||.|.||.....|.|.||:.  |....|..|:| .||.|||.|.|:.||.
EMBOSS_001       200 PEPEQEPVSEIQEEKPEPVL--EETAPEDAQKS-SSPAPADIAQTVQEDL
246

EMBOSS_001       248 RPSSWASVTSKNLPPGGVVPATGVPPHVVRVPSAQPRVEVKTETQTTAQR
297
                    |..||||||||||||.|.||.||:|||||:||::|||.|.|.|:|...||
EMBOSS_001       247 RTFSWASVTSKNLPPSGAVPVTGIPPHVVKVPASQPRPESKPESQIPPQR
296

EMBOSS_001       298 PQRDQRPRDQRPGPSPAHRTPRPGVVRE-GESGESEVRRTVRYPDSHQLF
346
                    ||||||.|:||.. .|..|.|||  :|| ||.|:.|.||.||:|||||||
EMBOSS_001       297 PQRDQRVREQRIN-IPPQRGPRP--IREAGEQGDIEPRRMVRHPDSHQLF
343

EMBOSS_001       347 VGNVPHDVDKNELKEFFEQYGTVLELRINSGGKLPNFGFVVFDDSEPVQK
396
                    :||:||:|||:|||:||:.||.|:||||||||||||||||||||||||||
EMBOSS_001       344 IGNLPHEVDKSELKDFFQSYGNVVELRINSGGKLPNFGFVVFDDSEPVQK
393

EMBOSS_001       397 ILNNRPIKLRGDVRLNVEEKKTRSAREGDRRDIRPRGPGGPRDRIGGS-R
445
                    :|:||||..||:||||||||||:||||||||.|.|||||||..:||. |
EMBOSS_001       394 VLSNRPIMFRGEVRLNVEEKKTRAAREGDRRDNRLRGPGGPRGGLGGGMR
443

EMBOSS_001       446 GPPTRGGMAQKPSFGAGRGTGPSE    469
                    ||| ||||.|||.||.|||..|.:
EMBOSS_001       444 GPP-RGGMVQKPGFGVGRGLAPRQ    466


#---------------------------------------
#---------------------------------------
```

## 7.3 Human *TIA1* cDNA aligned with Zebrafish *tia1* cDNA

```
#######################################
# Program: water
# Rundate: Sun 19 Sep 2021 13:44:23
# Commandline: water
#    -auto
#    -stdout
#    -asequence emboss_water-I20210919-134313-0715-96350247-p1m.asequence
#    -bsequence emboss_water-I20210919-134313-0715-96350247-p1m.bsequence
#    -datafile EDNAFULL
#    -gapopen 10.0
#    -gapextend 0.5
#    -aformat3 pair
#    -snucleotide1
#    -snucleotide2
# Align_format: pair
# Report_file: stdout
#######################################

#=======================================
#
# Aligned_sequences: 2
# 1: BC015944.1
# 2: BC066734.1
# Matrix: EDNAFULL
# Gap_penalty: 10.0
# Extend_penalty: 0.5
#
# Length: 1149
# Identity:     599/1149 (52.1%)
# Similarity:   599/1149 (52.1%)
# Gaps:         400/1149 (34.8%)
# Score: 1767.5
#
#
#=======================================

BC015944.1         2 GCGCCG-------CCGCGACAGCAGCAGCCATG--GA-GGACGAG----A     37
                     |||.||        ||    ||.||||| |.|||  || |||||||    |
BC066734.1        96 GCGTCGACCTTTTCC----CACCAGCA-CGATGATGATGGACGAGGACCA    140

BC015944.1        38 TGCCCAAGACTCTATACGTCGGTAACCTTTCCAGAGATGTGACAGAAGCT     87
                      |||.|.|||..|.||.|||||.|||||.|||||.||.||.||.||.||.
BC066734.1       141 -GCCGAGGACGTTGTATGTCGGGAACCTCTCCAGGGACGTTACGGAGGCC    189

BC015944.1        88 CTAATTCTGCAA-----CTCTTTAGCCAGATTGGACCTTGTAAAAACTGC    132
                     ||.||.||||||     ||||     |||||.||.||.||.||.|.|||.
BC066734.1       190 CTCATCCTGCAAGTGTTCTCT-----CAGATCGGCCCCTGCAAGAGCTGT    234

BC015944.1       133 AAAATGATTATGGATACAGCTGGAAATGATCCCTATTGTTTTGTGGAGTT    182
                     ||||||||..|.||||||.||||||||||.||.||.||.||||||||||||
BC066734.1       235 AAAATGATCCTTGATACAACTGGAAATGACCCATACTGCTTTGTGGAGTT    284

BC015944.1       183 TCATGAGCATCGTCATGCAGCTGCAGCATTAGCTGCTATGAATGGACGGA    232
                     ..|||||.|..|.|||||.||||||||..|.|||||.||||||||..|||
BC066734.1       285 CTATGAGAACAGACATGCTGCTGCAGCTCTGGCTGCCATGAATGGCAGGA    334

BC015944.1       233 AGATAATGGGTAAGGAAGTCAAAGTGAATTGGGCAACAACCCCTAGCAGT    282
                     ||||..|.||.|||||..|.|||||.||.|||||..||||.||.||||||
BC066734.1       335 AGATCTTAGGAAAGGATATGAAAGTCAACTGGGCCTCAACGCCAAGCAGT    384

BC015944.1       283 CAAAAGAAAGATACAAGCAGTAGTACCGTTGTCAGCACACAGCGTTCACA    332
                     ||||||||||||.|||||||
BC066734.1       385 CAAAAGAAAGACACAAGCA------------------------------    403
```

```
BC015944.1       333 AGATCATTTCCATGTCTTTGTTGGTGATCTCAGCCCAGAAATTACAACTG    382
                       ||||||||||.|||||||||||||.||.||||||||||..|.||.|
BC066734.1       404 --ATCATTTCCACGTCTTTGTTGGTGACCTGAGCCCAGAAATCTCGACAG    451

BC015944.1       383 AAGATATAAAAGCTGCTTTTGCACCATTTGGAAGAATATCAGATGCCCGA    432
                     |.|||.|.|.|||.||.|||||.||||||||||..|||||.|||||||||.
BC066734.1       452 ATGATGTCAGAGCAGCATTTGCTCCATTTGGAAAGATATCTGATGCCCGC    501

BC015944.1       433 GTGGTAAAAGACATGGCAACAGGAAAGTCTAAGGGATATGGCTTTGTCTC    482
                     |||||.||.||..||||.||||||||.|||||.||||||||.||..||||
BC066734.1       502 GTGGTGAAGGATCTGGCTACAGGAAAATCTAAAGGATATGGTTTCATCTC    551

BC015944.1       483 CTTTTTCAACAAATGGGATGCTGAAAACGCCATTCAACAGATGGGTGGCC    532
                     |||..|.|||||||||||||||.|||||..||.|||||.||.||||..|||||
BC066734.1       552 CTTCATTAACAAATGGGATGCAGAAAGTGCTATTCAGCAAATGAATGGCC    601

BC015944.1       533 AGTGGCTTGGTGGAAGACAAATCAGAACTAACTGGGCAACCCGAAAGCCT    582
                     |||||||.||.||.|||||.||||||||.||||||||.||..|.|||||.
BC066734.1       602 AGTGGCTGGGAGGCAGACAGATCAGAACAAACTGGGCCACAAGGAAGCCA    651

BC015944.1       583 CCCGCTCC--------------AAAGAG---------TACA-------TA    602
                     .|.|||||              ||.|||         .|||       ||
BC066734.1       652 TCAGCTCCCAAATCAAACAATGAAGGAGCCAGCAGCAAACACTTGTCCTA    701

BC015944.1       603 TGAG-------TG--------------TAG----------GTGTATTG--    619
                     .|||       ||              |||          ||.|||||
BC066734.1       702 CGAGGAGGTTCTGAACCAGTCGAGTCCTAGTAATTGCACCGTTTATTGTG    751

BC015944.1       620 -----------------------------------GAGA------------    623
                                                       ||||
BC066734.1       752 GTGGCATTGCTTCTGGCCTTTCAGATCAGCTCATGAGACAGACTTTCTCT    801

BC015944.1       624 ----------AGA-AAAGGAAATGTGGAATTTT---GGAGAAA-AATAC-    657
                               ||| ||.|||.||..|| .||||   .|||||| .||||
BC066734.1       802 CCGTTCGGCCAGATAATGGAGATCAGG-GTTTTCCCAGAGAAAGGATACT    850

BC015944.1       658 ----------GCTAGAT--------------------------------T    665
                               |.|.|||                                |
BC066734.1       851 CCTTTGTGAGGTTTGATTCTCATGAGGGTGCCGCTCATGCCATAGTGTCT    900

BC015944.1       666 TTAAATG---------TTAGAG-------CTGTTCCCGGAGACTTATTG-    698
                     .||||||         || |||       ||||    |.||...||.||
BC066734.1       901 GTAAATGGGACATGCATT-GAGGGCCACACTGT----GAAGTGCTACTGG    945

BC015944.1       699 ----CAGAA-----ATAGATGAGA-------AGCAAAT----------CA    722
                         .||||     |.|.||||||       |.|||||          ||
BC066734.1       946 GGTAAAGAAACGGCAGATATGAGATCCATGCAACAAATGCCAATGCCCCA    995

BC015944.1       723 --AGA--------------------------CTAC----------------    729
                       |||                          ||||
BC066734.1       996 GCAGAATAAACCCACTTATGCTGCCCAGCCCTACGGACAGTGGGGACAGT   1045

BC015944.1       730 --TAT--------TCA-----------AAAATGT----------------    742
                       |||        |||           |..||||
BC066734.1      1046 CATATGGCAACGGTCAGCAGATGGGTCAGTATGTGCCCAACGGCTGGCAG   1095

BC015944.1       743 ------ACTTA----GTTT----TCATTTTTGTAAT---------TATAA    769
                            |||||    ||.|    .||....||.|||         |||||
BC066734.1      1096 ATGCCCACTTATGGCGTCTACGGGCAGGCCTGGAATCAGCAGGGATATAA   1145

BC015944.1       770 ATAA-TATTATTT-------CTAAT------GTCAAGTCTCCTATTAAA    804
                     |||| ||..|.||       .||||      |||.|.||    ||||||
BC066734.1      1146 ATAAGTACAAATTTGGCTGATTAATCCCTCAGTCCAATC----ATTAAA   1190


#---------------------------------------
#---------------------------------------
```

## 7.4 Translated human TIA1 protein aligned with translated zebrafish Tia1 protein

```
########################################
# Program: water
# Rundate: Mon 20 Sep 2021 17:06:06
# Commandline: water
#    -auto
#    -stdout
#    -asequence emboss_water-I20210920-170604-0602-10844329-p2m.asequence
#    -bsequence emboss_water-I20210920-170604-0602-10844329-p2m.bsequence
#    -datafile EBLOSUM62
#    -gapopen 10.0
#    -gapextend 0.5
#    -aformat3 pair
#    -sprotein1
#    -sprotein2
# Align_format: pair
# Report_file: stdout
########################################

#=======================================
#
# Aligned_sequences: 2
# 1: zebrafish
# 2: human
# Matrix: EBLOSUM62
# Gap_penalty: 10.0
# Extend_penalty: 0.5
#
# Length: 194
# Identity:     154/194 (79.4%)
# Similarity:   176/194 (90.7%)
# Gaps:          11/194 ( 5.7%)
# Score: 844.0
#
#
#=======================================

zebrafish         40 MDEDQPRTLYVGNLSRDVTEALILQVFSQIGPCKSCKMILDTTGNDPYCF     89
                     |:::.|:|||||||||||||||||||:||||||||:||||:||.|||||||
human              9 MEDEMPKTLYVGNLSRDVTEALILQLFSQIGPCKNCKMIMDTAGNDPYCF     58

zebrafish         90 VEFYENRHAAAALAAMNGRKILGKDMKVNWASTPSSQKKDTS--------    131
                     |||:|:|||||||||||||||:||::||||||:||||||||||
human             59 VEFHEHRHAAAALAAMNGRKIMGKEVKVNWATTPSSQKKDTSSSTVVSTQ    108

zebrafish        132 ---NHFHVFVGDLSPEISTDDVRAAFAPFGKISDARVVKDLATGKSKGYG    178
                         :||||||||||||||:|:|::|||||||:|||||||||:|||||||||
human            109 RSQDHFHVFVGDLSPEITTEDIKAAFAPFGRISDARVVKDMATGKSKGYG    158

zebrafish        179 FISFINKWDAESAIQQMNGQWLGGRQIRTNWATRKPSAPKSNNE    222
                     |:||.||||||:||||||.||||||||||||||||||.|||||..|
human            159 FVSFFNKWDAENAIQQMGGQWLGGRQIRTNWATRKPPAPKSTYE    202


#---------------------------------------
#---------------------------------------
```

MACQUARIE University
SYDNEY·AUSTRALIA

09/12/2019

Dear Professor Julie Atkin,

**Re:"Generation of genetically modified organisms and cell lines to investigate and modify disorders of the nervous system. " 5974 - 52019597412350**

**NOTIFICATION OF A NOTIFIABLE LOW RISK DEALING (NLRD)**

The above application has been reviewed by the Institutional Biosafety Committee (IBC) and has been approved as an NLRD, effective 09/12/2019.

This approval is subject to the following standard conditions:

- The NLRD is conducted by persons with appropriate training and experience, within a facility certified to either Physical Containment level 1 (PC1) or PC2.
- Work requiring Quarantine Containment level 2 (QC2) does not commence until the facility has been certified

Please note the following standard requirements of approval:

1. Approval will be for a period of 5 years subject to the provision of annual reports. If, at the end of this period the project has been completed, abandoned, discontinued or not commenced for any reason, you are required to submit a Final Report. If you complete the work earlier than you had planned you must submit a Final Report as soon as the work is completed. Please contact the Committee Secretary at biosafety@mq.edu.au for a copy of the annual report.

Reporting: Annual progress reports are required for this project and a **Final Report for this project will be due on: 09/12/2024**

2. If you will be applying for or have applied for internal or external funding for the above project it is your responsibility to provide the Macquarie University's Research Grants Management Assistant with a copy of this email as soon as possible. Internal and External funding agencies will not be informed that you have final approval for your project and funds will not be released until the Research Grants Management Assistant has received a copy of this email.

If you need to provide a hard copy letter of approval to an external organisation as evidence that you have approval, please do not hesitate to contact the Committee Secretary at the address below.

Please retain a copy of this letter as this is your formal notification of final Biosafety approval. Also a copy of record submitted by Macquarie University to the OGTR.

Kind Regards,

**Professor Robert Willows**

Institutional Biosafety Committee Chair,
Macquarie University Research Office
Level 3, Research Hub, Building C5C East
Macquarie University, NSW 2109 Australia
T: +61 2 9850 4063
E: biosafety@mq.edu.au
W: mq.edu.au/research

# ANIMAL RESEARCH AUTHORITY (ARA)

**AEC Reference No.: 2015/033-36** **Date of Expiry:** 11 December 2021

*Online Project ID: 452*

***Full Approval Duration:*** *11 December 2015 to 31 December 2024*

This ARA remains in force until the Date of Expiry (unless suspended, cancelled or surrendered) **and will only be renewed upon receipt of a satisfactory Progress Report before expiry (see Approval email for submission details).**


**Principal Investigator:**
Professor Roger Chung
Faculty of Medicine, Health and Human Sciences
Macquarie University, NSW 2109
roger.chung@mq.edu.au
0402 808 958

**Associate Investigators:**

| | |
|---|---|
| Marco Morsch | 0449 126 528 |
| Emily Don | 0423 387 488 |
| Vinod Sundaramoorthy | 0430 198 649 |
| Lucy da Silva | 0478 143 417 |

**Others Participating:**

| | |
|---|---|
| Alison Hogan | 0401 857 972 |
| Rowan Radford | 0403 605 754 |
| Sharron Chow | 0413 536 028 |
| Dr Adam Svahn | 0403 003 200 |
| Katherine Robinson | 0402 734 322 |
| Ariuntugs Ultziikhutag | 0410 936 063 |
| Libing Fu | 0424 366 155 |
| Guoying Wang | 0415 928 329 |
| Andres Vidal-Itriago | 0434 635 818 |
| Natalie Scherer | 0491 082 379 |
| Cindy Maurel | 02 9850 2787 |
| Michael Lau | 0423 599 313 |
| Nicholas Kakaroubas | 0429 533 214 |
| Tyler Chapman | 0438 197 795 |
| Astrid Feiten | 0434 096 450 |
| Stephen Cull | 0410 095 812 |


**In case of emergency, please contact:**
*the Principal Investigator / Associate Investigator named above*
**or Animal Welfare Officer**: 9850 7758 / 0439 497 383

The above-named are authorised by MACQUARIE UNIVERSITY ANIMAL ETHICS COMMITTEE to conduct the following research:

**Title of the project:** **Using zebrafish to understand how the central nervous system responds to neuronal stress and death caused by neurodegenerative diseases**

**Purpose:** 5 - Research: Human or Animal Health and Welfare

**Aims:** To investigate:

1. How motor neuron disease (MND)-causing genes trigger dysfunction
2. How glia respond to motor neurons expressing MND disease, and how glial activation may influence disease progression.
3. How MND-causing proteins may cause the spreading wave of neurodegeneration that characterises MND.
4. Putative therapeutics that can rescue MND-like defects in motor neurons expressing MND-causing genes.

**Surgical Procedures category**: 9 - Production of Genetically Modified Animals

**All procedures must be performed as per the AEC-approved protocol, unless stated otherwise by the AEC and/or AWO.**

**Maximum numbers approved (for the Full Approval Duration):**

| Species | Strain | Age/Weight/Sex | Total | Supplier/Source |
|---|---|---|---|---|
| 23 - Fish | Zebrafish (*Danio rerio*) | Larvae | 15 000 | Bred In-house |
| 23 - Fish | Zebrafish (Danio rerio) | Adult | 7 200 | Bred In-house |
| | | | TOTAL 22 200 | |

**Location of research:**

| *Location* | *Full street address* |
|---|---|
| FMHHS Laboratory | Level 1, F10A, 2 Technology Place, Macquarie University, NSW 2109 |

**Amendments approved by the AEC since initial approval:**

1. Amendment #1 - Addition of Rola Bazzi as Animal Technician/Research Assistant (Executive approved 05/04/2016. Ratified by AEC 14 April 2016).
2. Amendment #2 - Addition of Dr Adam Svahn as Post-Doctoral Researcher (Executive approved. Ratified by AEC 16 June 2016).
3. Amendment #3 - Amend Zebrafish husbandry protocol to allow for the live collection of sperm and eggs for cryopreservation and IVF (Approved by AEC 16 June 2016).
4. Amendment #4 - Add Bianca Varney as weekend fish feeder and health check (Executive approved. Ratified by AEC 07/12/2016).
5. Amendment #5(a) - Additional substances for administration (Approved by AEC 07/12/2016).
6. Amendment #5(b) - Additional procedures (Approved by AEC 07/12/2016).
7. Amendment #6 - Add Alina Maschirow as Visiting Scholar (Executive approved. Ratified by AEC 16 February 2017).
8. Amendment #7- Add Katherine Robinson as Fish Feeder (Executive approved. Ratified by AEC 16 March 2017)
9. Amendment #8 - Add Ariuntugs Ulziikhutag as Fish Feeder (Executive approved. Ratified by AEC 16 March 2017)
10. Amendment #9 - Define the role of Fish Feeder (Executive approved. Ratified by AEC 12 April 2017)
11. Amendment #10 – Remove Dasha Monisha Syal from protocol (Executive approved. Ratified by AEC 20 July 2017).
12. Amendment #11 – Remove Bianca Varney from protocol (Executive approved. Ratified by AEC 20 July 2017).

**AEC Reference No.: 2015/033-36** **Date of Expiry:** 11 December 2021

**Amendments approved by the AEC since initial approval (cont'd):**

13. Amendment #12 – Remove Isabel Formella from protocol (Executive approved. Ratified by AEC 20 July 2017).
14. Amendment #13(b) - Add Libing Fu as PhD Student (Executive approved. Ratified by AEC 16 November 2017).
15. Amendment #13(c) - Add Guoying Wang as PhD student (Executive approved. Ratified by AEC 16 November 2017).
16. Amendment #14 - Add Andres Vidal-Itriago as PhD Student (Executive approved. Ratified by AEC at 22 March 2018 meeting).
17. Amendment #15 - Add Natalie Scherer as PhD Student (Executive approved. Ratified by AEC at 22 March 2018 meeting).
18. Amendment #16(a) - Remove Nicholas Cole (Approved by AEC at 22 March 2018 meeting).
19. Amendment #16(b) - Remove Rola Bazzi (Approved by AEC at 22 March 2018 meeting).
20. Amendment #16(c) - Remove Alina Maschirow (Approved by AEC at 22 March 2018 meeting).
21. Amendment #17 - Add Emily Don as Associate Investigator (Executive approved. Ratified by AEC at 22 March 2018 meeting).
22. Amendment - 01/11/2018 - Remove Jack Stoddart, Nicholas Cole and Serene Gwee from protocol (Approved by AEC 13 December 2018).
23. Amendment – 06/02/2019 - Add Lucy da Silva as Associate Investigator (Executive approved. Ratified by AEC at 14 February 2019 meeting).
24. Amendment – 04/06/2019 – Add Michael Udoh to project (Executive approved. Ratified by AEC 18 July 2019).
25. Amendment – 26/08/2019 – Addition of previously approved SOPs to project (Approved by AEC 19 September 2019).
26. Amendment – 17/09/2019 – Add Cindy Maurel to project (Executive approved. Ratified by AEC 17 October 2019).
27. Amendment – 29/11/2019 – Request extension of project until 12 December 2019 (Executive approved. Ratified by AEC 20/02/2020).
28. Amendment – 09/03/2020 – Add Michael Lau as Associate Investigator (Executive approved. Ratified by AEC 23/04/2020).
29. Amendment – 15/04/2020 – Add the approved SOP 'Genome Editing of Zebrafish' to the ARA (Approved by AEC 21/05/2020).
30. Amendment – 01/07/2020 – Add Nicholas Kakaroubas to protocol (Executive approved. Ratified by AEC 20 August 2020).
31. Amendment – 15/09/2020 – Add Tyler Chapman to protocol (Executive approved. Ratified by AEC 15 October 2020).
32. Amendment – 20/11/2020 – Add Astrid Feiten to protocol (Executive approved. Ratified by AEC 17 December 2020).
33. Amendment – 04/02/2021 - Add Stephen Cull to the protocol (Executive approved. To be ratified by AEC 18 March 2021).

**Conditions of Approval: N/A**

Being animal research carried out in accordance with the Code of Practice for a recognised research purpose and in connection with animals (other than exempt animals) that have been obtained from the holder of an animal suppliers licence.

**A/Prof. Simon McMullan** (Chair, Animal Ethics Committee) **Approval Date: 09 February 2021**

# ANIMAL RESEARCH AUTHORITY (ARA)

MACQUARIE University

**AEC Reference No.: 2015/034-29** **Date of Expiry:** 10 December 2020

***Full Approval Duration:*** *11 December 2015 to 10 December 2020*

This ARA remains in force until the Date of Expiry (unless suspended, cancelled or surrendered) **and will only be renewed upon receipt of a satisfactory Progress Report before expiry (see Approval email for submission details).**

**Principal Investigator:**

**Dr Angela Laird**
Faculty of Medicine and Health Sciences
Macquarie University, NSW 2109
angela.laird@mq.edu.au
0416 808 108

**Associate Investigators:**

| | |
|---|---|
| Marco Morsch | 0449 126 528 |
| Roger Chung | 0402 808 958 |
| Emily Don | 0423 387 488 |

**Others Partipating:**

| | |
|---|---|
| Alison Hogan | 0401 857 972 |
| Jennifer Fifita | 0433 979 754 |
| Yagiz Aksoy | 0431 955 280 |
| Rowan Radford | 0403 605 754 |
| Sharlynn Wu | 0450 252 404 |
| Serene Gwee | 0411 514 831 |
| Sharron Chow | 0413 536 028 |
| Jack Stoddart | 0402 682 745 |
| Erin Lynch | 0431 106 315 |
| Hamideh Shahheydari | 0413 243 183 |
| Katherine Robinson | 0402 734 322 |
| Ariuntugs Ultziikhutag | 0410 936 063 |
| Maxine Watchon | 0481 451 897 |
| Kristy Yuan | 0430 039 958 |
| Emma Perri | 0400 068 242 |
| Sina Shadfar | 0431 107 710 |
| Reka Toth | 0434 893 254 |
| Luan Luu | 0430 115 691 |
| Claire Winnick | 0415 777 021 |
| Madelaine Tym | 0490 496 794 |
| Caitlin Lucas | 0411 679 538 |
| Zachary Frangos | 0418 752 119 |
| Nicholas Kakaroubas | 0420 533 214 |

**In case of emergency, please contact:**
*the Principal Investigator / Associate Investigator named above*
**or Animal Welfare Officer**: 9850 7758 / 0439 497 383

The above-named are authorised by MACQUARIE UNIVERSITY ANIMAL ETHICS COMMITTEE to conduct the following research:

**Title of the project:** **Zebrafish models of neurodegenerative diseases**

**Purpose:** **5 - Research: Human or Animal Health and Welfare**

**Aims**: **To create fish models of neurodegenerative diseases using zebrafish**

**Surgical Procedures category**: **9 - Production of Genetically Modified Animals**

**All procedures must be performed as per the AEC-approved protocol, unless stated otherwise by the AEC and/or AWO.**

**Maximum numbers approved (for the Full Approval Duration):**

| Species | Strain | Age/Weight/Sex | Total | Supplier/Source |
|---|---|---|---|---|
| 23 - Fish | Zebrafish (*Danio rerio*) | Larvae | 30, 552 | Bred In-house |
| | Zebrafish (Danio rerio) | Adult | 12,200 | |
| | Zebrafish (Danio rerio) | Adults and Larvae | 90 | |
| | Zebrafish (Marine Facility) | Adults | 3000 | |
| | | | TOTAL 45,842 | |

**Location of research:**

| *Location* | *Full street address* |
|---|---|
| FMHS Laboratory | Level 1, F10A, 2 Technology Place, Macquarie University, NSW 2109 |

**Amendments approved by the AEC since initial approval:**

1. ***Amendment #1*** *- Add Erin Lynch as Student. (Executive Approved. Ratified by AEC 18 February 2016).*
2. ***Amendment #2*** *- Add Dr Elinor Hortle as Associate Investigator. (Executive Approved. Ratified by AEC 18 February 2016).*
3. ***Amendment #3*** *- Add Dr Hamideh Shahheydari as Researcher. (Executive Approved. Ratified by AEC 18 February 2016).*
4. ***Amendment #4*** *- Add Rola Bazzi as Animal Technician/Research Assistant. (Executive Approved. Ratified by AEC 17 March 2016).*
5. ***Amendment #5(a)*** *- Amend experimental design and* ***Amendment #5(b)*** *- Amend procedure (Approved by the AEC 14 April 2016).*
6. **Amendment #6** - Amend Zebrafish husbandry protocol to allow for the live collection of sperm and eggs for cryopreservation and IVF. (Approved by the AEC 16 June 2016).

**AEC Reference No.: 2015/034-29** **Date of Expiry:** 10 December 2020

**Amendments approved by the AEC since initial approval (Cont'd)**

7. ***Amendment #7*** *- Add Bianca Varney as weekend fish feeder & health check (Executive approved. Ratified by AEC 07/12/2016).*
8. ***Amendment #8*** *- Amend experimental procedure (Executive approved. Ratified by AEC 07/12/2016).*
9. ***Amendment #9*** *- Additional procedure (Approved by AEC 07/12/2016).*
10. ***Amendment #10*** *- Additional 2, 800 adult zebrafish (Approved by AEC 16/03/2017).*
11. ***Amendment #11*** *- Add Katherine Robinson as Fish Feeder (Approved by AEC 16/03/2017).*
12. ***Amendment #12*** *- Add Ariuntugs Ulziikhutag as Fish Feeder (Approved by AEC 16/03/2017).*
13. ***Amendment #13*** *– Add Maxine Watchon as PhD Student (Approved by AEC 16/03/2017).*
14. ***Amendment #14*** *- Add Kristy Yuan as Research Assistant (Approved by AEC 16/03/2017).*
15. ***Amendment #15*** *- Add Angela Laird as Chief Investigator (Approved by AEC 16/03/2017).*
16. ***Amendment #16*** *- Additional behavioural testing to detect changes in baseline activity, cognition and memory. (Approved by AEC 16/03/2017).*
17. ***Amendment #17*** *- Additional 90 adult zebrafish to include 30 zebrafish added as adults (three groups of n=10) and 60 zebrafish raised from embryos to adults (three groups of n=20) (Approved by AEC 16/03/2017).*
18. ***Amendment #18*** *- Add Emma Perri as PhD student (Executive approved. Ratified by AEC 12/04/2017).*
19. ***Amendment #19*** *- Define the role of Fish Feeder (Executive approved. Ratified by AEC 12/04/2017).*
20. ***Amendment #20*** *– Remove Joel Berliner from protocol (Executive approved. Ratified by AEC 20 July 2017).*
21. ***Amendment #21*** *– Remove Vinod Sundaramoorthy from protocol (Executive approved. Ratified by AEC 20 July 2017).*
22. ***Amendment #22*** *– Remove Elinor Hortle from protocol (Executive approved. Ratified by AEC 20 July 2017)…*
23. ***Amendment #23*** *– Remove Dasha Monisha Syal from protocol (Executive approved. Ratified by AEC 20 July 2017).*
24. ***Amendment #24*** *– Remove Isabel Formella from protocol (Executive approved. Ratified by AEC 20 July 2017).*
25. ***Amendment #25*** *– Remove Bianca Varney from protocol (Executive approved. Ratified by AEC 20 July 2017).*
26. ***Amendment #26(a)*** *- Additional procedure involving administration of substances (Approved by AEC 20 July 2017).*
27. ***Amendment #26(b)*** *- Additional 15,552 embryo and larval zebrafish for these treatments to be tested on (Approved by AEC 20 July 2017).*
28. ***Amendment #27*** *- Add Sina Shadfar as PhD Candidate (Executive approved. Ratified by AEC 17 August 2017).*
29. ***Amendment #28*** *- Add Reka Petra Toth as Student (Executive approved. Ratified by AEC 17 August 2017).*
30. ***Amendment #29*** *- Add Luan Luu as Research Fellow (Executive approved. Ratified by AEC 21 September 2017).*
31. ***Amendment #30(a)*** *- Remove Nicholas Cole from protocol (Approved by AEC 15 February 2018).*
32. ***Amendment #30(b)*** *- Remove Rola Bazzi from protocol (Approved by AEC 15 February 2018).*
33. ***Amendment #31*** *- Add Claire Winnick as Research Assistant (Executive approved. Ratified by AEC 22 March 2018).*
34. ***Amendment #32*** *- Add Madelaine Tym to protocol (Executive approved. Ratified by AEC 24 May 2018).*
35. ***Amendment –*** *10/05/2018 – Add Caitlin Lucas to the protocol (Executive approved. Ratified by AEC 21 June 2018).*
36. ***Amendment –*** *01/11/2018 – Additional 2,200 adult Zebrafish requested (taking total no. of adult Zebrafish to 12,200) (Approved by AEC 13 December 2018).*
37. ***Amendment –*** *26/02/2019 – Add Zachary Frangos to protocol (Executive approved. Ratified by AEC 11 April 2019).*
38. ***Amendment –*** *17/07/2019 – Amend experimental procedure, technique, design - euthanise nine fish (three animals from three different lines) to take terminal blood samples from them. These samples will then be processed to identify whether the protein is present. (Executive approved. Ratified by AEC 15 August 2019).*
39. ***Amendment –*** *14/08/2019 – Additional experiment (hypoxia) (Executive approved. Ratified by AEC 19 September 2019).*
40. ***Amendment –*** *10/10/2019 – Add Sharlynn Wu to project (Executive approved. Ratified by AEC 14 November 2019).*
41. ***Amendment*** *– 24/10/2019 – Additional 3,000 animals requested (taking total to 45,842) (Approved by the AEC 14 November 2019).*
42. ***Amendment*** *– 10/03/2020 – Add Nicholas Kakaroubas to protocol (Executive approved. To be ratified by AEC 23 April 2020).*

**Conditions of Approval:**

1. ***Amendments #2 & #3 -*** *Approved subject to strict supervision until competency established.*

Being animal research carried out in accordance with the Code of Practice for a recognised research purpose and in connection with animals (other than exempt animals) that have been obtained from the holder of an animal suppliers license.

**A/Prof. Nathan Hart** (Chair, Animal Ethics Committee) **Approval Date:** 13 March 2020